HYDROCRACKING OF ASSAM CRUDE RESIDUE FOR THE PRODUCTION OF KEROSENE AND DIESEL OILS

A Thesis Submitted
In Partial Fulfilment of the Requirements
for the Degree of
DOCTOR OF PHILOSOPHY

By
NITYANAND CHOUDHARY

to the

DEPARTMENT OF CHEMICAL ENGINEERING
INDIAN INSTITUTE OF TECHNOLOGY KANPUR
FEBRUARY, 1977

2 MAY 1978

TO

THE MEMORY OF MY

FATHER, SRI SARJU CHOUDHARY

and

BROTHER, SRI RATNESHWAR CHOUDHARY

CERTIFICATE

Certified that the work,"Hydrocracking of Assam Crude Residue for the Production of Kerosene and Diesel Oils", has been carried out under our supervision and that the work has not been submitted elsewhere for a degree.

February 17, 1977

(A.K.Singhal)
Assistant Professor
of Chemical Engineering

(D.N.Saraf)
Associate Professor of
Chemical Engineering

CHE-1977-D-CHO-HYD

ACKNOWLEDGEMENTS

It is with great pleasure and deep gratitude that the author acknowledges the help and guidance of Professors D.N. Saraf and A.K. Singhal of Chemical Engineering Departmen the supervisors for present investigation. Their clear, deep insight to the many problems encountered during the period of this research has been a constant source of inspiration, stimulation and enlightenment.

The author is thankful to Professor D.Devaprabhakara Department of Chemistry for providing High Pressure Parr Autoclave, and Professor K.V.G.K. Gokhale, Department of Civil Engineering for assisting in DTA measurements.

The assistance provided by Dr. L.M. Pandey, Defence Research Laboratory (Materials), Kanpur for DTA and TG analyse of the catalyst samples, F.C.I., Sindri for determination of physical properties of the catalysts and I.I.P., Dehradun for characterization of feed-stock is gratefully acknowledged

The author expresses his appreciation for his colleagues, Messrs Govind Ram for x-ray, P.S. Murli, R.K. Gupta, B.S.R. Murthy, Vinay Kumar, R.K. Sharma, P.K. Bajpai and many others who helped in many ways.

The cooperation rendered by the staff of the Chemical Engineering Workshop, the services of Glass Blowing Shop and Central Workshop are gratefully acknowledged. Mr. J.S. Virdi was particularly helpful in fabrication jobs.

and the author is thankful to him.

Thanks are also due to Mr. B.S. Pandey for his excellent typing, and Mr. D.S. Panesar for preparing the drawings.

Author

CONTENTS

List of Tables ... viii

List of Figures ... ix

Synopsis ... xi

CHAPTER

1 INTRODUCTION ... 1

1.1 Selection of Feed-Stock 5

1.2 Selection of Catalyst 5

1.3 Objective and Scope of the Present Investigation ... 6

2 LITERATURE REVIEW ...

2.1 Hydrocracking Process ... 8

2.1.1 Processes ... 8

2.1.2 Catalysts ... 12

2.1.3 Reactions ... 25

3 EXPERIMENTAL METHODS

3.1 Materials Used ... 34

3.2 Process Description ... 40

3.2.1 Experimental Set-up 40

3.2.2 Procedure ... 42

3.3 Analytical Methods ... 44

3.3.1 Distillation ... 44

3.3.2 Hydrocarbon Type by Fluorescent Indicator Adsorption 44

4 CATALYST CHARACTERIZATION

4.1 Literature Review ... 47

4.1.1 Zeolite Activity Improvement Methods 47

4.1.2 Ion-Exchange ... 49

4.2 Method of Preparation ... 52

4.3 Methods of Characterization 54

4.3.1 Chemical Composition 54

4.3.2 X-ray Powder Analysis 58
4.3.3 Thermogravimetric and Differential Thermal Analysis 60
4.3.4 Surface Area, Pore Volume and Pore Size Distribution 61

4.4 Characterization Results 62
4.4.1 Chemical Composition 62
4.4.1.1 Ion Exchange 62
4.4.1.2 Chemical Composition 66
4.4.2 X-ray Diffraction Patterns 66
4.4.3 Differential Thermal Analysis and Thermogravimetric Results 69
4.4.4 Surface Area, Pore Volume and Pore Size Distribution 78

5 RESULTS AND DISCUSSION

5.1 Lanthanum Exchanged Zeolite X Catalysts 80
5.1.1 Effect of Reaction Temperature 82
5.1.2 Effect of Hydrogen Charging Pressure 87
5.1.3 Effect of Charge to Catalyst Weight Ratio ... 90
5.1.4 Effect of Reaction Time 92
5.1.5 Effect of Degree of Exchange 94

5.2 Nickel Exchanged Zeolite X Catalyst 98
5.2.1 Effect of Reaction Temperature 98
5.2.2 Effect of Hydrogen Charging Pressure 103
5.2.3 Effect of Reaction Time 105
5.3 Conventional Silica-Alumina Catalyst 105
5.4 Effect of Particle Size of LaX Catalyst 107
5.5 Lanthanum Exchanged Zeolite Y Catalyst 109
5.6 Effect of Temperature Variation During Reaction Time ... 113

6 CONCLUSIONS AND RECOMMENDATIONS

6.1 Conclusions ... 117
6.2 Recommendations ... 118

BIBLIOGRAPHY ... 121

APPENDIX

A X-RAY POWDER DIFFRACTION DATA FOR DIFFERENT ZEOLITE CATALYSTS ... 130

B EXPERIMENTAL RESULTS ... 141

LIST OF TABLES

TABLE		Page
1.1	Pattern of Petroleum Products' Production	2
3.1	Physico-Chemical Characteristics of the Feed-Stock ...	35
3.2	Properties of Zeolites	36
3.3	Physico-Chemical Analyses of Fluid Cracking Catalysts ...	37
3.4	Chemical Properties of Nickel Nitrate	39
4.1	Chemical Composition of Zeolite Catalysts	57
4.2	Lanthanum Ion-Exchange Results	63
4.3	Unit Cell Parameters of Zeolite Catalysts	67
4.4	Physical Properties of Catalysts	79
5.1	Range of Variables Covered	81
A.1	X-Ray Data for NaX-100 ...	130
A.2	Reported Data for NaX-100	132
A.3	X-Ray Data for LaX-58 ...	133
A.4	X-Ray Data for LaX-79 ...	135
A.5	X-Ray Data for LaX-96 ...	137
A.6	X-Ray Data for NiX-80 ...	139
B.1	Operating Conditions ...	141
B.2	Product Characteristics...	147

LIST OF FIGURES

FIGURE		Page
3.1	Experimental Set-up ...	41
4.1	Sodium Calibration Curve ...	55
4.2	Thermogravimetric Curves for NaX-100, LaX-58, LaX-81 and LaX-96 Catalysts	70
4.3	Thermogravimetric Curves for LaX-79, LaX-81, NiX-80 and Silica-Alumina Catalysts	71
4.4	Differential Thermogravimetric Curves for NaX-100, LaX-58, LaX-81, and LaX-96 Catalysts	72
4.5	Differential Thermogravimetric Curves for LaX-79, LaX-81, NiX-80 and Silica-Alumina Catalysts ...	73
4.6	Variation of the Number of Water Molecules with the Degree of Exchange	74
4.7	Trace of DTA Thermograms for LaX-58, LaX-79, LaX-96 and LaY-86 Catalysts	75
5.1	Effect of Temperature on Product Distribution for LaX-79 ...	83
5.2	Effect of Temperature on Product Distribution for LaX-96 ...	84
5.3	Batch Pressure Variation with Reaction Time for LaX-96 ...	88
5.4	Effect of Hydrogen Charging Pressure on Product Distribution for LaX-96	89
5.5	Effect of Charge to Catalyst Weight Ratio on Product Distribution ...	91
5.6	Effect of Reaction Time on Product Distribution for LaX-96 ...	93
5.7	A Comparison of the Performance of LaX Catalysts Having Different Degree of Exchange ...	95

Figure		Page
5.8	Effect of Temperature on Product Distribution for NiX-80 ...	99
5.9	A Comparison between LaX, NiX and Silica-Alumina Catalysts ...	101
5.10	Effect of Hydrogen Charging Pressure on Product Distribution for NiX-80	104
5.11	Effect of Reaction Time on Product Distribution for NiX-80 ...	106
5.12	Effect of Temperature on Product Distribution for -20 +35 Mesh LaX-96*	108
5.13	Effect of Reaction Time on Product Distribution for -20 +35 Mesh Lax-96*	110
5.14	Effect of Temperature on Product Distribution for -20 +35 Mesh LaY-86*	111
5.15	Effect of Hydrogen Charging Pressure on Product Distribution for -20 +35 Mesh LaY-86* ...	112
5.16	Effect of Reaction Time on Product Distribution for -20 +35 Mesh LaY-86*	113
5.17	Variation in Temperature with Reaction Time for -20 +35 Mesh LaX-96* During a Run ...	115
5.18	Variation in Pressure with Reaction Time for -20 +35 Mesh LaX-96* during a Run	116
5.19	Variation in Temperature with Reaction Time for -20 +35 Mesh LaY-86* During a Run ...	117

HYDROCRACKING OF ASSAM CRUDE RESIDUE FOR THE PRODUCTION OF KEROSENE AND DIESEL OILS

A Thesis Submitted
In Partial Fulfilment of the Requirements
For the Degree of

DOCTOR OF PHILOSOPHY

by

NITYANAND CHOUDHARY

to the
DEPARTMENT OF CHEMICAL ENGINEERING
Indian Institute of Technology, Kanpur

February 1977

SYNOPSIS

Hydrocracking of Assam crude residue obtained from Gauhati Refinery was investigated in a rocking type batch reactor. The study was aimed to develop a suitable catalyst and choose the optimum operating conditions which would result in the maximum yield of kerosene-diesel fractions (boiling in the range 140 to 340^{o}C). Zeolite based catalysts were preferred because of their supercracking activity as compared to the conventional silica-alumina catalysts. Zeolite type X(NaX) was used in the form of 1/16 inch pellets. Sodium cation in parent NaX was substituted with a rare earth element, La^{+++}, or a transition metal, Ni^{++} to various degrees of exchange to increase hydrogenating activity of the zeolite catalyst. The incorporation of these active metal ions into the lattice of the zeolite was found to enhance the cracking activity also.

The bifunctional catalysts used in this investigation were characterized by X-ray diffraction, flame photometry, pore size distribution, surface area, pore volume, differential thermal analysis and thermogravimetric tests. Reproducible results were obtained with these catalysts when activated by heating above 400°C followed by outgassing for about an hour. This ensured that the catalyst was uniformly activated prior to its use.

The effect of process variables including temperature, hydrogen charging pressure, charge to catalyst ratio, reaction time, the degree of ion-exchange and the nature of the cation in the catalyst, on the conversion of residuum and the distribution of the products was examined. The conversion which represents the overall cracking activity of the catalyst is defined as the weight per cent of residuum converted to liquid products having a maximum boiling point as the reaction temperature. The range of variables covered in this study are as follows:

1. Reaction temperature, °C	330-470
2. Hydrogen charging pressure, psi	400-1300
3. Charge to catalyst ratio	13-40
4. Reaction time, min.	15-270
5. Catalysts: (a) Lanthanum exchanged zeolites X and Y	
(b) Nickel exchanged zeolite X	
(c) Conventional silica-alumina	

6. Degree of exchange, per cent

(a) Lanthanum cation	
zeolite X	58,79,81,96
zeolite Y	86
(b) Nickel cation	
zeolite X	80

All the parameters studied influenced the conversion and the yield of the products. However, the influence of temperature was found to be most significant. The yield of a product is defined as volume per cent of liquid hydrocarbon boiling in a specified range. With LaX catalyst, the total conversion to liquid products and the yield of kerosene-diesel fraction increased with increasing temperature; attained a maximum around 400°C and then decreased with further rise in temperature. Reaction temperature below 350°C gave little conversion. In the pressure range studied, the conversion and the yield of kerosene-diesel fraction increased with increasing hydrogen pressure. The conversion decreased linearly with increasing charge to catalyst ratio. The reaction time for maximum conversion was found to be a function of operating conditions, the degree of ion-exchange and the nature of cation in the catalyst. The conversion was found to increase with increasing degree of exchange of Na^{+} with La^{3+}. This behaviour of the catalyst has been explained using the concept of cation distribution in the zeolite structure and the dependence of the cracking activity on the nature, number and strength of

acid sites in the catalyst. A more acidic catalyst gave higher conversion and better yield of middle distillates.

With nickel exchanged catalyst (NiX), a linear increase in the conversion and decrease in the yield of kerosene-diesel fraction were observed with temperature rise in the range of 370-455°C. The effect of hydrogen charging pressure on the conversion and the yield of kerosene-diesel fraction was analogous to that obtained with LaX catalyst. The use of NiX catalyst did not improve either the conversion, or the yield of the desired product or its quality. This has been attributed to partial loss of crystal structure in nickel exchanged NaX zeolites.

The degree of saturation of kerosene defined as volume per cent of saturated hydrocarbons, as measured by Fluorescent Indicator Adsorption Test (ASTM D-1319/66) was usually high. The quality of kerosene obtained in runs having high conversion was invariably high. The degree of saturation as high as 80 per cent was obtained under certain conditions of operation.

The catalysts studied had very high activity and the distribution of the products obtained was also favourable for middle distillate production. Same catalyst was used in several repetitive runs without any loss of activity. It is expected that these catalysts would succeed in withstanding more severe conditions in actual plant trials. The data obtained in this study are likely to be of great use in the rational design of industrial reactors.

CHAPTER 1

INTRODUCTION

The pattern of consumption of various petroleum products in India is quite different from that of Western countries. Whereas, there is a maximum demand for gasoline in the U.S., its demand in India is very limited because of very few cars on the roads. What we need most are diesel-kerosene fractions. Public transport: buses, trucks, diesel-loco-engines; diesel pump sets etc. all need diesel fuel. The development of diesel car will further enhance the importance of this fuel [8]. The only source of illumination in most of our villages is still kerosene lamps. City dwellers to a great extent, rely on kerosene fuel for cooking. Superior kerosene is used as jet fuel. It is, therefore, necessary that our refineries, unlike their Western counterparts, try to maximize the production of kerosene-diesel fractions. Table 1.1, which contains the relative amounts of various products that are processed, indicates that gasoline is the largest volume product in the U.S.A., while distillate and residual fuels predominate in the rest of the world [30]. Above 50 per cent middle distillate requirement is a typical characteristic of Indian need [5] and is in far excess of that of the other regions which range between 25-35 per cent only.

TABLE 1.1: PATTERN OF PETROLEUM PRODUCTS' PRODUCTION [5,30]

Refining yield of products, per cent	U.S.A.	Central and Western Europe	Middle East	Far East	India
Light distillate	50	14	12	14	17
Middle distillates	30	33	31	25	53
Fuel Oils, Lube Oils, etc.	6	33	46	40	24
Others	14	20	11	21	6

In 1975, India imported nearly 14 million tons of crude oil and produced another 8 million tons. The total kerosene and diesel oils consumed were 5 and 6 million tons, respectively. Another 6 million tons of fuel oil was used. At the present rate of growth, by 1980 we need a total of more than 45 million tons of petroleum products of which kerosene would be 9, diesel 13 and fuel oil 10 million tons. If this 10 million tons of fuel oil is hydrocracked, it can give about 7 to 8 million tons of kerosene-diesel fractions. This means an import of more than 10 million tons per year of crude oil can be curtailed which tantamounts to a saving of several billions of rupees in foreign exchange.

It is true that a given crude oil has a fixed composition and when distilled can yield only fixed amounts of gasoline,

kerosene, diesel or any other product. However, since the demand for various products is not in proportion to their presence in the crude oil, technology has been developed to convert the surplus fractions into deficit ones to meet the demand of the society. This is the reason why catalytic processes are finding ever increasing use in petroleum refining. It is possible to polymerize lighter gases to yield heavier products and crack heavy cuts into lighter ones, either thermally or catalytically.

As discussed earlier, in this country, the need for gasoline is meagre which could be further curtailed by suitable governmental measures. But we cannot possibly limit the use of middle distillates which means that we should look for processes which can convert the heavy fractions like furnace oil, distillation residue etc. into kerosene-diesel fractions. One known method to do this is hydrocracking. Lighter gases like propane, butane, etc. can also be polymerized to yield kerosene-diesel fractions but these can be better utilized as petrochemical feed stock.

Substantial quantity of fuel oil and other residues are available from the refining processes. If these are reserved only for high priority uses like upgrading the same by hydrocracking to render additional middle distillates, our requirement of the refining capacity can be reduced. The

Fuel Policy Committee of India for the Fifth Five Year Plan has gone carefully into this aspect of better utilization of our resources and has made a strong case for setting up hydrocracking facilities [70]. The committee found that by establishing adequate hydrocracking facilities, 'it is possible to meet most of the requirements of middle distillates, motor gasoline and naphtha which are not easily substitutable by other fuels and we would be dependent on imports mainly for fuel oil which can be substituted by coal or coal gas'.

Hydrocracking has been used by Western oil refiners to get more gasoline, but it is equally possible to use this technique to increase the production of kerosene or diesel. Since this problem is special to India, detailed technology is not generally available from advanced countries unlike most of the other technologies. Besides, the implication of heavy economic impact of importing technology, the high import cost of patent-clear equipment, over-pricing of materials, regulation of current operation, installation and adjustment of the purchased machinery, and the need for 'appropriate technology' clearly indicate the choice for indigenous technology [7]. Fortunately, for the present problem, enough information is already existing which could be harnessed to generate the missing links and perfect the technology indigenously. This will

have to be done if India wants to survive this oil crisis because it cannot simply afford to import all the oil it needs at the existing price level. Further, in view of the global trend to augment crude supply from coal crude, hydrocracking processes assume special significance, since coal crude being highly aromatic with a high nitrogen content is unsuitable for other catalytic processes [6].

1.1 Selection of Feed-Stock:

In light of the above discussion, the choice of topped residue as hydrocracking feed-stock becomes obvious. Availability, low-cost and better utilization of residuum were the major factors considered in choosing residuum as the feed-stock for this study. Assam crude is a mixed base crude and has a high paraffin-wax content. As such its residue has very limited utilization and is used mainly as industrial fuel. Vacuum distillation of this residue for the production of lubricating oils would fail to yield good lubricants because of high wax content. However, this residue makes an excellent hydrocracking feed-stock for the production of middle distillates.

1.2 Selection of Catalyst:

The selection of the catalyst, examined in greater detail in Chapter 2, was made on the basis of known higher cracking activity, greater tolerance to nitrogen and sulfur

poisoning, and significant hydrogen shifting action of the catalyst. In respect of all these, zeolite catalysts are superior to conventional silica-alumina catalysts. Zeolite catalysts were, therefore, selected for the cracking of heavy residuum molecules. For the hydrogenation of unsaturated cracked hydrocarbon molecules, rare earth-and transition-metal cations were used. Ion-exchange was used to introduce the active hydrogenating metal cations like lanthanum and nickel. This ensured uniform and fine dispersion of the metal cations[91]. The choice of these cations was made on the basis that lanthanum exchanged zeolite catalysts possess strong cracking activity and high thermal stability [91, 92, 95, 123], while nickel ions exhibit strong hydrogenating-dehydrogenating activities. It was hoped that the performance of these two cations would throw light on the relative importance of these two activities of the catalyst in the hydrocracking of Assam crude residue.

1.3 Objective and Scope of the Present Investigation:

The aim of the present work was to develop a process for hydrocracking of Assam crude residue to maximize the production of kerosene-diesel fractions, boiling in the range of 140-340^{o}C. The development of a suitable catalyst that can effectively handle this typical residue becomes a prerequisite for this process study by

virtue of the key position that the catalyst occupies in this catalytic process. The hydrocracking catalysts, processes and the reactions have been reviewed in Chapter 2 of this dissertation. Chapter 3 deals with the experimental procedure and methods of analysis that were used to characterize the products. The preparation and characterization of the catalysts have been discussed in Chapter 4. The results of hydrocracking of Assam crude residue have been presented in Chapter 5. In the same chapter, the effects of various parameters like reaction temperature, hydrogen charging pressure, reaction time, charge to catalyst weight ratio, degree of ion exchange, and the nature of cations in the zeolite catalysts are discussed. A comparative study between the different catalysts used is also included.

=======

CHAPTER 2

LITERATURE REVIEW

2.1 Hydrocracking Processes:

During the past decade hydrocracking has taken shape into a major refining process. Ever since the announcement of the modern version of hydrocracking, the worldwide onstream capacity has increased steadily. At the beginning of the year 1973, the total hydroprocessing capacity of Western Europe was 4,631,000 barrels/day [42], while the total hydrocracking capacity of U.S.A. and Canada at the same time were 865,050 and 51,700 bbl/day, respectively [23]. Hydrocracking is extensively practised commercially in petroleum refining to produce high quality gasoline, jet fuel, low pour point diesel fuel, high quality lubricants and LPG. Limited use of hydrocracking to produce light paraffins and aromatics has also been reported [105, 113].

Hydrocracking is the most versatile of modern petroleum processes. Flexibility of operation in respect of both the feed stock and product have been achieved. This flexibility in operation is assigned to the development of specific families of the catalyst, the design of processing schemes, that allow these catalysts to function efficiently, and

the optimum refining relationships between hydrocracking and other refining processes. Whereas the commercial feedstocks range from naphtha to residue, there is wide choice for the end product of a hydrocracker. It is possible to produce high octane gasoline at one time and middle distillates at another time. If needed, the proportion of motor and jet fuel production can be varied to meet the variation in demand pattern.

Advances in hydrocracking processes have been reviewed from time to time [77, 105, 106, 111, 116]. Recently, Choudhary and Saraf [28] have extensively reviewed the hydrocracking processes. Molenda et al. [72] have described the significance of hydrocracking process in modern refining. Murphy et al. [77] have established the superiority of hydrocracking to fluid catalytic cracking and have discussed their relative effects on overall refining systems. Catalytic cracking works best on stocks that have high hydrogen content and are not too aromatic in nature. For highly aromatic stocks hydrocracking is much more effective [30]. Factors responsible for the recent increase in hydrocracking capacity, refining scheme incorporating various types of hydrocrackers and its future application under European conditions have been discussed by Winsor [125]. Scott and Patterson [105] have considered the commercial processes and their worldwide

applications. The hydrocracking of feed-stocks too contaminated to be catalytically cracked, integration of hydrocracking and other refining processes, and advances in residuum hydroprocessing have been discussed by these authors. Scott and Bridge [106] have described the state of hydrocracking technology and their catalytic requirements for a wide range of applications. The relation between the laboratory kinetic measurements and the actual performance in commercial units have also been discussed. Nelson [81, 82] has written a series of review articles dealing with various aspects of hydrocracking such as the prediction of quality of the product in terms of octane rating and characterization factor, the distribution of products and yields, and design factors including hydrogen requirement, amount of heat liberated in the exothermic reaction, etc. Stormont [113] has reported the initial commercial success of many processes that followed the modern version of hydrocracking.

The effect of pressure on hydrocracking over a D-6 type chromia-alumina catalyst was investigated by Abidova et al. [1]. The hydrocracking activity of the catalyst was evaluated in terms of the extent of conversion into diesel fractions. Between 380 and 400°C an increase in pressure gave a higher yield of diesel fraction while at higher temperature (450-475°C) an optimum pressure was reached and further increase in pressure decreased the yield of diesel

fraction. Filimonov et al. [44] have experimentally shown that an increase in temperature results in a gradual decrease in the reactions of aromatic and benzonaphthene hydrocarbons, and increase in the reactions of paraffin and naphthene hydrocarbons. Chernozhukov et al. [27] have reported the effect of operating conditions on the hydrocarbon composition of aviation fuel obtained from hydrocracking of petroleum residues. Manshilin et al. [69] and Musial and Rutkowski [78] have reported the effect of hydrodynamic conditions on hydrocracking product pattern. It is possible to predict the conversion of petroleum vacuum residue from the hydrodynamic conditions prevailing during hydrocracking [77]. Chernakova et al. [26] developed empirical equations to calculate the thermal effects of the product depending on the degree of conversion of the raw material and hydrogen consumption. Mathematical descriptions of the products of hydrocracking and use of microkinetic equations to determine the yield have been reported [86, 126, 127]. Stangeland and Kittrell [112] studied the selectivity of jet fuel. Qader et al. [95] have indicated that by operating the process at relatively higher severity of hydrocracking, gasoline production can be maximized. The cracking severities depend on the quality of feed-stock, reaction temperature and pressure, and activity and selectivity of the catalyst.

Seven hydrocracking processes offered for licensing have been enlisted with details of flow diagrams, commercial applications, operating capacities and conditions by Scott and Patterson [105]. The major distinctive features of these processes are (i) the type of catalyst, (ii) the contacting pattern of the reactants with the catalyst and (iii) the number of reaction stages employed in a particular process.

2.2 Hydrocracking Catalysts:

The history of hydrocracking catalyst, that follows, clearly shows the dependence of hydrocracking process on the development of catalyst of requisite activity and selectivity. The beginning of hydrocracking may be pinned down to the year 1927 when the first Bergius plant for hydrogenating brown coal at Leuna, Germany, was put on stream. This led to supplementary processes for hydrocracking of vaporizable middle oils from coaltar in Germany, England, and a little later, in the United States of America [57].

Pelleted tungsten sulfide was the most successful early hydrocracking catalyst. Operating conditions were 250 atm. pressure and 400°C temperature with hydrogen circulation rate of 1700-2700 volumes(STP) per volume of oil fed. Multiple beds of catalyst with cold hydrogen injection was used to control temperature of this exothermic

reaction. The catalyst had very good tolerance for high concentrations of impurities like nitrogen, sulfur and oxygen compounds, but it failed miserably to produce high octane gasoline even from highly aromatic feeds because of extensive hydrogenation. By 1935, tungsten sulfide on montmorillonite catalyst was developed which succeeded partly to avoid this oversaturation of gasoline but its nitrogen tolerance was poor and hence coaltar oil had to be pretreated before hydrocracking. In 1937, ESSO used tungsten sulfide on HF-treated montmorillonite catalyst to obtain aviation gasoline.

The European coaltar hydrogenerator used two-stage operation to obtain good octane gasoline. Unsupported tungsten sulfide was used in the first stage for the removal of nitrogen and its compounds by suitably adjusting the operating parameters so that aromatic saturation was minimized. Tungsten sulfide supported on HF-treated montmorillonite was used in second or hydrocracking stage. Iron on HF-treated montmorillonite catalyst developed by ICI, England, in 1939 proved to be a good catalyst for their second stage hydrocracker.

Nickel on HF-treated montmorillonite catalyst developed by ESSO could produce better antiknock quality gasoline but fairly rapid sulfur poisoning of nickel was its serious

limitation. Two-stage hydrocracking, using tungsten sulfide on HF-treated montmorillonite in the first stage to remove sulfur, and nickel on HF-treated montmorillonite for the second stage was commercially practised during 1940-44 to produce gasoline [116]. Further development resulted in nickel on silica-alumina catalyst which was more nitrogen resistant. At a given conversion level of the feed, this catalyst preserved still more aromatics in the gasoline fraction to further enhance its octane rating [16, 17, 52, 106, 116].

The hydrocracking catalyst is a dual functional one. The two functions it serves are (i) cracking of high molecular weight hydrocarbons, and (ii) hydrogenation of the unsaturates either formed during the cracking step or otherwise present in the feed-stock. A typical cracking catalyst is silica-alumina and a base or noble metal serves as a hydrogenating catalyst. In a way, hydrogenation helps cracking. The metal hydrogenation sites keep the acid sites of cracking catalyst clean and active by hydrogenating the coke precursors before coke accumulates and deactivates the catalyst. This cooperation between these two activities depends on the amount of metal deposited on the acidic support, increasing with increase in metal loading until a critical limit is reached [98].

Cracking Catalysts:

Almost all commercial cracking catalysts are combinations of silica-alumina. They are (i) the acid-treated aluminosilicates, (ii) the amorphous synthetic silica-alumina combinations, and (iii) the crystalline synthetic silica-alumina combinations (known as Molecular Sieve Zeolites). All of these have high temperature acid sites and their catalytic activity is attributed to their acidity[13,51,57,75,80,83,123].

In case of amorphous silica-alumina, both Lewis and Bronsted acid sites operate, their ratio being dependent on the degree of catalyst hydration [85, 116]. The composition of silica-alumina determines the number of active sites and their specific activity. Generally speaking, the catalysts having highest number of acid sites are the most active ones [119, 120].

Recently, interest in molecular sieve zeolites has been greatly intensified. Zeolite X, Y and mordenite have been used. The increased commercial application of zeolite as compared to the conventional silica-alumina catalyst could be ascribed to its following properties [58, 83, 92, 123].

- Well defined crystalline structure.
- Very large surface area which is highly polar in nature
- Reproducibility of the various forms.

-Well defined pore structure which produces ion sieving effect.

-Excellent thermal stability and ease of manipulation.

-Exchangeable cations facilitating the introduction of catalytically active metals in the highest degree of dispersion.

-More than 10,000 times active than conventional silica-alumina cracking catalyst.

-Higher reactivity for hydrogen transfer between hydrocarbon species leading to higher production of paraffin and aromatic hydrocarbons.

Because of these properties, zeolite catalysts have been reported to give

-25 per cent higher gasoline yield.

-Greater conversion resulting in less recycle.

-Higher throughput rates.

-Lower C_1 to C_3 hydrocarbons and coke production.

-2 to 3 times higher amounts of iso-structural products.

The superiority of zeolite catalyst is well borne out by Fedorov [43] who claimed that if the silica-alumina catalyst presently being employed in 40 catalytic cracking units of USSR be replaced by zeolites, there would be a net saving of 40 million rubles by way of additional production of gasoline.

The source of cracking activity of zeolites and nature of active sites is not resolved completely, however, it is believed that in most of the cases Bronsted acid sites catalyze carbonium type of reactions [99, 120]. These acid sites can be introduced by exchange with a multivalent cation or by introduction of exchangeable ions which can be thermally decomposed to protons. In the understanding of active sites, significant contributions have been made by infrared and thermal analytical studies [4, 45, 116, 117-120].

Zeolite crystal lattice has both small and big holes which are interconnected and regularly spaced. 5 Å and 8Å are two sizes of 'windows' with 'rooms' of 13 Å. Orderly silica-alumina tetrahedra make the walls of cages and super-cages. Whereas amorphous silica-alumina may be viewed as a graft polymer of alumina on a backbone of silica having no ion-exchange capacity, zeolites may be regarded as a copolymer of alumina and silica. Regularly spaced alumina and silica form the backbone of the copolymer. Each atom of aluminum and silicon is joined by a single valence bond to each of four oxygen atoms. There is a negative charge in the copolymer for every aluminum atom because aluminum has a positive valence of 3. These negatively charged sites are balanced usually by sodium metal cations in the synthesized forms of X and Y zeolites which can subsequently be exchanged with multivalent cations if needed. Rare earth ions when introduced in the

zeolite by ion exchange, induce high polarity and strong acidity to its surface required in carbonium ion type reactions, enhance thermal stability of zeolites, and, catalyze coke burning reactions [50, 83, 124]. Maher et al. [68] have discussed the relationship between activity and different rare earth cations. Correlation of existing literature data for the dependence of the catalytic activity of X and Y zeolites on structure, chemical composition, and temperature has been proposed by Jerocki et al. [59].

There is distribution of strength over the zeolite catalyst surface, some being stronger than others. Strongest sites are not the most favourable ones because the slow rate of desorption can retard the catalytic reaction and may give rise to side reactions. The most favourable sites are the weak ones which are sufficiently strong to accomplish the desired chemical conversion. Amorphous silica-alumina has a higher percentage of the total acidity in its strong acid range. The presence of relatively large amount of very strong acid sites cause (i) overcracking to C_3 to C_4 hydrocarbons at the expense of C_5^+ gasoline and (ii) formation of more condensed ring aromatics that cannot desorb from the catalyst surface resulting in increased coke production [83]. The olefin intermediates which give rise to coke formation on silica-alumina catalysts are 'preserved' by fast hydrogen transfer and are converted to paraffins, naphthenes and

single ring aromatics with zeolite catalyst. The acidity of zeolite catalyst depends on the nature of cation, the extent of ion exchange, the Si/Al ratio of the lattice, the heat treatment of the zeolite and the amount of 'bound' water. Consequently, total acidity may vary from essentially zero to 14 or more times that of silica-alumina. Increased cracking selectivity results from the disappearance of the strong acid sites which is obtained by giving a hydrothermal treatment to the zeolite by subjecting it to a steam pressure of 1 atm for 17 hours at high temperature [75]. Weisz has related the selectivity of zeolite catalysts to the size of cages and supercages present in zeolite lattice [123]. This higher activity of zeolite catalyst may be used for increased liquid yields, greater selectivity for midbarrel product or in reduced catalyst inventory [117].

Some of the major points of agreement between amorphous and crystalline silica-alumina catalysts are that (i) both owe their activity to their acidity, (ii) show promotional effect of olefins; and (iii) act through carbonium ion mechanisms. The main points of dissimilarity between the two catalysts lie in the difference in ion-exchange activity and in acidity distribution as mentioned earlier. Zeolite, being a superior cracking catalyst, permits a decrease in the reaction temperature for the same level of conversion of the feed-stock. Both activity and selectivity advantages

have been reported [83]. These advantages may partly be assigned to 50 to 70 times greater number of 'active sites' in the zeolites as compared to silica-alumina catalysts [76].

Hydrogenating Catalysts:

The major hydrogenating catalysts are platinum, nickel, palladium, molybdenum, cobalt etc. These may be modified by promotion with another metal or by some pretreatment such as sulfiding [1, 39]. Rare earth metals on zeolite support also accomplish hydrogenation reactions. Voorhies and Smith [116] have shown that nickel can produce higher octane gasoline than either tungsten or iron. Higher boiling product formation with a decreased amount of light hydrocarbons is favoured if nickel is replaced by a noble metal. Coonradt and Garwood [31] reported better selectivity to a liquid product with a platinum catalyst than with rhodium, ruthenium, osmium, or iridium. A better service with platinum catalyst is ensured if the feed is pretreated to remove sulfur and nitrogen.

The relationship between the hydrogenating activity of supported Pt-catalyst and catalyst acidity was studied by Larson et al. [66]. They observed that with increasing platinum content, selective adsorption of platinum by acid sites causes a reduction in catalyst activity. With a strong hydrogenating catalyst such as platinum on silica-alumina, extensive direct

isomerization resulting in high ratio of intermediate to low molecular weight paraffin was obtained. This indicates less secondary splitting which can be used advantageously to minimize the ratio of gas to liquid products and the hydrogen consumption [31].

Nitrogen compounds depress the hydrocracking activity of both the noble metal and base metal catalysts but noble metals can better preserve their activity and selectivity, if operated at high temperature to maintain the same level of conversion. Base metal catalysts suffer much deterioration with time. Nitrogen causes irreversible loss of activity for platinum or nickel sulfide on silica-alumina, however, it is possible to regain the activity of platinum catalyst on certain other supports [16, 17, 116].

Cracking and hydrogenating activities of the hydrocracking catalyst depend on their respective composition in the overall catalyst, operating conditions, and composition of charge stock. In any specific application, the best choice of hydrocracking catalyst demands a peculiar balance between the cracking and hydrogenating-dehydrogenating components of the catalyst. A catalyst has to be 'tailored' depending on the feed-stock to be handled and the end product desired. As an example, the catalyst characteristics for the production of middle distillates from gas oil are moderate

acidity and strong hydrogenating activity with moderate to high porosity while that for the production of gasoline from the same feed-stock become strong acidity and moderate hydrogenating activity with low to moderate porosity. The selection of a proper catalyst, that would meet effectively the requirements for a given feed-stock may be made by considering the following factors:

Nature of the Feed-Stock:

The basic constituents in a feed affect the acidic component of hydrocracking catalyst. If the feed-stock is known to contain basic compounds of nitrogen, a zeolite catalyst should be preferred to conventional silica-alumina catalyst since the former is more nitrogen resistant. Also in the presence of nitrogen, catalyst temperature must be raised to sustain conversion. Pretreatment of the feed-stock to remove nitrogen compounds is commercially practised.

Acidity of the Catalyst:

Acidity of the catalyst determines the operating temperature of the process but it has limited effect on the type of reactions. By changing the relative hydrogenation activity of the catalyst, acidity can have major effects on the products [31]. Scott and Bridge [106] have compared the effect of catalyst acid strength for Arabian straight

run vacuum gas-oil hydrocracked over a moderately acidic catalyst in a two-stage plant. In a single stage operation, mild acidity catalyst can effectively produce low-freezing point jet fuel and, if operated at higher cut points, low pour point diesel from high pour-point feed-stock. If strongly acidic catalyst is employed in the second-stage of a two-stage plant, product distribution similar to single stage plant is obtained. However, with lower consumption of hydrogen, superior products like jet fuel having lower smoke-point and naphtha of higher octane number are obtained.

Mass Transfer Limitation:

Porosity is an important parameter of the catalyst. If the intrinsic reaction rate is high as compared with the diffusive influx of the reactants within the catalyst particle to the 'active sites', the catalyst is not being used effectively. In such a case the reaction rate and selectivity both become functions of particle size [106]. This change in selectivity has been used to advantage by Chen and Weisz [24]. When processing heavy feeds, catalysts having high pore volume and pore diameter should be used. Increasing catalyst porosity or decreasing the catalyst particle size can alleviate the problem of pore diffusion limitation. However, the use of small particles of catalyst has the attendant problem of pressure over-shooting unless an ebulated bed type reactor is

used. In case of residual hydrocracking, 1/32 in. catalyst particles have given a better performance than 1/16 in. catalyst particles [47]. Empirical correlation to evaluate liquid phase effective diffusivity in fine pores, where the pore size is of the order of the size of the adsorbed molecule, is available [101].

Catalyst Poisons:

Inorganic salts, water, metals, and organic compounds of sulfur, nitrogen, or oxygen present in crude oil act as poisons for the hydrocracking catalyst. Each of these foreign constituents affect the catalyst in a different way. Sulfur compounds inhibit the hydrogenation activity while nitrogen compounds inhibit the cracking activity of the catalyst. The metal contaminants in petroleum are deposited on the catalyst. These deposits, when in the active state promote various dehydrogenating reactions and increase coke production tendency. Oxygen compounds do not pose any serious problem to the refiner although it is reported to cause permanent catalyst deactivation under certain conditions [79].

Type of Hydrocracking:

Depending upon the feed stock used, two types of hydrocracking are being practised industrially. If the feed-stock is a heavy distillate obtained from straight run refining or

cracking operation, it is called distillate hydrocracking. Residual hydrocracking is the name given to the process if the feed-stock happens to be the residue of straight-run refining. These residuals are usually lower in API gravity, and higher in carbon residues and carbon to hydrogen ratios as compared to the distillates. Galbreath and van Driesen [47] have shown that residual hydrocracking is clearly a different process than the distillate hydrocracking. In the residuum hydrocracking, a different type of catalyst is used at relatively higher temperature. This difference in the catalyst is caused by metals and asphaltenes present in the feed-stock. Thc thermal mode of cracking prevails in case of residuum hydrocracking whereas it is catalytic when distillate feed is used.

The selection of the catalyst is, thus, governed chiefly by the type of feed used, the type of product desired, operating conditions of the process, contacting pattern of the reactants, and the type of hydrocracker.

2.3 Hydrocracking Reactions:

Reactions occurring during hydrocracking have been studied extensively. The chemistry of hydrocracking is essentially the carbonium ion chemistry of catalytic cracking coupled with that of hydrogenation. Almost all the initial reactions of catalytic cracking take place but the presence

of hydrogen inhibits some of the secondary reactions. This is why similar products are formed in these two refining processes. Like catalytic cracking, very small amounts of C_1 and C_2 fractions are produced in hydrocracking but unlike in the former process, only saturated products are formed in the latter. This difference is due to the presence of hydrogen and that of the hydrogenating component in the catalyst. C_4 fractions rich in isobutane are formed because of the great tendency to form tert-butylcarbonium ion [114]. The catalyst remains active for a relatively longer period as the olefins and other catalyst deactivating materials are rapidly hydrogenated. So coke formation is suppressed and regeneration of catalyst is minimized. In hydrocracking process, even at lower temperature rapid cracking was accomplished because of hydrogenation and relatively high working pressure [114].

Reaction temperature and the relationship of acidity to the hydrogenating-dehydrogenating activity are chiefly responsible to decide the product distribution. Although the hydrocarbon processes are complex in nature yet the overall reaction kinetics can be expressed in simple terms. The mechanism proposed by Qader and Hill [96] to explain product distribution in hydrocracking of gas-oil with nickel (6 per cent) tungsten (19 per cent) sulfide on silica-alumina

catalyst envisaged a combination of simultaneous and consecutive bond-breaking reactions followed by isomerization and hydrogenation. They reported that hydrocracking, hydrodesulfurization, and hydrodenitrogenation reactions were first order with the cracking reactions on the acidic sites of the catalyst being rate controlling. In another study of hydrocracking of polycyclic aromatics, Qader [94] observed the sequential occurrence of hydrogenation, isomerization, and cracking reactions. Hydrocracking reactions followed first-order kinetics and the kinetic data were compatible with the dual site mechanism of Langmuir-Hinshel-wood.

Langlois and Sullivan [64] have reviewed the chemistry of hydrocracking. When the reactants are paraffins, cycloparaffins or alkylaromatics, the products obtained from both hydrocracking and catalytic cracking are similar, but when the reactants are polycyclic aromatics, wide difference in the product from these two refining processes are obtained. This comprehensive review should be referred to for further details. The following paragraphs deal with the classwise salient features of hydrocracking reactions.

Reactions of Paraffins:

The paraffin hydrocracking reactions can be related to the mechanisms proposed for catalytic cracking of paraffins. It starts with the formation of olefins at metallic centers

and the formation of carbonium ions from these olefins at acidic centers. Olefins, being the precursors of carbonium ions, can hydrocrack more readily than paraffins. This explains why a small amount of olefins when added to the feedstock increases the cracking rate of some of the hydrocarbons [89, 103,104, 114, 124]. Carbon-carbon bond cleavage hydrogen transfer, hydrogenation-dehydrogenation, isomerization, disproportionation, and cyclization are the reactions that can take place with varying degrees of importance. Extensive catalytic cracking followed by hydrogenation to form isoparaffins appears to be the primary reaction of the paraffins [64, 116].

Generally, isoparaffins react in the same way as n-paraffins with the only difference in rate which is much more rapid in case of isoparaffins. The effluent stream from hydrocracking of n-paraffins contains only a small quantity of isoparaffins with the same molecular weight as the reactant. This appears reasonable as any isoparaffin formed may readily undergo subsequent reaction.

A characteristic of this family of hydrocarbons is that with increase in molecular weight of the paraffin reactants there is a corresponding increase in the hydrocracking rate. Flinn et al. [46] have reported 95 per cent conversion of n-hexadecane at conditions of operation at which only 53 per cent n-octane was converted. Another distinctive

feature of paraffin hydrocracking is the presence of very high ratios of branched-to-straight chain paraffins in the product stream. This iso-to-normal ratio of product paraffins is substantially greater than the thermodynamic equilibrium [16,17,39]. Hydroisomerization, disproportionation and other side reactions contribute to this high ratio by converting n-paraffins formed during cracking step into branched products. This high ratio of iso-to-normal paraffins has also been related to the catalyst used. A lower iso-to-normal ratio may be expected if a strong hydrogenating catalyst is used [51, 54].

The preferential adsorption of other families of hydrocarbons on the catalytic sites may inhibit the reactions of n-paraffins in a mixture [12,116]. Use of shape selective zeolite catalyst for the selective hydrocracking of normal paraffins in the presence of branched paraffins have been reported [24, 123]. With these catalysts only those molecules of reactant and product which conform to a particular size and shape can arrive at or depart from 'active sites'. Thus the geometrical configuration of the catalyst plays a limiting role.

Reaction of Cycloparaffins:

A typical cracking reaction known as paring reaction takes place to selectively remove the methyl groups from the

cycloparaffin rings without severely affecting the ring itself [12, 39, 64]. This cracking reaction gives one acyclic and one cyclic product containing four carbons less than the parent cycloparaffin molecule. The main acyclic product is isobutane. There is a high ratio of iso-to-normal paraffin present in the product which is far greater than the thermodynamic ratio. A steep fall in both selectivity and cracking rate is reported if C_{10} cycloparaffin reactants are replaced by C_9 cycloparaffins. Over 100 times greater rate of cracking is reported for C_{10} cycloparaffins than that for C_9 cycloparaffins [39].

The composition of the product from 1, 2-diethyl, n-butyl-, sec-butyl-, isobutyl-, and tert-butyl-cyclohexanes were found to be similar irrespective of the structure of the reactant. Decrease in temperature results in higher selectivity for the paring reaction of polymethylcyclohexanes. Cracking of cycloparaffins is preceded by extensive isomerization.

The hydrocracking of a multiple ring naphthene such as decaline is more rapid than that of the corresponding n-paraffins. Higher iso-to-normal ratios of light paraffins and large yields of single-ring naphthenes are found. At conventional process conditions, single-ring naphthenes are resistant to further hydrocracking. These naphthenes contain a higher ratio of methyl cyclopentane to cyclohexane far in

excess of thermodynamic equilibria. The C_5 rings are desirable to produce good octane gasoline directly but are not amenable to subsequent reforming needed for further octane improvement [12].

Reactions of Alkylaromatics:

In the hydrocracking of alkylaromatics, isomerization, dealkylation, paring, and cyclization are the reactions that take place. Normally the effluent stream from the hydrocracking of aromatics shows wider variation and greater dependence on the structure of the reactants than that from the hydrocracking of cycloparaffins. Hydrocracking of alkylbenzenes containing side chains of 3 to 5 carbon atoms gives relatively simple products. The larger the alkyl side chains, the more complex the product distribution and a new reaction known as cyclization is observed [39,46]. The presence of a considerable quantity of C_9-C_{12} polycyclic hydrocarbons especially tetralins and indanes in the product is intriguing since the formation of these bicyclic species is thermodynamically unfavourable. However, only little tetralin is formed in the hydrocracking of n-butylbenzene. A suitable mechanism to explain the formation of tetralin and indane type hydrocarbons is available [15].

Hydrocracking of polyalkylbenzenes gives light isoparaffins and C_{10} and C_{11} methylbenzenes as the principal product. Ring cleavage is almost absent and hydrogenolysis to

form methane is at a minimum. Mechanisms to explain the product distribution are available [64].

Aromatic products from hydrocracking, generally form mixtures approximating thermodynamic equilibrium. This is because these can undergo secondary reactions including alkyl transfer and migration of alkyl groups around the rings. The products from cracking of cycloparaffins, on the contrary, are generally far from thermodynamic equilibrium distribution as they do not react extensively. While the ring is conserved with both the families of hydrocarbons, only alkylaromatics undergo cyclization. If nonacidic catalyst is used, successive removal of methyl groups from the side chains is the principal reaction and the isomerization reaction is at a minimum [15]. Commercial usages of both catalytic and thermal hydrogenolysis to produce gasoline and naphthalene have been reported [122].

Reactions of Polycyclic Aromatics:

The principal reaction in the hydrocracking of polycyclic aromatics is reported to proceed through a multiple mechanism of hydrogenation, isomerization, and cracking [94] and also via a different route of hydrogenation and isomerization coupled with alkylation, paring and cracking reactions [46, 64].

Unlike other classes of hydrocarbons, the product obtained from hydrocracking and catalytic cracking of

polycyclic aromatics are distinctly different. Catalytic cracking of phenanthrene over acidic catalyst produced only coke and small amount of gases while the hydrocracking of the same gave low molecular weight cyclic products [64]. This difference in the product is caused by the hydrogenating component of the catalyst and excess of hydrogen present in hydrocracking. After hydrogenation, these aromatics which are refractory stocks in catalytic cracking are converted into readily cracked naphthenes. This hydrogenation is effective only at higher severity of the reaction [2,40,116].

Di- and polycyclic aromatics joined by only one bond rather than by two common carbon atoms are readily cleaved by hydrogen and converted into single ring aromatics [54]. To produce high octane gasoline, the partial hydrogenation of polycyclic aromatics, followed by extensive splitting of the saturated rings to form monocyclic aromatics, is a significant reaction. These monocyclic aromatics enhance the octane rating of gasoline. A strong hydrogenating catalyst would undesirably hydrogenate them and thereby necessitate the use of subsequent reforming for octane improvement [116]. Activity and selectivity of different catalyst systems were investigated by Qader et al.[96]. Cobalt sulfide on silica (low)-alumina was found to be most active catalyst in the hydrocracking of polycyclic aromatic hydrocarbons.

CHAPTER 3

EXPERIMENTAL METHODS

3.1 Material Used:

Assam Crude Residue: Reduced crude obtained from Gauhati Refinery processing crude oil from Assam oil fields was used as the feed-stock in this study. Its physico-chemical characteristics are given in Table 3.1. Besides these, the qualitative tests in accordance with the procedure of Vogel [115a] indicated the presence of nickel, iron and cobalt metal ions. However, the quantitative analyses for these metals could not be carried out because of the partial solvency of the feed-stock.

Zeolite Molecular Sieves: Synthetic molecular sieves type X (NaX) and Y(NaY) supplied by Linde Division of Union Carbide, U.S.A. were used to prepare hydrocracking catalysts. The physico-chemical properties of these molecular sieves are recorded in Table 3.2.

Silica-Alumina: This conventional fluid cracking catalyst was obtained from Hindustan Petroleum Corporation Limited, Bombay. The relevant data for this low alumina catalyst are given in Table 3.3.

TABLE 3.1: THE PHYSICO-CHEMICAL CHARACTERISTICS OF THE FEED-STOCK

Density at 15°C, kg/lit	0.9408
Relative density at 60/60 °F	0.9414
API gravity at 60°F	18.8
Molecular weight (calculated)	408

ASTM D-1160 Distillation Data (under reduced pressure)

IBP at 760 mm Hg	281°C
5 per cent volume recovered at 760 mm Hg	323°C
10 per cent volume recovered at 760 mm Hg	351°C
20 per cent volume recovered at 760 mm Hg	392°C
30 per cent volume recovered at 760 mm Hg	420°C
40 per cent volume recovered at 760 mm Hg	440°C
50 per cent volume recovered at 760 mm Hg	461°C
60 per cent volume recovered at 760 mm Hg	475°C
70 per cent volume recovered at 760 mm Hg	497°C
80 per cent volume recovered at 760 mm Hg	540°C

Elementary Composition

Carbon, per cent (weight)	86.32
Hydrogen, per cent (weight)	10.31
Nitrogen, per cent (weight)	2.50
Others, per cent (")	0.87
Total	100.00

TABLE 3.2: PROPERTIES OF ZEOLITES

Type X (SK-20)[α]	
Chemical formula	$Na_{86}[(AlO_2)_{86}(SiO_2)_{106}]\cdot X\ H_2O$
Properties of Pellets	
Nominal pore diameter	10 Å
Extrudate dimension	1/16 inch
Apparent bulk density	38 lbs/cuft
Crush strength	12 lbs
Equilibrium H_2O capacity	28.5 per cent weight
Heat of adsorption (max)	1800 Btu/lb H_2O
Molecules adsorbed	<10Å effective dia.
Molecules excluded	>10Å effective dia. e.g. $(C_4F_9)_3N$
Type Y (SK-40)[αα]	
Typical chemical composition (anhydrous basis of zeolite portion)	
SiO_2	63.5 wt. per cent
Al_2O_3	23.5 wt. per cent
Na_2O	13.0 wt. per cent
Cl^-	> 0.05 wt. per cent
F^-	> 0.05 wt. per cent

[α] Bulletin F-23, Union Carbide Corporation, Molecular Sieve Department, 270 Park Ave., New York, N.Y. 10017, U.S.A.

[αα] Bulletin F-10A, Union Carbide Corporation, Molecular Sieve Department, 270 Park Ave., New York, N.Y. 10017, U.S.A.

TABLE 3.3: THE PHYSICO-CHEMICAL ANALYSES OF FLUID CRACKING CATALYST

Chemical (weight per cent dry basis)	
Alumina	13.00
Sodium oxide (Na_2O)	0.02
Iron (Fe)	0.04
Sulphate (SO_4)	0.60
Loss on ignition at 800°C	53.00
Physical (after thermal deactivation, 3 hours at 538°C)	
Pore volume (cc/gm)	0.73
Average bulk density (gm/cc)	0.48
Particle Size Distribution (micromesh sieve: wt. per cent)	
0 - 20 microns	2
0 - 40 microns	18
0 - 80 microns	80
0 - 105 microns	93
0 - 150 microns	99
Average particle size, microns	60

Rare Earth Salts: Rare Earths Division of the Rare Earths India, Ltd., Alwaye, Kerala supplied lanthanum chloride having a purity of atleast 99.9 per cent. It was used for exchanging Na^+ ions of zeolites of type X and Y. The stock solution for the interference study of lanthanum on sodium in the flame photometric determination of the concentration of Na^+ ion in the mixture was also made from this salt.

Nickel Nitrate: BDH, A Division of Glaxo Laboratories (India) Ltd. provided analytical grade nickel nitrate which was employed in the preparation of nickel exchanged zeolite catalyst. A typical analysis of the assay as provided by the supplier is presented in Table 3.4.

Silica Gel: Silica gel grade 923, 100-200 mesh supplied by Koch Light Laboratories Ltd., Colnbrook, Bucks, England and chromatographic grade silica gel obtained from Acme Synthetic Chemicals (India) were used in the Fluorescent Indicator Adsorption tests.

FIA Dye: The dye consisted of a mixture of Sudan III together with an olefin and aromatic indicating dye dissolved in xylene. It was obtained from Defence Material and Stores, Research and Development Establishment, Kanpur.

TABLE 3.4: CHEMICAL PROPERTIES OF NICKEL NITRATE

Chemical formula	$Ni(NO_3)\cdot 6H_2O$
Minimum assay (ex.N)	98 per cent
Maximum limit of impurities	
Chloride (Cl)	0.005 per cent
Sulphate (SO_4)	0.05 per cent
Cobalt (Co)	0.1 per cent
Iron (Fe)	0.02 per cent

3.2 Process Description:

3.2.1 Experimental Set-up:

A one-liter high pressure Autoclave (Series 4000, Parr Instrument Co., Molline, U.S.A.) was used in the present work. The experimental set-up consisted mainly of an assembly of a) reactor housed in an annular furnace fitted with a rocking mechanism, b) residue charging gun, c) hydrogen charging assembly, d) condensing coil immersed in a water-bath, and e) oil-gas separator. A schematic diagram of the set-up is illustrated in Figure 3.1. Mixing of the reactants and the catalyst in the autoclave was achieved by rocking the heater and autoclave assembly by 30° up and down about the horizontal axis of rotation. Heating of the autoclave and its contents was accomplished by an electrical heater. The temperature was manually controlled by regulating the voltage input to the heater through an autotransformer. The semi solid feed-stock choked the charging-port of the autoclave and, thereby, necessitated the use of relatively larger port. The head of the autoclave was suitably modified to meet this requirement. A residue charging gun was devised to feed the charge-stock into the autoclave. A sectional view of the gun is included in Figure 3.1. It worked on the principle of positive displacement.

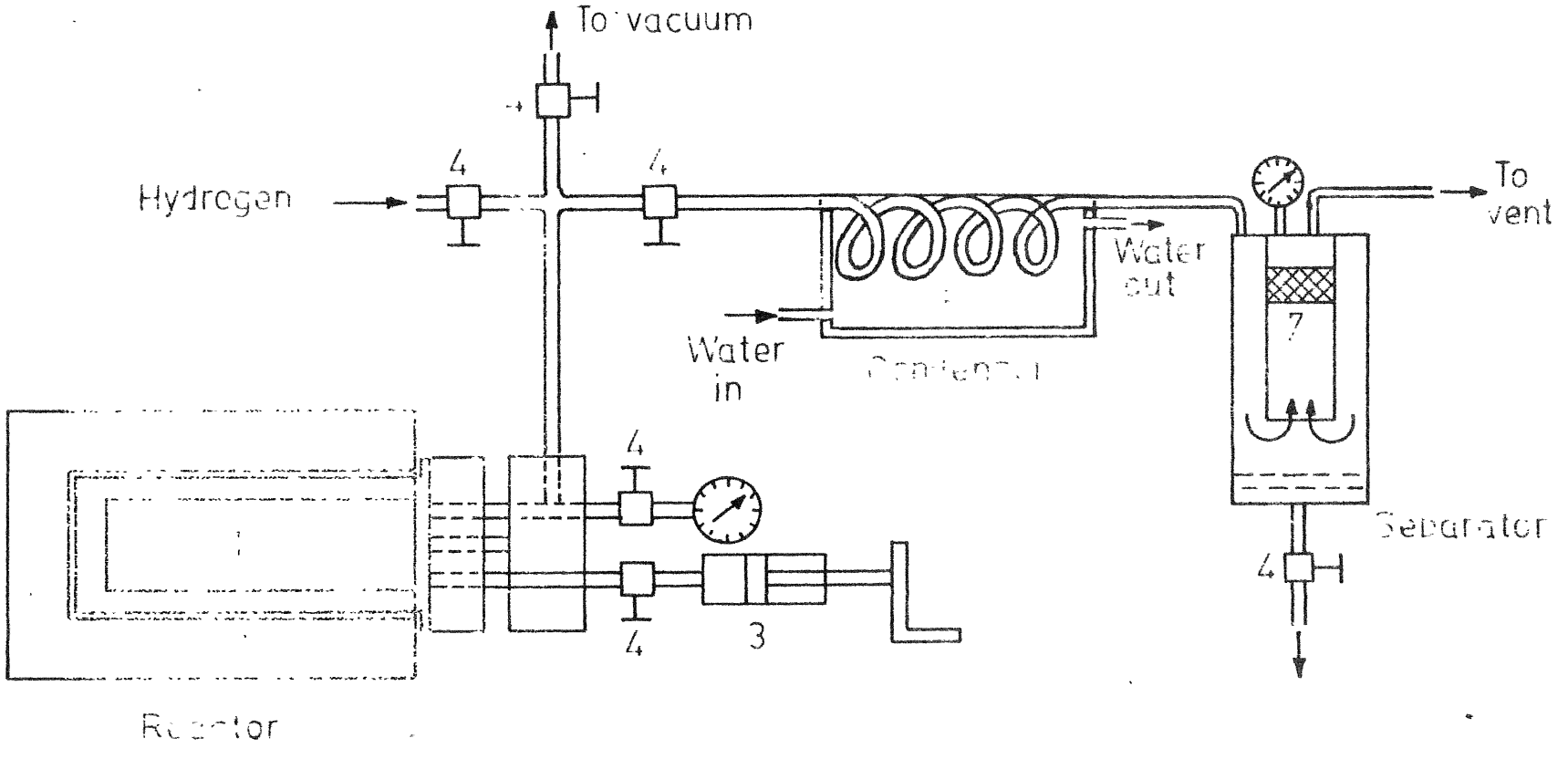

1. Reactor
2. Heater
3. Charging gun
4. Valves
5. Condenser
6. Separator
7. Wire mesh plug

Fig. 3.1 - Schematic diagram.

At the completion of a reaction period, since the reaction products existed in gaseous form, the exit stream had to be cooled down to ambient temperature in order to condense the gaseous hydrocarbons. To achieve this, a coil of about 30 ft length of high pressure stainless-tubing immersed in a water-bath was used. The phase separation of the reaction mixture was obtained in an oil-gas separator, the detail of construction of which is shown in Figure 3.1. The separator is a stainless steel cylindrical chamber in which the product stream enters at the top and impinges on the inner wall tangentially. The inner concentric cylindrical tube is provided with a wire-mesh screen plug to retain any entrained liquid droplets escaping with the gas being vented into the atmosphere through it. A bottom opening in the separator was used to withdraw the liquid product collected in the lower part of the separator.

3.2.2 Procedure:

Before starting each experimental run, the autoclave was cleaned properly, rinsed with acetone and dried. A weighed amount of the catalyst (10 grams) was taken in the autoclave which was then sealed and pressure tested with hydrogen upto about 2000 psi. Hydrogen was subsequently released. The autoclave was inserted into its heater housing and heated at least upto 400^{o}C. At that temperature the autoclave was

evacuated to 10^{-2} torr for an hour to complete the activation of the catalyst prior to its use. Generally the activation of the catalyst was done at a temperature 20-30°C higher than the operating temperature. For the set of runs using the same batch of catalyst in subsequent runs, unconverted residue of the earlier run was converted into product and consequently a pressure rise was observed. When this pressure was released through a condenser and separator assembly, liquid product was obtained, the amount of which was a function of the conversion in the previous run.

A known quantity of residuum (130 grams) was then vacuum sucked into the autoclave from the charging gun. Because of the semi-solid nature of the feed-stock, it was necessary to use a charging gun through which the residuum could be pushed into the reactor by means of a piston. Hydrogen was charged upto a particular batch pressure and rocking was started. This marked the initiation of reaction. At the end of the reaction time, the withdrawal of the contents of the autoclave was started in a regulated way, slowly releasing the pressure, after connecting the autoclave to the oil gas separator through the condenser. The dry gas was vented into the atmosphere. The liquid product that collected in the lower part of the separator was withdrawn through a bottom opening and analyzed for its quality.

At the end of an experimental run, the autoclave was taken out of its furnace housing when the same had attained ambient temperature for cleaning and preparing for the next run. The hard crust of carbon and coke deposited in the autoclave was removed by cutting out chips with a sharp edged chisel and/or drilling the same with the help of a hand-tool, somewhat analogous to the drill-bit used in oil-well drilling.

3.3 Analytical Methods:

3.3.1 Distillation:

The liquid product withdrawn from the separator was distilled in a batch distillation column to obtain different fractions. The distillation assembly was provided with a flask of shortneck-height, a condenser and a thermowell. The shortneck-height flask was used to minimize the condensation of the distillate in the reboiler. The thermowell facilitated accurate temperature measurements. No glass joints were used to avoid any leakage. Records of initial boiling temperature and condensate volume collected at a temperature of the boiling liquid were made. The different cuts separated from the liquid products were naphtha (upto 140°C), Kerosene (140-280°C), diesel (280-340°C), and finally gas oil (above 340°C).

3.3.2 Type of Hydrocarbons:

The type of hydrocarbons in the product was determined

by using Fluorscent Indicator Adsorption (FIA) test. In accordance with the ASTM D1319-66 test procedure, a glass adsorption column was made. The analyser section of the FIA column was made of 1.5 mm glass capillary whose outer diameter was 7.5 mm. The charging and separating sections of the column were made to the specification of this test. The two sections of the column were held together by mounting a piece of polyethylene tubing over the junction of these two pieces. The internal surface of this column was made moisture free and dry before filling and packing the same with activated silica-gel. Use of electrical vibrator for 4 to 5 minutes ensured proper packing of silica gel in the column. About 0.75 ml of kerosene (140-280°C) added with a very small quantity of the dye, enough to cover the tip of a needle, was injected into the charging section of the column. Amyl alcohol was added to desorb the sample and nitrogen was passed at 10-15 psig to force it down the column. The hydrocarbons are separated according to their adsorption affinities into aromatics, olefins, and saturates. The fluoroscent dyes are also separated selectively with the hydrocarbon types and make the boundaries of the aromatic, olefin, and saturates zones visible under ultraviolet light. The volume percentage of each hydrocarbon types was calculated from the length of each zone in the column.

About 12 initial FIA experiments were conducted to standardize the column and to find a substitute to silica gel grade 923 because of its nonavailability. Samples of known composition were used. Acme's chromatographic grade silica gel, 100-200 mesh size, was found to give reproducible results with about 5 per cent higher value of saturates.

CHAPTER 4

CATALYST CHARACTERIZATION

4.1 Literature Review:

4.1.1 Zeolite Activity Improvement Methods:

The various ways of improving the catalytic activity of zeolite catalyst are (1) active metal loading using impregnation or ion-exchange, (2) decationation, (3) dealumination, and (4) addition of proton source. Whereas metal loading and decationation have been extensively used, dealumination is relatively recent in origin. A few limited studies on the addition of proton source have been reported.

The cations, whose function is to neutralize one excess charge per aluminum ion in the crystal lattice of zeolite, attach themselves loosely to the oxygen atoms at the corners of the tetrahedra. These cations can be replaced by simple ion-exchange with mono-, di-, and tri-valent ions which may be used in the form of a simple or complex salt. These catalytically active metals can also be deposited on the tiny crystals of zeolite in a supporting matrix. In contrast to the bulk adsorption or impregnation method, ion-exchange produces a uniform, extremely fine dispersion of these metals ions throughout the body of the catalyst which ensures the most efficient use of these metal catalysts [91].

Decationation is a special case of ion-exchange involving exchange of Na^+ cations with thermally decomposable ammonium ions and subsequent heating to liberate ammonia gas with the formation of a proton-containing intermediate. Shallow-bed calcination of ammonium zeolite permitting rapid diffusion of gaseous products from the sample produced hydrogen zeolite, while deep-bed calcination, impedding removal of gaseous products yielded ultrastable faujasite [60]. Both hydrogen form and ultrastable zeolites possess high catalytic activity. Whereas ultrastable zeolite has excellent thermal stability, hydrogen form is even less stable than the parent zeolite.

Dealumination, of late, has become a subject of study. Two major types of aluminum sites are recognized, about 30-35 per cent are weakly acidic while the rest are strongly acidic. The extraction of aluminum begins with the selective removal of aluminum atoms having the lowest acidities. The aluminum atoms associated with the strong acidity are removed only when those of the first type are exhausted. The vacated aluminum atom sites are occupied by silicon atoms. The removal of aluminum atom increases thermal stability and catalytic activity and changes acidity distribution. Total number of Bronsted sites does not change but their strength is increased [10, 11].

Besides these, strong acidity can be developed in alkalimetal zeolites by the addition of a proton source such as hydrochloric acid, carbon dioxide or propyl chloride [62, 65]. The improvement in acidity because of the presence of carbon dioxide is ascribed to the impurities in the zeolite in the form of Ca^{2+} ions, while the promoting of propyl chloride is complex and intriguing because of the suppression of the catalytic activity of the active catalysts like HX and CaX.

4.1.2 Ion Exchange:

Zeolite ion-exchange can be accomplished by slurrying it in a solution of the appropriate salt. The exchanged zeolite is filtered and washed free of soluble salts with distilled water. The use of distilled water prevents the formation of protonated form of zeolite. Repeated equilibration is needed to achieve higher degree of exchange. The degree of exchange that can be achieved depends on the following factors [20,109].

(i) Operating Temperature: Elevated temperature favours exchange.

(ii) Radii of the exchanging cations: For cations of same valence too large an ion cannot pass through six membered ring of the sodalite cage, and hence ionic selectivity decreases with increasing radius of the cation.

(iii) Valence of the incoming ions: More complete exchange can usually be accomplished with monovalent ions rather than with polyvalent ions.

(iv) Silica/alumina ratio of the zeolite: Higher degree of exchange can be obtained with lower silica/alumina ratio (but higher silica/alumina ratio zeolites possess higher stability and activity).

(v) Water molecules per cation: The more the number of water molecules for a cation in the zeolite the lower will be the degree of exchange obtained at ambient temperature. Since the hydrated cations are too big to enter the smaller cages, stripping of water molecules necessitates higher temperature exchange. This explains the dependence of maximum loading limit on temperature.

(vi) Solvent: Both the selectivity and the rate of exchange decrease with decreasing dielectric constant of the solvent, however, aqueous solutions have been used extensively.

(vii) Concentration of the cation species in the solution: zeolite preferentially selects the ions with highest charge at low total normality

and the ions with lowest charge at high normality.

The present state of understanding of the zeolite ion-exchange which was first reported by Way [121] as early as 1850 may be summarized as follows [9, 20, 109].

Ion-exchange in zeolites X and Y are distinguished by double sieving effects which are caused by the presence of two independent 3-dimensional networks of cavities. The network of sodalite and hexagonalprisms is dense and contains little water while the network of large cages is open and highly hydrated. The cation sites in the network of large cages prefer higher charged ions and among monovalent ions this preference depends on aluminum content of the zeolite. In zeolite X, the preference of higher charged ions decreases with increasing ion size, while in zeolite Y this thermodynamic preference decreases with increasing ionic hydration energy. But in the network of small cages of zeolites X and Y, ions with smallest radius and lowest charge are preferred. The polyvalent exchange for sodium ion takes place in two steps, one step being many orders of magnitude slower than the other. The slower step is associated with the exchange of those 16 Na^+ ions in a unit cell which are located in small cages. The beginning of the exchange from the smaller cages marks the end of the gradual increase in acidity as well as activity of the zeolite catalyst. Further exchange brings about a rapid

change in both the acidity and activity of the sample. The incoming ions may not occupy the same site as the outgoing ions did as evidenced in Sr^{2+}-Na^{+} and Cs^{+}-Na^{+} systems [109].

4.2 Catalyst Preparation:

Zeolite NaX, in the form of 1/16 inch pellets as supplied by Linde Division of Union Carbide Corporation, was used to prepare the hydrocracking catalyst. Sodium ions in the parent NaX were substituted with the desired cations through conventional ion-exchange method [32, 109]. The two cations that were deployed in this study were lanthanum (La^{3+}), and nickel (Ni^{2+}) ions.

Lanthanum exchanged zeolite X (LaX) was prepared by slurrying pellets of NaX in an aqueous solution of lanthanum chloride. Ion-exchange of Na^{+} with La^{+++} was allowed to take place at a constant temperature of 70°C while the contents were continuously shaken. The amount of salt solution used in each treatment of the zeolite was in large excess of that of the number of La^{3+} cations needed for complete exchange. Usually a four fold excess of lanthanum ions was employed. 12 gram of zeolite was equilibrated with 200 ml of one normal solution of the desired salt. After equilibration, the solid was filtered and washed free of soluble salt by adding enough distilled water. Low level of exchange, when required was obtained by allowing the zeolite to exchange

with a calculated amount of cations in the solution. Several equilibrations were needed to achieve higher degree of exchange. Intermediate heat-treatment of the partially exchanged zeolite sample before starting fresh equilibration was found to be particularly helpful in accelerating the residual ion-exchange. This is due to the redistribution of cations among different sites as a result of which residual sodium ions in inaccessible sites migrate into more accessible ones [37]. Heat treatment consisted of gradually heating the zeolite upto 300 - 350°C for about one hour. Similarly, LaY-86* and LaX-96* were prepared from -20 + 35 mesh sizes of these zeolites.

Nickel exchanged zeolite (NiX) was prepared by equilibrating NaX in aqueous solution of nickel nitrate essentially in the same way as followed in the preparation of LaX. Care was taken to avoid any pH increase and precipitation of basic nickel salt. Several subsequent fresh solutions were used to achieve a degree of exchange greater than 50 per cent. Filtered and washed zeolites after ion-exchange, were stored in a desiccator over saturated ammonium chloride solution. All the catalyst samples, as discussed in Section 3.2.2., were calcined in the autoclave just before using it in the reaction.

* The zeolite catalysts contain about 10 per cent sodium silicate as binder.

4.3 Characterization Methods:

4.3.1 Chemical Composition of Zeolite Catalysts:

The evaluation of the degree of exchange achieved was done from the determination of the concentration of sodium ions in the equilibrating solutions. The Systronic Flame Photometer Type 121 MK-1 was used to find the concentration of sodium ions in the filtrate. A sodium calibration curve is shown in Figure 4.1. Stock-solutions required in the calibration of the instrument were prepared in accordance with the procedure due to Dean [33].

Since the equilibrating solutions contained sodium and lanthanum ions in one system and sodium and nickel ions in the other, an attempt was made to check if the presence of these foreign ions affected the determination of sodium ions in any way. To evaluate the effect of the presence of lanthanum ions, five sets of experiments with six samples in each set, were conducted. Samples in each set had a fixed concentration of sodium ions but different samples contained different concentration of lanthanum ions which was varied between 0-80 milligram per liter. The deflection reading for each sample in all sets was found to be independent of the concentration of lanthanum ion. The flame photometric deflections corresponding to solutions with or without lanthanum ion were identically the same as long as the sodium ion

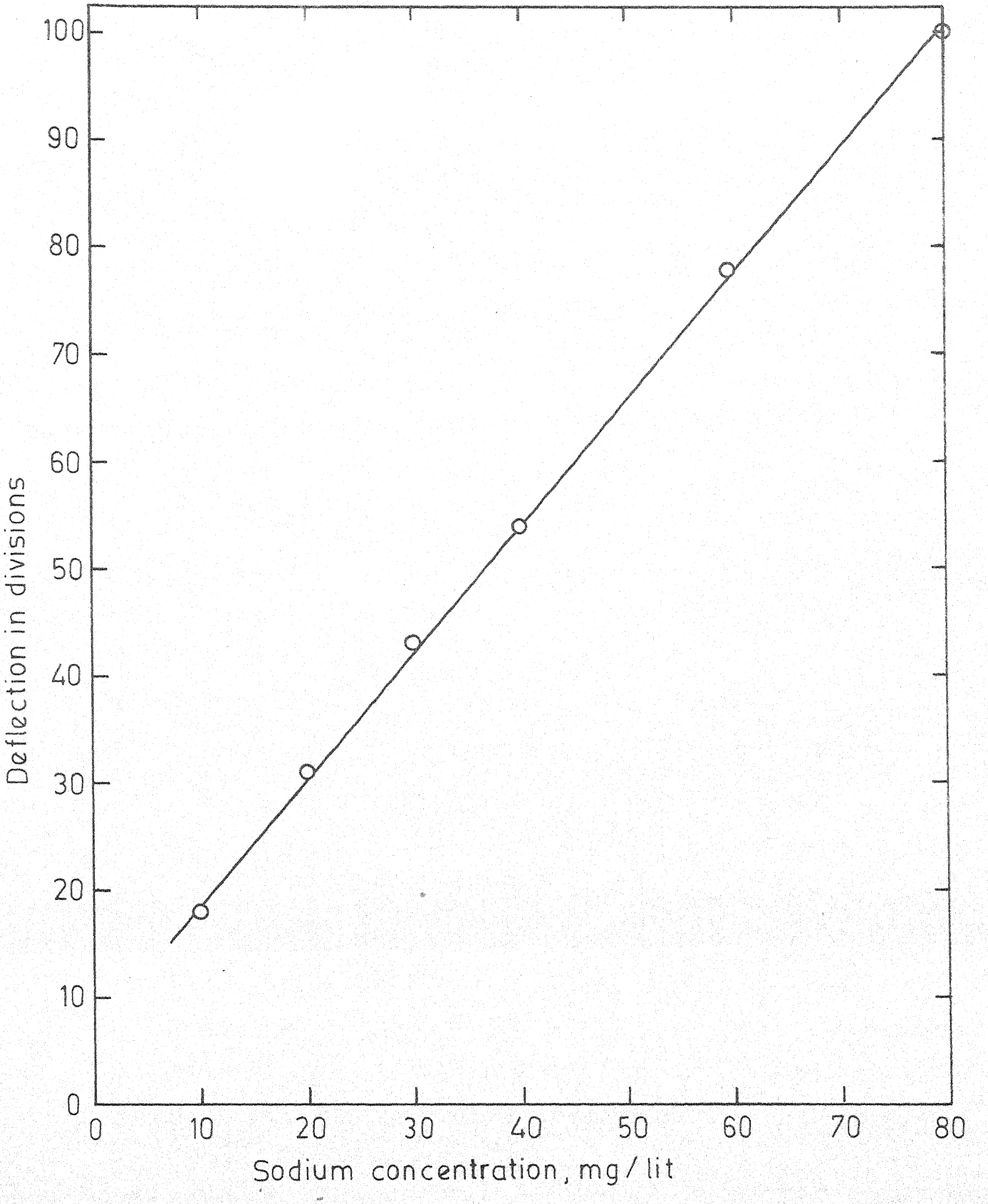

Fig. 4.1 -Sodium calibration curve.

concentration was same. Similar set of experiments in presence of nickel ions revealed no interference of nickel with sodium ions. Hence the calibration chart for pure sodium (Figure 4.1) was used to convert the flame photometric deflection into equivalent concentration of sodium in milligram per liter for both systems.

The concentration of sodium ions in the filtrate was used to calculate the degree of ion-exchange in the catalyst[3] as follows. The total number of sodium milliequivalents was first computed. This amount of sodium was replaced by equivalent amount of lanthanum (or nickel) in the zeolite. Knowing the original milliequivalent of sodium in the parent zeolite (Table 4.1), Na^+ remaining in the matrix was found. From these, the degrees of exchange of lanthanum and nickel cations were calculated as $[3La^{3+}/(3La^{3+}+Na^+)] \times 100$ and $[2Ni^{2+}/(2Ni^{2+}+Na^+)] \times 100$, respectively. Here La^{3+}, Ni^{2+} and Na^+ are the milliequivalents of cations present in the zeolite. The numeral appearing after the zeolite index indicates the extent of sodium ion replacement. For example, LaX-96 denotes a X type zeolite sample in which 96 per cent of the exchangeable sodium ions have been substituted by lanthanum. The unit cell composition of these exchanged zeolites are given in Table 4.1.

4.3.2 X-Ray Powder Analysis:

X-ray analysis is used to uniquely characterize a catalyst. It can help determine the physical form of the catalyst in regard to its crystallinity. It is also used to locate the position of different cations in the crystal lattice. In zeolite catalysts x-ray analysis reveals the loss in crystal structure caused during ion exchange or calcination etc. Since the position of the cations in the zeolite lattice greatly influences the catalytic activity, the determination of exact location of these cations is of utmost interest. However, in the present study the use of this technique was limited to ascertaining the crystallinity and determining various characteristic parameters of the unit cell.

When a monochromatic beam of x-rays strikes an atom in a crystal, tightly bound electrons are set into oscillation and radiate x-rays of same wave length as that of the incident beam. This is called diffraction. Every crystalline substance scatters the x-rays in a particular diffraction pattern, depending on its atomic and molecular structure. The shape and size of a unit cell fix the angular position of peaks and relative intensities of these peaks are governed by the number and positions of atoms within the unit cell. The relationship between the wavelength of the x-ray beam, λ ,

the angle of diffraction, θ, and the interplanar distance, d, is governed by the Bragg equation [19].

$$2d \sin\theta = n\lambda \qquad (4.1)$$

where, n, the order of diffraction, is usually first order. For a cubic crystal, as in case of zeolite types X and Y, lattice parameter (a), Miller indices (h k l) and interplanar distance (d) bear a relationship,

$$a = d\sqrt{h^2 + k^2 + l^2} \qquad (4.2)$$

For the purpose of indexing the powder pattern, analytical method subject to the constraint was used.

$$\frac{\sin^2\theta}{h^2+k^2+l^2} = \frac{\sin^2\theta}{S} = \frac{\lambda^2}{4a^2} = \text{constant} \qquad (4.3)$$

Since the sum, $S = h^2+k^2+l^2$ is always an integer, and $\lambda^2/4a^2$ is a constant for a given pattern, indexing of a cubic system can be done by finding a set of integers S which will give a constant quotient when the observed $\sin^2\theta$ is divided by them, one by one.

The x-ray measurements of hydrated zeolite samples were made on a General Electric Company's apparatus equipped with XRD-6 x-ray generator, SPG-4 Detector system, SPG-2 Diffractometer and xenon filled counter. Copper (K_α) target (λ =1.5418) was used. Beta-radiations were cut off by the use of a filter. Samples were scanned in the range 5 to 80°

at a rate 2^{o}/min with a chart speed of 1" /min. The peak positions were checked by collecting point-to-point intensity data with a receiving slit of 0.1^{o} at 30 KVA and 20 mA. Permoquartz standard sample was used for zero-error adjustment.

4.3.3 Differential Thermal Analysis and Thermogravimetry:

Differential thermal analysis data in conjunction with thermogravimetric results make it possible to determine dehydration temperatures and to ascertain the sequence of dehydration steps. The use of these techniques and a host of others is rapidly increasing, not only to obtain the dehydration characteristics of zeolite catalysts but also to characterize, identify, and distinguish one form from the other [32, 63, 100]. Differential thermal analysis (DTA) establishes the temperatures at which thermal reactions take place within a sample when it is heated continuously to an elevated temperature. It also determines the intensity and general character of such reactions which are characteristic of the material under test. The amount of divergence from the base line reflects the difference in temperature between the sample and a reference which is usually α-Al_2O_3, a thermally inert material. When a thermal reaction takes place in the sample, the temperature of the sample becomes greater or less than that of the reference, depending on whether the reaction is exothermic or endothermic.

These exo- and endo-thermic peaks are attributed to the vaporization of water and/or crystallographic phase transition that takes place within the specimen. The low temperature endo-therm, in DTA curves of zeolites type X and Y, represents the loss of water. The high temperature exotherm is due to the loss of structure of the zeolite. In the present study DTA measurements were made on a Dupont 900 apparatus equipped with a high temperature cell and using calibrated Platinum/ Platinum - 13 per cent Rhodium thermocouples under atmospheric conditions.

Thermogravimetry (TG) measures the loss in weight of the specimen under investigation as the temperature is increased at a predetermined rate. Dynamic method of determining the dehydration curve with a heating rate of $10^{o}C$ per minute and simultaneously recording the weight of the sample was followed. A Cahn thermogravimetric apparatus with a programmed temperature rise was used under atmospheric conditions. Differential thermogravimetry determined from thermogravimetric data, follows the rate of weight change of the sample as a function of temperature, $dW/dt = f(T)$.

4.3.4 Surface Area, Pore Volume and Pore Size Distribution:

The importance of the surface area of the catalyst in heterogeneous catalysis can hardly be over-emphasized. It has a profound effect on the amount of gas adsorbed and on its

catalytic activity. The dependence of the rate of adsorption and catalytic reactions on surface makes it imperative to have a reliable measure of surface area. The knowledge of surface area makes it possible to compare the performance of different catalysts, that have different surface area, by using the intrinsic activity per unit surface. Since major catalytic surface is in the interior of the solid particle, void volume, sizes of the pores and their distribution are of paramount significance. The size of the pore, if of molecular dimension, can significantly control the access of the reactants to and from the active centers situated in the interior portion of the catalyst.

Surface area of all the catalyst samples were calculated from nitrogen adsorption isotherms using BET apparatus. Pore volume and pore size distribution were measured by a mercury porosimeter, Winslow Porosimeter for 15,000 psi range.

4.4 Characterization Results:

4.4.1 Chemical Composition:

4.4.1.1 Ion Exchange: The results of the preparation of lanthanum exchanged zeolite, type X, are summarized in Table 4.2. A close scrutiny of these data leads to the following conclusions:

1. The degree of exchange obtained in the first equilibration is a function of the number of days for which

TABLE 4.2: LANTHANUM ION - EXCHANGE RESULTS

Catalyst	Equilibrium Batch	No. of days of equilibration	Conc. of Na^+ in the filtrate of the batch	Isotherm Coordinates		Degree of Exchange
				S_{La}	Z_{La}	
LaX[a]-80	NIK-111	2	640	0.840	0.569	49.4
	NIK-112	2	252	0.945	0.765	19.5
	NIK-113	2	66	0.986	0.815	4.8
	NIK-114	4	44	0.990	0.849	3.5
	NIK-115	2	36	0.992	0.877	2.8
LaX-79	NIK-121	3	800	0.826	0.620	61.5
	NIK-122	5	120	0.974	0.714	8.5
	NIK-123	4	20	0.996	0.728	1.5
	NIK-124	2	92[b]	0.970	0.799	6.5
	NIK-125	2	13	0.997	0.809	1.0
LaX-96	NIK-131	5	900	-	-	69.5
	NIK-132	4	204	-	-	15.5
	NIK-133	25	144[b]	-	-	11.0
LaX-81	NIK-161	17[c]	1050	-	-	81.0

[a] 12 gram of zeolite type X was equilibrated with 200 ml of normal solution.

[b] The zeolite sample was given heat treatment before starting this batch equilibration

[c] The equilibration was performed at ambient temperature with occassional heating upto 70°C for one hour.

it is allowed to continue. The first equilibration proceeding for two-, three-, and five- days produced 50 (NIK-111), 62(NIK-121), and 70(NIK-131) per cent replacement of sodium ions, respectively. It may be nevertheless, noted that the increment in the degree of exchange decreases as the number of days in the first equilibration increases.

2. The contribution of the first equilibration towards the extent of exchange is quite substantial, while the share of the subsequent exchanges keep diminishing. This indicates that the substitution of sodium ions becomes increasingly difficult, as the concentration of the residual ions in the lattice of zeolite diminishes. This is in accord with the literature [9, 20, 36, 37, 63, 109]. The cations in the hexagonal prisms (SI sites) of zeolite X and Y are the most difficult ones to exchange. This is caused by the size of the apperture (2.4 Å) that connects the sodalite cage with supercage. With ionic radius of 1.15 Å, lathanum ion should be able to reach SI sites. Since its hydrated ion radius is 3.96 Å, the inability of La^{3+} ions, therefore, stems from its hydrated sheath. This accounts for the low level of exchange at room temperature since the stripping of water molecules is thermodynamically unfavourable under these conditions. To circumvent this limitation, usually high temperature exchange is done.

3. Intermediate heat-treatment of the partially exchanged zeolite sample before starting afresh equilibration is particularly helpful in accelerating the residual ion-exchange. The increased concentration of sodium ion in the filtrate of batches NIK-124 and NIK-133 demonstrate this phenomenon. This is due to redistribution of cations among different sites. On dehydration, exchanged cations that are located in the channels coordinated with water molecules may migrate to SI sites as a result of which residual sodium ions are displaced to accessible sites [14, 20, 37]. The maximum degree of exchange obtained at 70°C, which is 96 per cent in this study, is higher than the reported 92 per cent at 82°C [109]. This higher level of exchange even at lower temperature of operation may solely be attributed to the intermediate heat-treatment of the zeolite sample. Dyer and Molyneux [37] reported a similar increase on heat treatment.

4. The coordinates of Na^{+}-La^{3+} exchange isotherm included in Table 4.2 were calculated in accordance with the procedure of Sherry [109]. Z_{La} represents the equivalent fraction of La^{3+} ions in the zeolite phase, as defined by

$$Z_{La} = \frac{\text{Milliequivalents } La^{3+}/\text{gram zeolite}}{\text{Milliequivalents } (La^{3+}+Na^{+})/\text{gram zeolite}} \quad (4.4)$$

and S_{La} is the equivalent fraction of La^{3+} ions in the solution phase, defined as

$$S_{La} = \frac{\text{Normality of } La^{3+}}{\text{Total normality}} \qquad (4.5)$$

The values of these coordinates indicate a higher selectivity of lanthanum ion in the solution phase as compared to the zeolite phase. This is due to the use of concentrated solution in ion exchange. It has been shown that the selectivity of higher charged ions in the zeolite phase may be increased by employing very dilute solution [109].

4.4.1.2 Chemical Composition: Table 4.1 gives the chemical composition of a unit cell of zeolite type X and Y catalysts. The degree of exchange as determined by Flame Photometry has been discussed in detail in previous subsection. The number of water molecules in a unit cell as determined from the TG analysis and DTA exo- and endo-therm temperatures are also included.

4.4.2 X-Ray Diffraction Patterns:

The interplanar specings (d), Miller indices (hkl), and relative intensity for the zeolite samples are given in Tables A-1 to A-6 in Appendix A. The reported data for NaX-100 is also included for comparison in Table A-2[21]. The best value of the lattice parameter, a, for each sample was determined by using least square technique. The computed a values of the exchanged zeolite samples are presented in Table 4.3. The Si/Al ratio and the number of aluminum atoms

TABLE 4.3: UNIT CELL PARAMETER OF ZEOLITE CATALYSTS

Catalyst	Degree of Exchange Per cent	Unit Cell Parameter Å
NaX-100 (Si/Al = 1.25)	100	24.93 [21]
NaX-100 (Si/Al=1.23)	100	24.9954
LaX-58	58	25.0215
LaX-79	79	25.0252
LaX-96	96	25.0243
NiX-80	80	25.0197

per unit cell (PUC) were obtained by employing the correlation of Dempsey and Olson [34]. For NaX sample the Si/Al ratio was 1.23 giving 86 aluminum atoms per unit cell. The d values obtained in this study were in agreement with those reported by Breck and Flanigen [21], but the match of intensity data was not that close. This may be due to the difference in Si/Al ratio in them since it governs the number and positions of atoms within a unit cell.

The replacement of sodium ions causes an increase in the lattice parameter of the zeolite,however, the dependence of its values on the degree of exchange is complex. While the value of lattice parameter, a, increased with the degree of exchange upto 79 per cent, it remained essentially constant with further increase in the extent of exchange (Table 4.3).

The degree of exchange with La^{3+} cations affected the point-to-point intensity data as well. With increasing degree of La^{3+} substitution, the intensities of some lower angle peaks decreased whereas those of medium angle peaks increased. Some higher angle peaks which were absent in NaX-100 were also observed in the exchanged samples. These differences suggest a different site selectivity for lanthanum cations as compared to sodium ions in the zeolite framework. This is in accord with the literature [14, 20, 61, 63, 97, 110].

The peak intensities of nickel exchanged samples were lower than those of either lanthanum exchanged or the parent NaX-100 sample. Some of the peaks were virtually missing. An explanation for these differences could be found in the increase in the temperature factor which is caused by nickel cation exchange in zeolite X. The increased thermal vibrational energy makes the zeolite structure less stable. This is in accord with other workers [36, 55, 93, 108]. Serpinskii et al. [108] have reported studies on adsorption of propane on nickel exchanged type X zeolites. They observed a decrease in the adsorption volume with increase in nickel exchange which they attributed, along with other factors, to partial loss in crystal structure.

4.4.3 Differential Thermal Analysis and Thermogravimetric Results:

Thermogravimetric (TG) curves of weight loss against temperature were determined for the different types of catalysts used in this study and are shown in Figures 4.2 and 4.3. Since differential thermogravimetric (DTG) curves can provide information on the different types of intrazeolitic water binding, these curves were obtained from the corresponding TG curves by finding loss in weight (ΔW) with increment in temperature (ΔT). These curves are shown in Figures 4.4 and 4.5. Figure 4.6 shows the variation of the number of water molecules with the degree of La^{3+} cation exchange. Differential

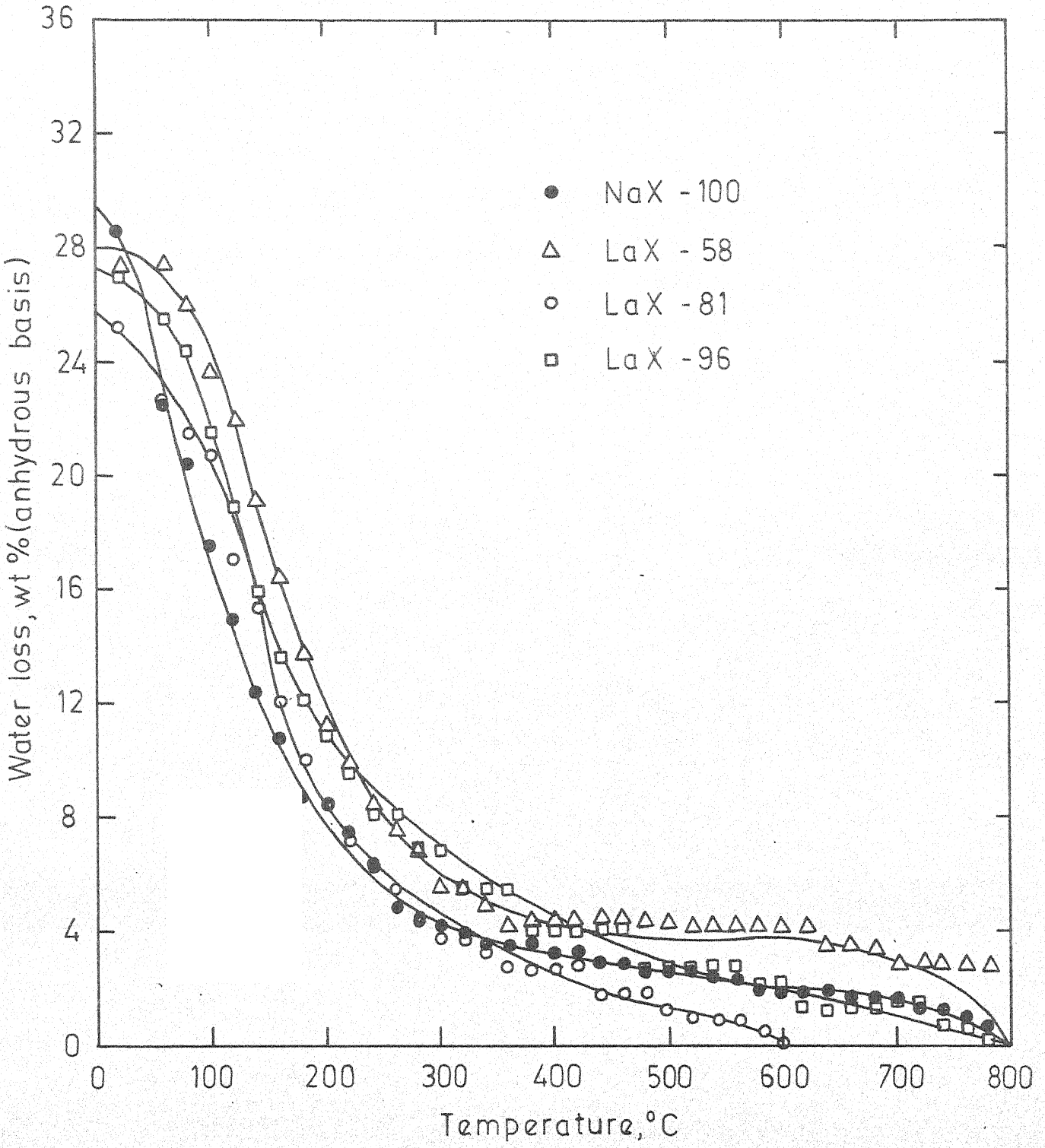

Fig. 4.2 - Thermogravimetric curves for NaX-100, LaX-58, LaX-81, and LaX-96 catalysts.

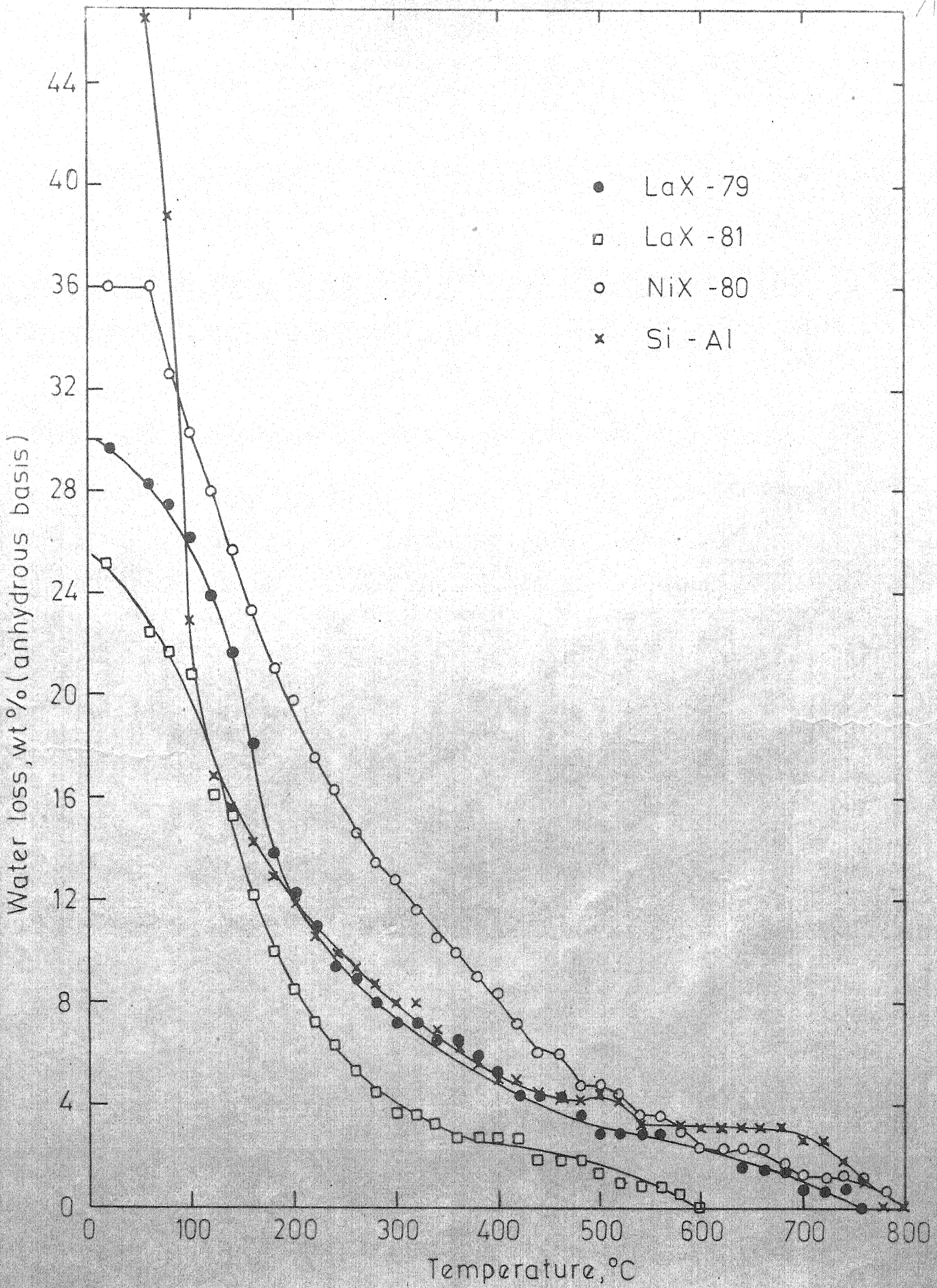

Fig. 4.3 - Thermogravimetric curves for LaX-79, LaX-81, NiX-80 and silica-alumina catalysts.

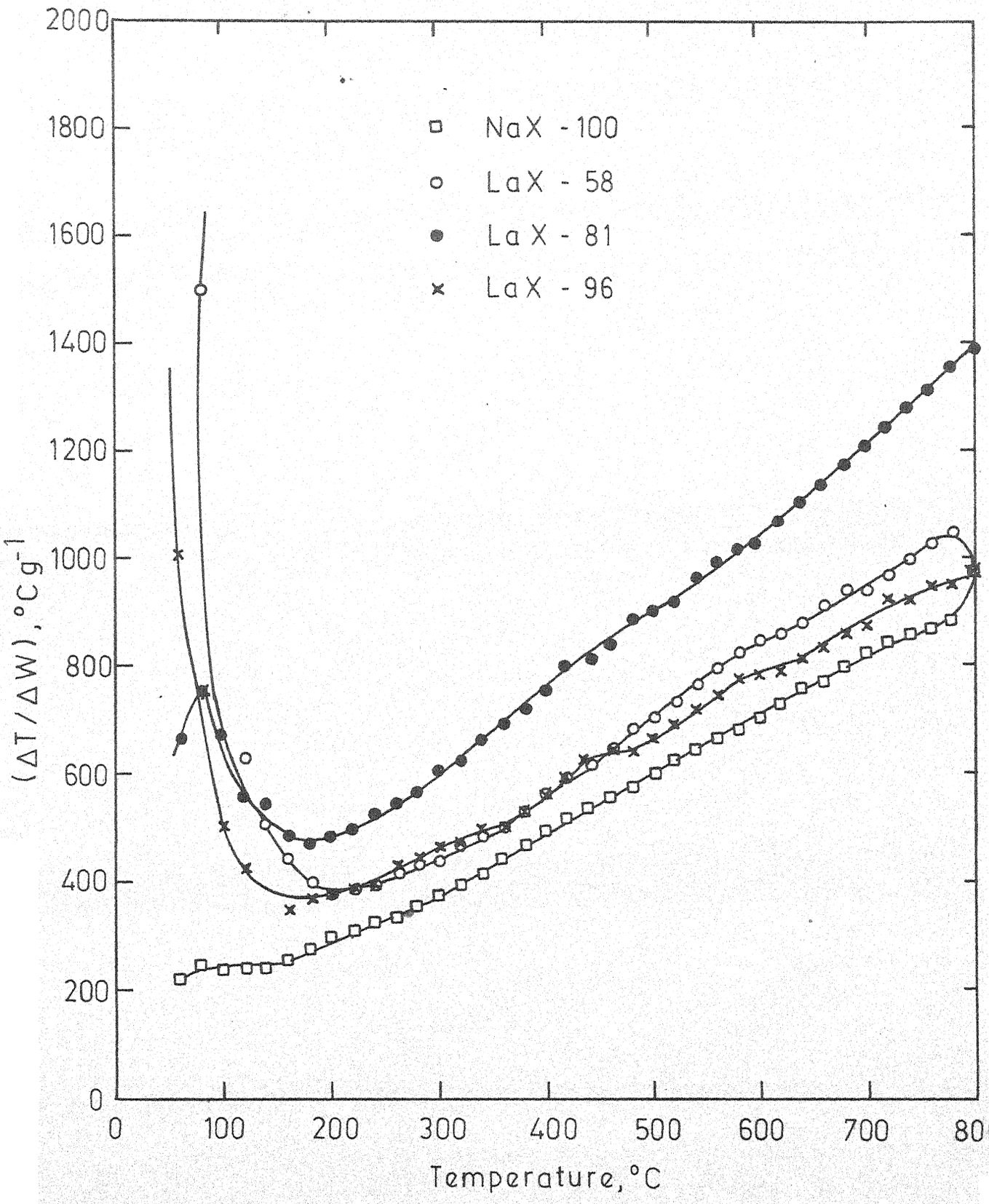

Fig.4.4 - Differential thermogravimetric curve for NaX-100, LaX-58, LaX-81 and LaX-96 catalysts.

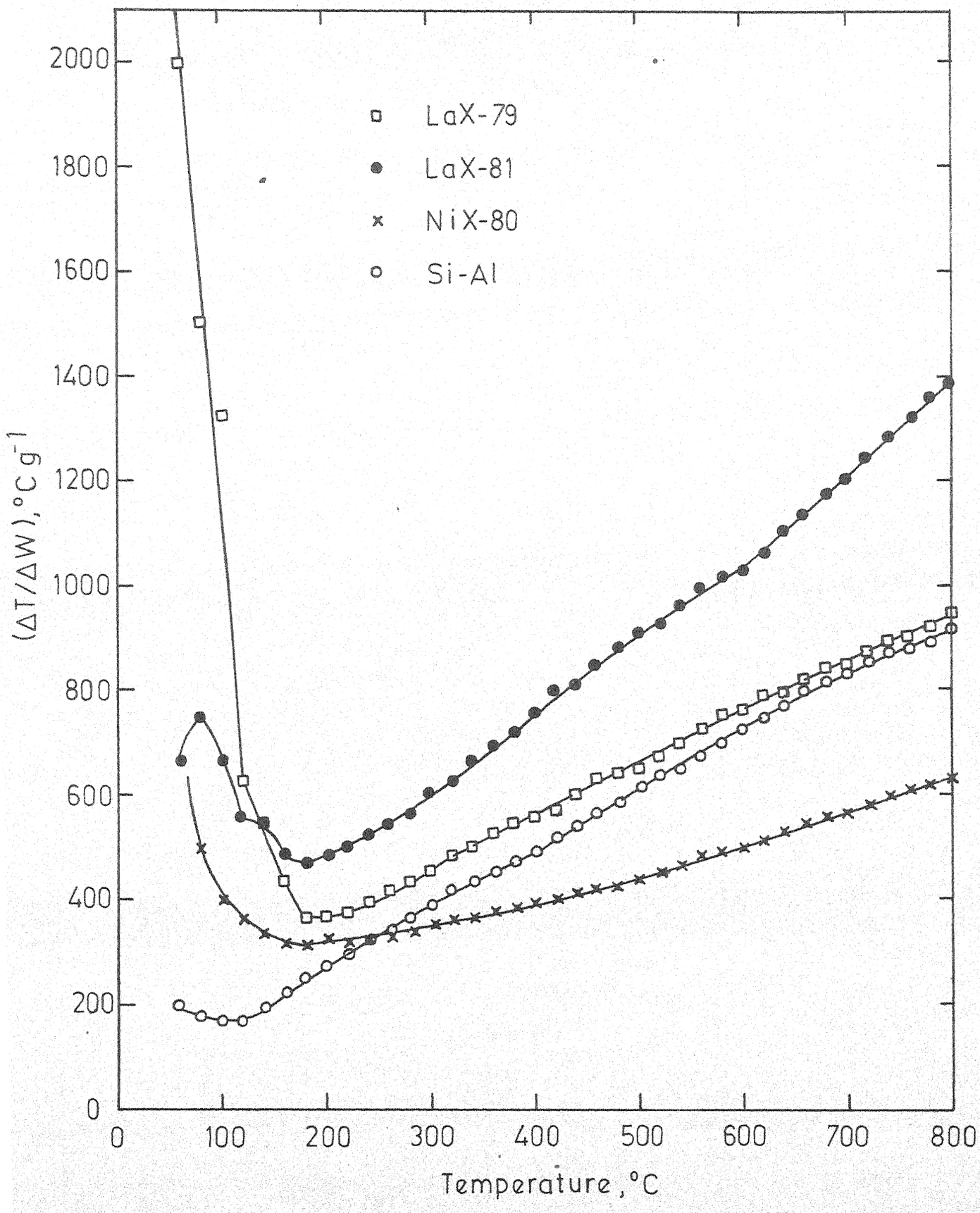

Fig. 4.5 -Differential thermogravimetric curves for LaX-79, LaX-81, NiX-80 and silica alumina catalysts.

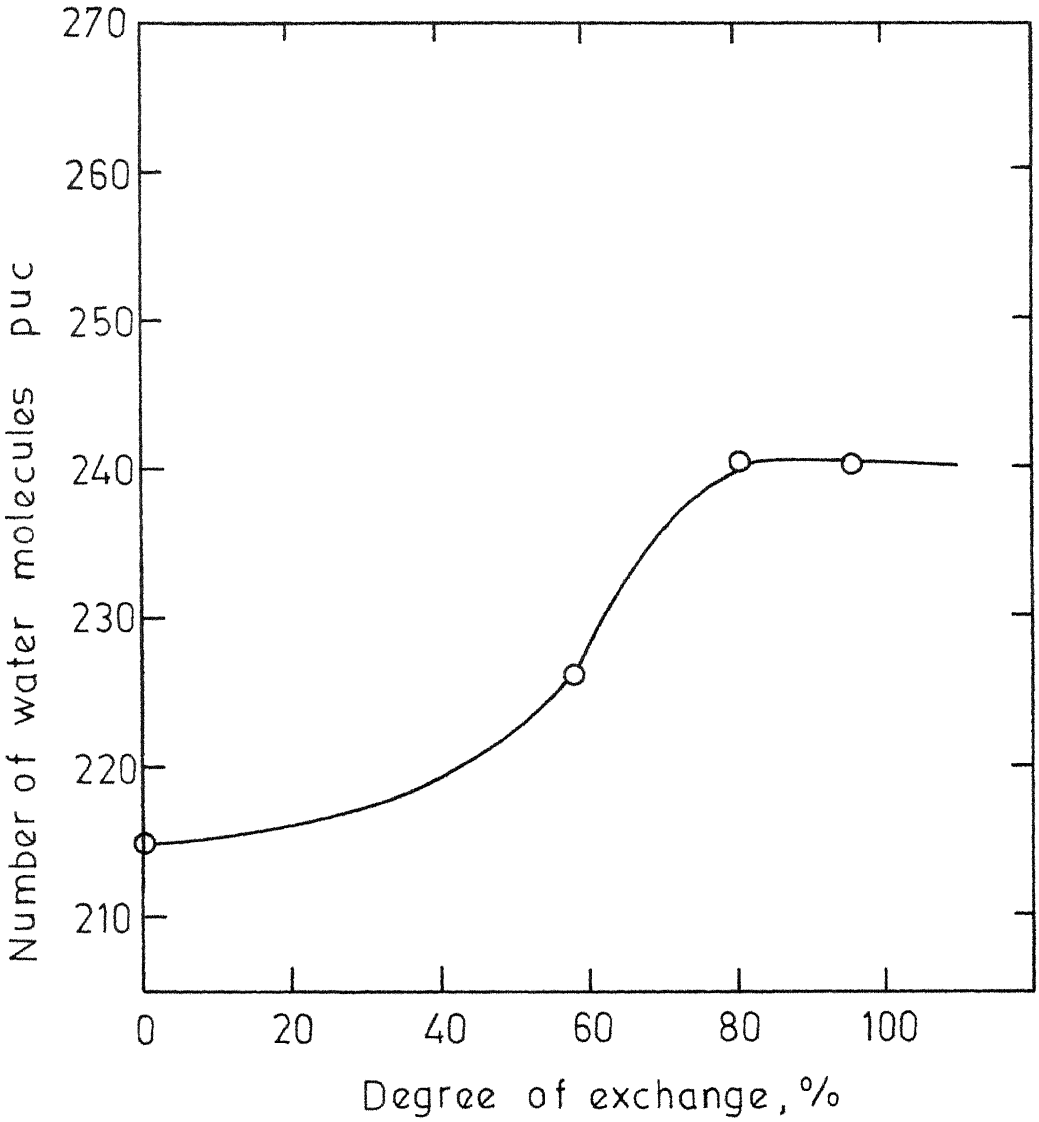

Fig.4.6 - Variation in the number of water molecules with the degree of exchange.

thermal analysis (DTA) curves for some of the zeolite catalysts are given in Figure 4.7.

The saturation water content of the zeolite samples were determined from thermogravimetric measurements. Zeolite catalyst samples were kept in a desiccator over saturated ammonium chloride solution for a minimum of two weeks prior to its use in thermogravimetric measurements. This was to ensure the attainment of saturation water by zeolite samples. Because of the difference in atomic weights of lanthanum and nickel cations used, one gram each of these exchanged zeolites do not contain the same number of unit cells. Therefore, the results of these zeolite samples are expressed on the basis of a unit cell and recorded in Table 4.2. It is to be noted that NiX-80 contains about 20 per cent more water molecules than LaX-81 does. Nearly 8 per cent higher number density of water for LaX-79 as compared to that of LaX-81 may be attributed to fine particle size of the former as against 1/16 inch pellets used in the latter.

DTA curves of zeolite X and Y (Figure 4.7) indicate a continuous loss of water over a broad range of temperature commencing from slightly above room temperature to about 350°C with a maximum at about 200°C. To demonstrate that the endothermic peak of the DTA curves were associated with water loss, thermogravimetric curves (Figures 4.2 - 4.5) were

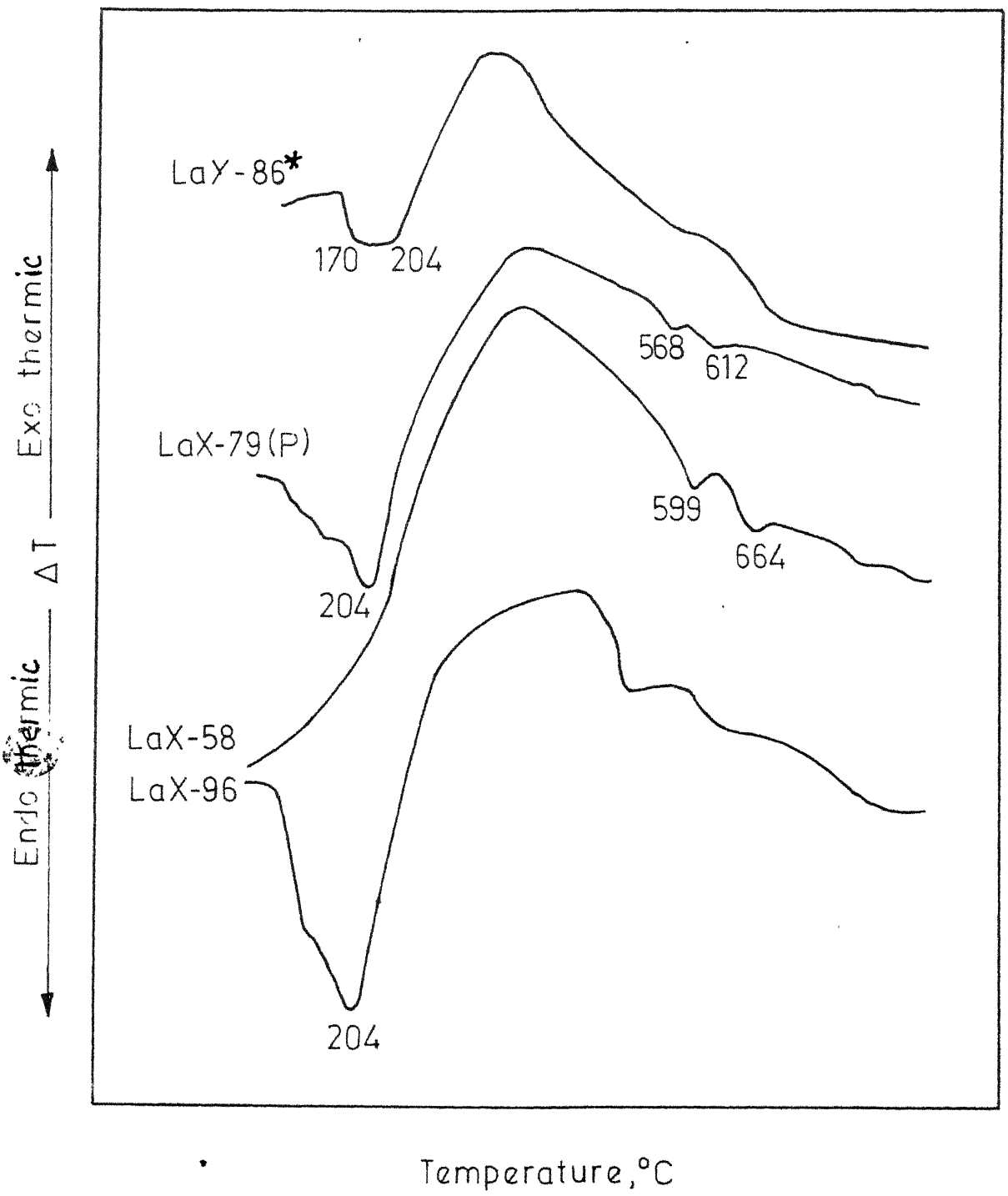

Fig. 4.7 -Trace of DTA thermograms for LaX-58, LaX-79, LaX-96 and LaY-86* catalysts.

determined. Figures 4.2 and 4.3 show that water loss from faujasite zeolite occurs in stages, in agreement with the DTA curves, indicating thereby that zeolites contain water bound in different ways. While the low temperature DTA endotherms pertain to the dehydration of the zeolite, high temperature endotherms are due to the loss of water from hydroxylated cations in the structure of the zeolites [20]. The existence of these additional endotherms for polyvalent exchanged zeolites e.g. calcium and lanthanum exchanged faujasites have been reported [20].

The water content of the faujasite type zeolite increases with a decrease in the cation radius and an increase in its valency. The size and the number of cations in a unit cell obviously affect the number of water molecules which can be contained in the unit cell. To elucidate this dependence of the water content, zeolites having about the same degree of exchange with different cations such as lanthanum and nickel were chosen. Figure 4.3 shows a comparison of the variation of weight loss with temperature for these two catalysts. It is clear that for NiX-80, not only the total weight loss is more than that for LaX-81 but also it remains higher throughout the range of heating. But the number of cations in these two samples are different. A unit cell of LaX-81 contains 23.2 La^{3+} ions, whereas that of NiX-80 is having 34.4 Ni^{2+} ions

(Table 4.1). Based on the number density of cations, NiX-80 should be able to accommodate less water molecules. But actually, NiX-80 contains 285 water molecules per unit cell as compared to only 241 in case of LaX-81. However, nickel with a radius of 0.72 Å [100] is about five-eighth the size of a lanthanum ion, as a result of which the total volume of these cations, on a unit cell basis, is only about 40 per cent of that occupied by lanthanum ions. This explains the higher water content of NiX-80 as compared to that of LaX-81. The appearance of the DTG minima for these zeolites essentially at the same temperature (Figure 4.5) indicates a similar binding of water molecules with these cations.

It may be seen from Figure 4.6, which is a correlation between the number of water molecules and the degree of lanthanum exchange, that the water molecules increase in number as the degree of exchange increases upto about 82 per cent beyond which there is no increase in water content. This shows an association of water with the cations, since those exchanged beyond 82 per cent, after which SI sites starts taking part, are not available for association with water. In the presence of water, nonetheless, La^{3+} ions from SI sites move to SI' and other accessible sites [12,77,101] and hence the non-availability of these ions for association with water does not seem to provide sufficient explanation for non-increasing water content at

higher level of exchange. However, the presence of these additional La^{3+} ions in the supercage appears to make it too much crowded for more water molecules to enter. This is in agreement with the results of Coughlan and Carroll [32].

4.4.4 Surface Area, Pore Volume and Pore Size Distribution:

Table 4.4 gives physical properties including surface area, pore volume, pore size distribution, true density and apparent density for all the catalysts used in this study. Surface area seems to decrease with increase in degree of lanthanum exchange. NiX-80, the only nickel exchanged catalyst studied, showed a much smaller surface area compared to LaX catalysts. This is in line with the observation made earlier in section 4.4.2 indicating partial loss of structure. A large number of pores (about 60 per cent) were present in very small size range (4-60 Å) in case of NiX-80 whereas LaX catalyst contained only 25 to 30 per cent pores in this range. Nearly 60 per cent of volume was contributed by small pores (4-60Å) in case of amorphous silica-alumina catalyst. Also the data indicate that the exchange of sodium with other cations result in a reduction in pore volume of the zeolite catalyst. This is found to be valid for both nickel and lanthanum ions.

TABLE 4.4: PHYSICAL PROPERTIES OF CATALYSTS

S.No.	Catalyst	True density g/cc (by He)	Apparent density g/cc (by Hg)	Pore Volume cc/g	S_2A m^2/g.	Pore Size Distribution(per cent by Volume)						
						4-60Å	60-100Å	100-200Å	200-300 Å	300-400 Å	400-500 Å	500 - 75000
1	NiX-80	0.3666	0.6852	0.3186	217.0	57.7	5.10	6.1	3.7	2.5	2.9	22.0
2	NaX-100	0.3627	0.7550	0.3923	450.01	29.2	3.2	4.2	3.2	2.1	2.1	56.0
3	LaX-58	0.3365	0.7035	0.3670	454.8	23.8	3.2	4.9	3.3	2.2	2.3	60.3
4	LaX-79	0.3686	0.9212	0.5526	348.2	20.3	3.2	2.6	1.7	1.7	1.6	68.9
5	LaX-81	0.3709	0.6900	0.3191	413.6	22.5	3.0	4.9	2.7	2.1	2.4	62.4
6	LaX-96	0.3208	0.6827	0.3619	326.9	31.7	2.4	3.0	3.7	2.0	1.4	55.8
7	LaY-86*	0.3193	0.7569	0.4376	503.4	29.4	0.9	1.1	0.4	0.4	1.2	66.6
8	Si-Al	0.4368	1.2459	0.8091	600.0	61.7	11.7	4.5	1.6	0.7	0.6	19.2

CHAPTER 5

RESULTS AND DISCUSSION

The results of hydrocracking of Assam crude residue are presented in this Chapter. The effect of the process variables including temperature, hydrogen charging pressure, reaction time, charge-to-catalyst weight ratio, the degree of ion-exchange and the nature of cations in the catalyst on the conversion of residuum and the distribution of the products are also discussed. The catalysts studied were various lanthanum exchanged zeolites of type X and Y, nickel substitute zeolite X and conventional silica-alumina. The physico-chemical properties of these catalysts have already been discussed in Chapter 4. The important properties of the feed-stock are given inTable 3.3. The range of the process parameters covered in this study are summarized in Table 5.1.

Experimental results obtained on an isothermal batch reactor are given in Appendix B. Table B.1 contains the operational details and the conversion obtained for each run and Table B.2 gives the record of product characteristics. The conversion, which represents the overall cracking activity of the catalyst, is defined as the weight per cent of the feed-stock converted to liquid products having a maximum boiling point as the reaction temperature. The yield of a product is

TABLE 5.1: THE RANGE OF VARIABLES COVERED

S.No.	Variables	Range
1.	Reaction temperature, ^{o}C	330-470
2.	Hydrogen charging pressure, psi	400-1300
3.	Charge to catalyst weight ratio	13-40
4.	Reaction time, min	15-270
5.	Catalysts:	
	a. Lanthanum exchanged zeolites X and Y	
	b. Nickel exchanged zeolite X	
	c. Conventional silica-alumina	
6.	Degree of exchange, per cent	
	a. Lanthanum cation	
	Type X	58,79,81,96
	Type Y	86
	b. Nickel cation	
	Type X	80

defined as the volume per cent of liquid hydrocarbons boiling in a specified range, e.g. the yield of kerosene is the volume per cent of hydrocarbons boiling between 140-280°C.

5.1.1 Effect of Reaction Temperature:

The temperature was measured through a chromel-alumel thermocouple inserted in a thermowell located in the bottom of the autoclave. The conversion and the distribution of products over LaX-79 and LaX-96 are shown in Figures 5.1 and 5.2, respectively. The scatter of data points in these figures is primarily because of temperature fluctuations during a run. Because of manual operation, a precise temperature control could not be achieved particularly in these runs. In certain cases, the temperature fluctuations were as high as ± 15°C.

With LaX-79 catalyst, the conversion, first increased with increasing temperature between 350-395°C, it attained a maximum and then decreased with further rise in temperature. The yields of kerosene (140-280°C) and middle distillates (140-340°C) decreased linearly with increasing temperature. The yields of gas oil increased linearly with temperature whereas that of naphtha showed a minimum at about 395°C. The pattern of conversion with LaX-96 was similar to that obtained with LaX-79. But the distribution of the products obtained was distinctly different from that with LaX-79 catalyst because of higher cracking activity of LaX-96. The yields of

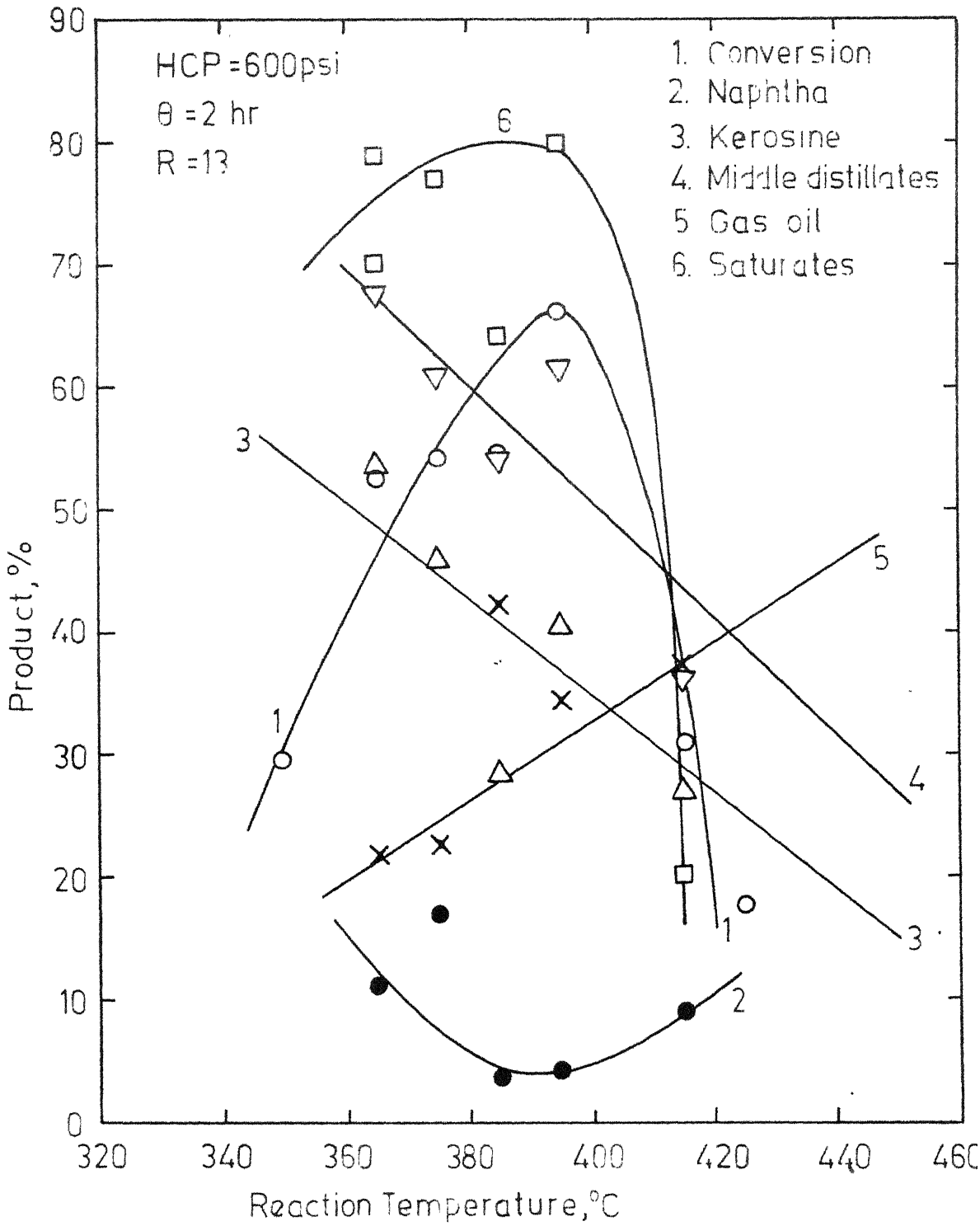

Fig 5.1 - Effect of temperature on product distributio for LaX - 79.

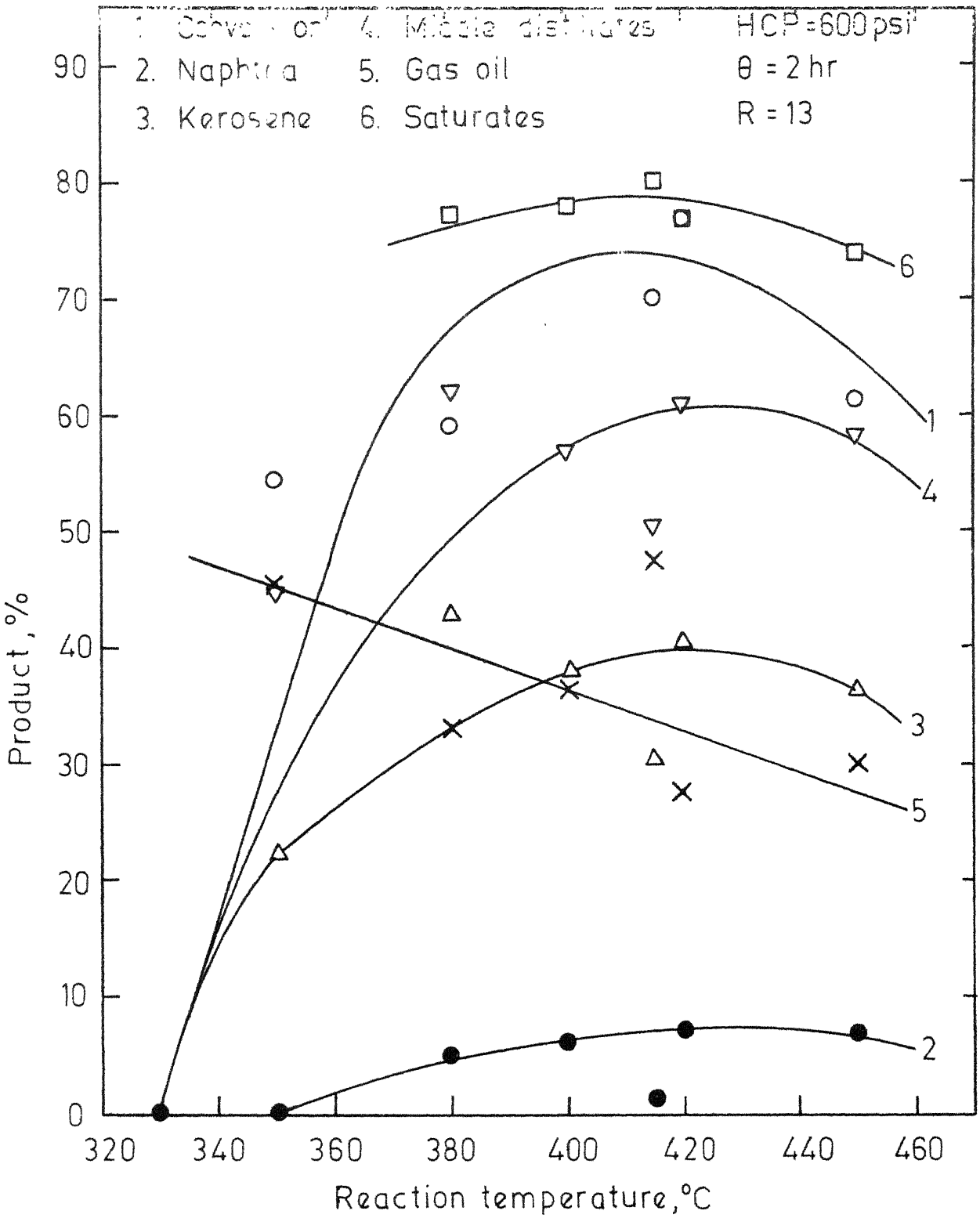

Fig. 5.2 - Effect of temperature on product distribution for LaX-96.

naphtha, kerosene, and middle distillates first increased with an increase in temperature and then showed a decreasing trend at higher temperatures. However, the yield of gas oil decreased with increasing temperature. These results are in close agreement with those obtained by Qader and Hill [96].

A cracking reaction mechanism may be postulated in which the feed molecules disappear to form gas oil, middle distillates, naphtha, gas and coke. As the operating temperature rises, the cracking severity increases resulting in subsequent cracking of gas oil into middle distillates, naphtha, gas and coke. As the cracking severity further rises, middle distillates also starts cracking simultaneously to naphtha, gas and coke. Naphtha, in turn, cracks to give gas and coke. Thus as the temperature rises, the proportion of gas and coke formation also rises and consequently the total conversion which accounts only for liquid products decreases. This cracking mechanism also explains why the yield of products formed pass through maxima. The increase in reaction temperature increases the reaction rate very much but does not affect the conversion as much [49].

The degree of saturation of kerosene defined as the volume per cent of saturated hydrocarbons was measured by Fluorescent Indicator Adsorption method (ASTM D-1319/66T). The degree of saturation first increased with increase in temperature

up to about 400°C and then started decreasing (Figures 5.1 and 5.2) at higher temperature, as the hydrogenation-cracking equilibrium shifts towards cracking reaction [2,40], the decrease in the degree of saturation of kerosene becomes apparent. Further, experimental data show a close relationship between the degree of saturation of kerosene and the total conversion of residuum. Irrespective of the level of operating temperature, if the total conversion was high, the degree of saturation was invariably high. On the other hand, when the conversion was low, the degree of saturation of kerosene was also low. Thus total conversion of residuum can serve to indicate qualitatively the degree of saturation of kerosene produced. The degree of saturation as high as 80 per cent was obtained under certain conditions of operation. This may be attributed to the greater hydrogen-transfer ability of the zeolite catalyst [123], and the higher severity of operation (temperature, HCP, and reaction time) [2,40]. Although, because of the colour of diesel fraction, above test could not be applied to diesel oil for its degree of saturation determination, but it is expected to be of the same order of magnitude as in case of kerosene. This gives an indication of high quality of middle distillates obtained by this technique.

Since LaX-96 was found to give better conversion along with higher yields of middle distillates, further studies were made using this catalyst only.

Effect of Hydrogen Charging Pressure:

Hydrogen charging pressure (HCP) is the pressure in the autoclave immediately after charging of hydrogen at the reaction temperature. As the reaction progressed, the pressure in the reactor increased continuously attaining a final value much higher than the charging pressure. The pressure rise, ΔP in a batch was a function of operating temperature, charging pressure and batch time. Figure 5.3 shows variation of pressure with reaction time in a few typical runs. The increase in pressure was because of formation of lighter products from the cracking of large residuum molecules.

The effect of hydrogen charging pressure on the conversion and the distribution of the products is illustrated in Figure 5.4. The conversion of the feed and the yields of naphtha, kerosene, and middle distillates increased gradually with increase in hydrogen pressure in the whole range of study. The yield of gas oil decreased with hydrogen pressure increase. Increase in the conversion with hydrogen pressure is in agreement with results of Gary and Handwerk [49].

The effect of hydrogen pressure on the conversion was only marginal. In the entire range of hydrogen charging pressure studied, between 700-1300, psi, the conversion increased only by 4 per cent. However, the production of kerosene increased by 20 per cent in the same range. A similar

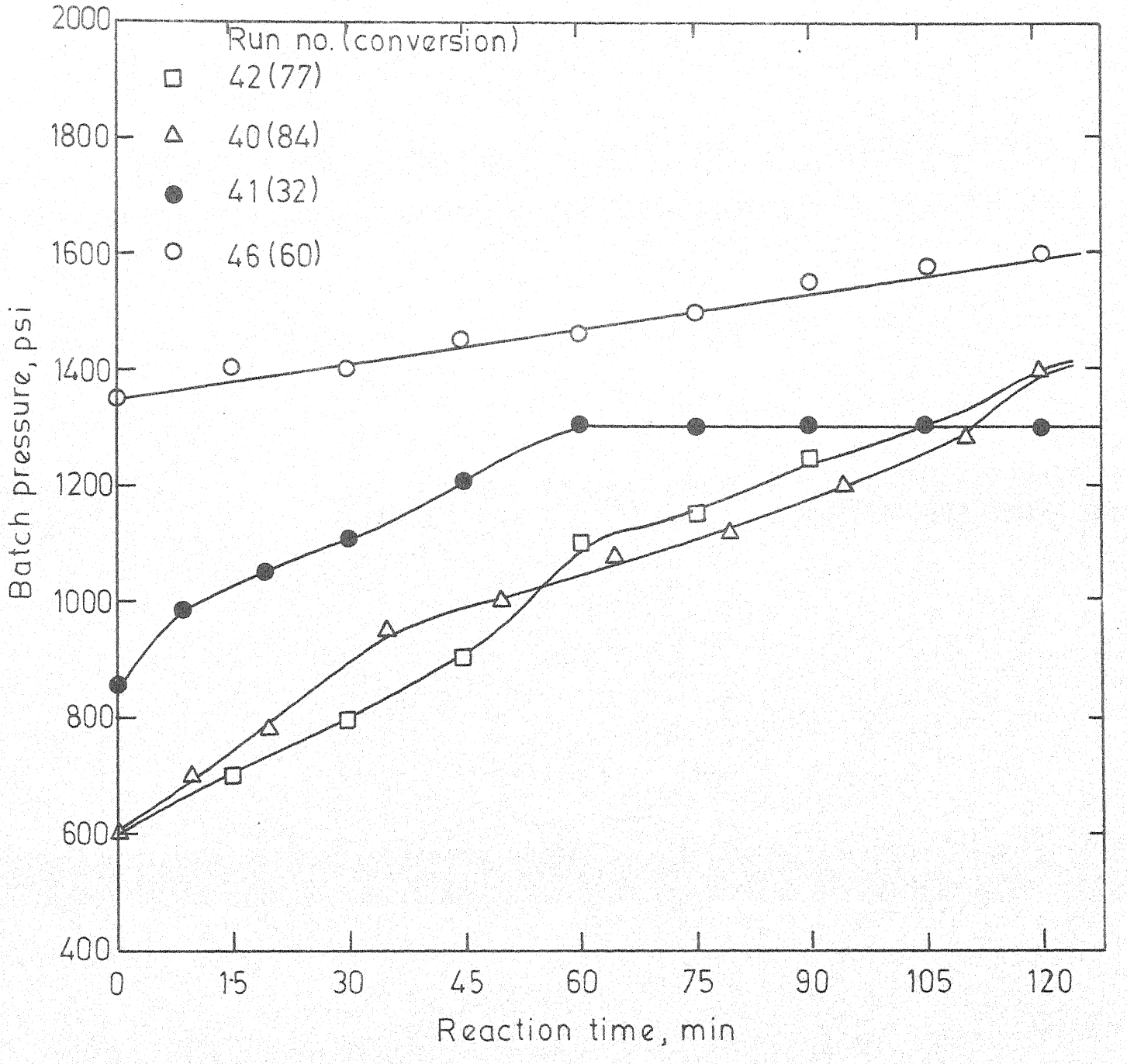

Fig.5.3 - Batch pressure variation with reaction time for LaX-96 during a run.

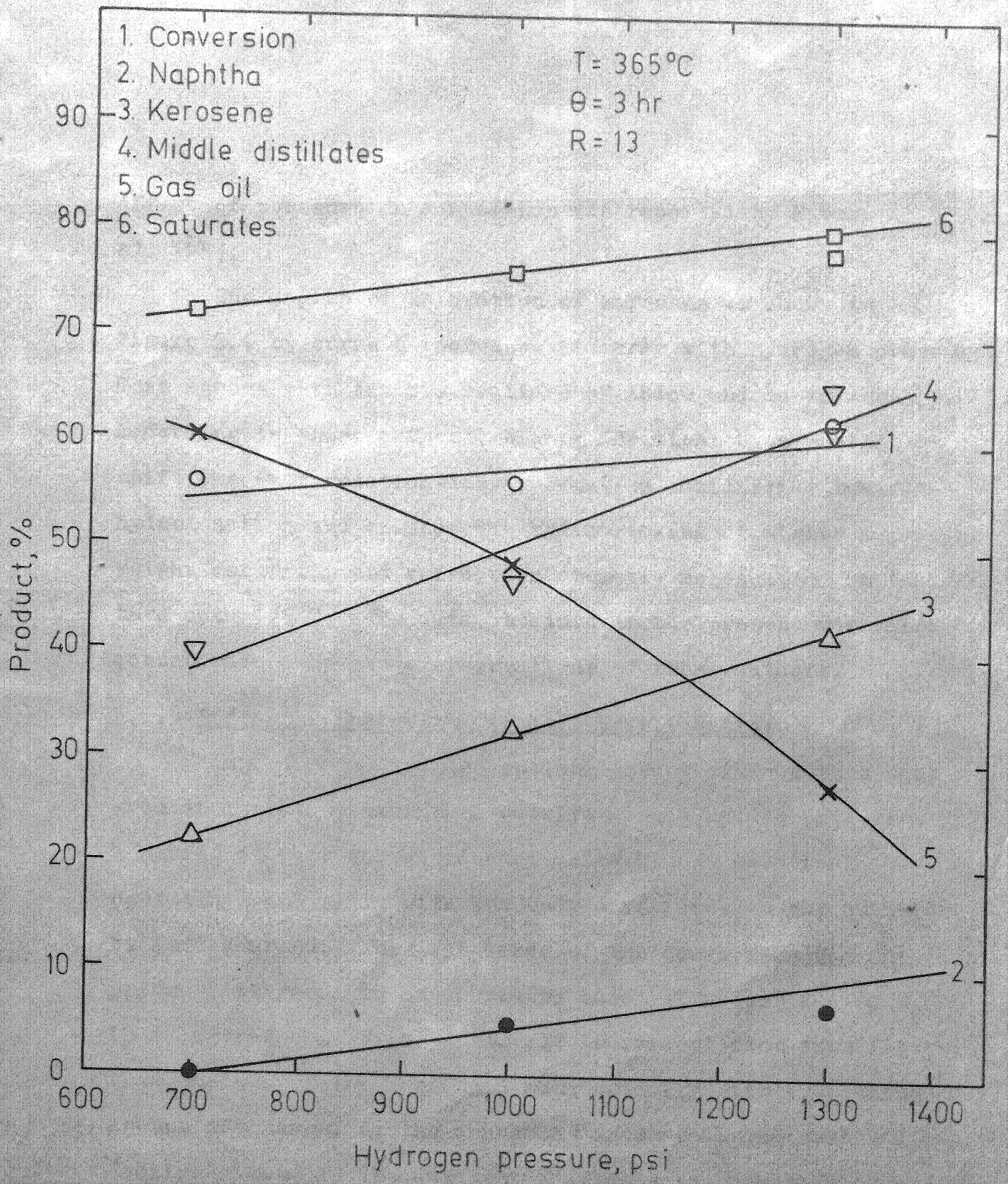

Fig. 5.4- Effect of hydrogen charging pressure on product distribution for LaX-96.

effect of pressure on conversion was reported by Fabuss et al. [41].

The degree of saturation of kerosene as shown in Figure 5.4 by curve 6 increased linearly with hydrogen pressu This agrees with the observations of Abdou and co-workers [2,4 According to these authors, higher HCP might be expected to shift the hydrogenation-dehydrogenation equilibrium towards hydrogenation and enhance the hydrocracking of higher molecula weight paraffins and refractory aromatic molecules at a tempe ture upto 425°C. The data obtained in the present work also corroborate the above observations of these authors.

5.1.3 Effect of Charge to Catalyst Weight Ratio:

In order to find the optimum amount of feed that each gram of lanthanum exchanged catalyst could handle effectively, a series of runs were conducted under almost identical operating conditions with the only difference in the quantity of feed charged. The dependence of the conversion and the product distribution on charge to catalyst weight ratio, R, is illustrated in Figure 5.5. It is evident from this figure that the conversion decreased monotonically with increasing amount of charge. As the charge is increased, the number of 'active sites' in the catalyst available to each gram of char is decreased and the conversion is lowered. The yields of

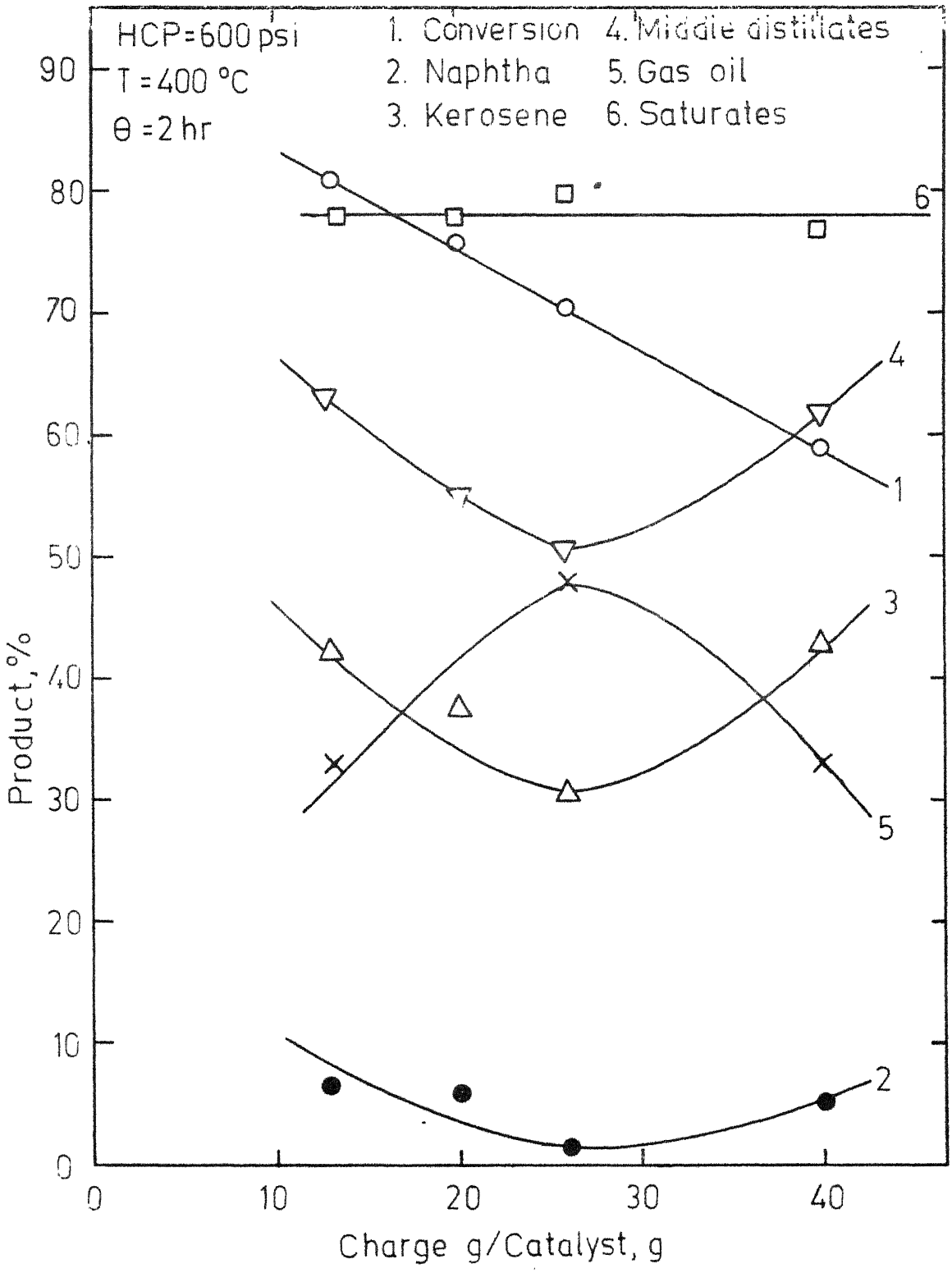

Fig. 5.5 - Effect of charge to catalyst weight ratio on product distribution for LaX - 96.

kerosene, and middle distillates passed through minima but the yield of gas oil had a maximum at R = 26. These data compare well with those of Otouma and Arai [87] who studied the cracking of gas-oil over LaX catalysts. Increasing charge to catalyst weight ratio produces almost no change in the degree of saturation of kerosene obtained.

5.1.4 Effect of Reaction Time:

The effect of reaction time on the conversion and distribution of products obtained from hydrocracking of residuum over LaX-96 catalyst is shown in Figure 5.6. At reaction temperature of 400°C, HCP of 600 psi, and R=13, the conversion increased with increase in reaction time between 1 to 2 hr, attained a maximum conversion of 77 per cent at 2 hr and then decreased for higher batch times. Batch reaction times of 1 hr and 3 hr gave conversion at 54 per cent. The effect of batch time on the yields of naphtha and middle distillates was found to be similar to that on the conversion, while that of gas oil followed a reverse trend with a minimum at 2 hr.

The effect of reaction time on the degree of saturation of kerosene is also included in Figure 5.6. As the reaction time was increased, the degree of saturation decreased linearly but only slightly.

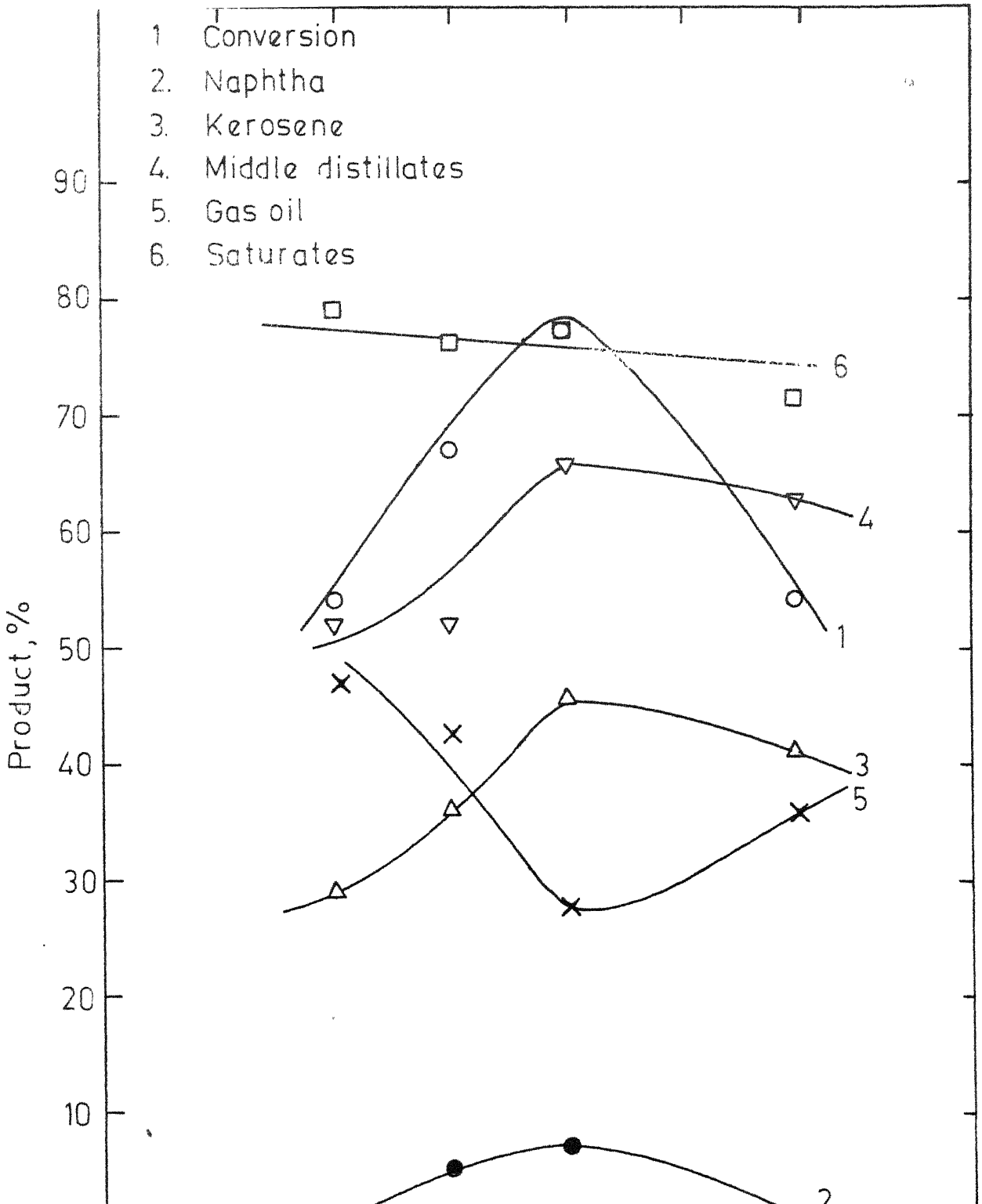

Fig.5.6 - Effect of reaction time on product distributic.. for LaX-96.

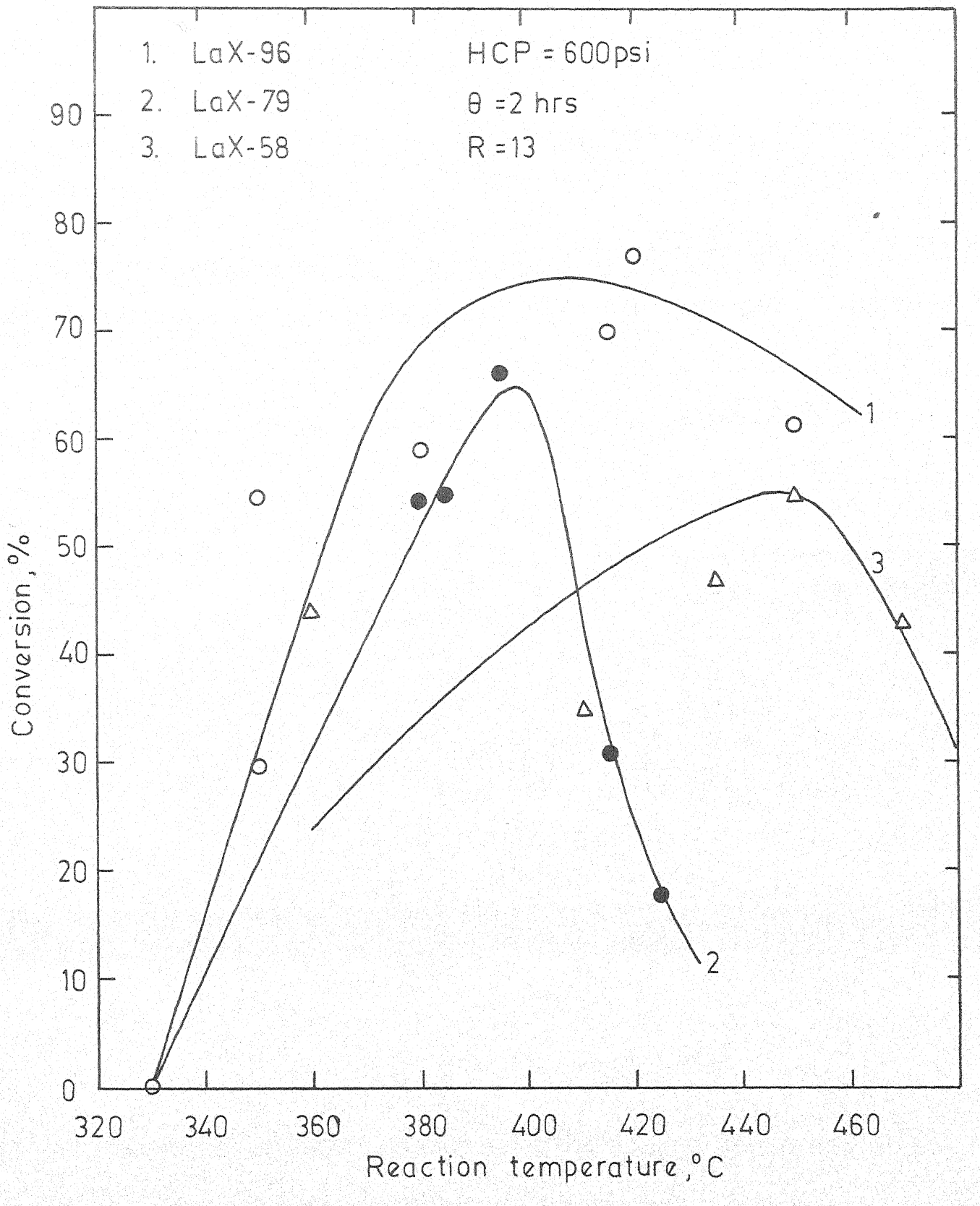

Fig. 5.7 - A comparison of the performance of LaX catalysts having different degree of exchange.

as compared to the distillate hydrocracking and did not need a strong cracking catalyst as thermal mode of cracking prevailed in this process. In the present investigation, however, thermal mode of cracking could not have been significant in the range of temperature studied and in all likelihood it was the cracking activity of the catalyst which controlled the conversion.

There are five types of cation positions in faujasite type zeolite structure. Some of these are easily available to cations while others are not. This complex cation siting accounts for the variation in its activity as a result of cation exchange. Bennett and Smith [14, 20, 110] on the basis of x-ray data, place lanthanum ions in various sites of LaX-8 as 11.8 in SI, 2.5 in SI' and 1.5 in SII after calcination at 420°C. This indicates a strong preference of lanthanum ions to fill up the SI sites. However, this distribution of cation cannot explain high acidity of lanthanum exchanged zeolites even at low level of exchange [61] and the observed activity of this catalyst. This fact must have its explanati in a partial migration of lanthanum ions from SI sites to more accessible ones which concurs with the finding of Bennet and Smith who reported migration of lanthanum ions during calcination. The dehydration study of rare earth exchanged faujasites indicate that rare earth ions tend to bind one

water molecule [18,20, 110]. It is worthy of note that lanthanum ions prefer SI' when some residual water molecules are available.

The distribution of cations affects the acidity of these catalysts. If the cations take positions in SI sites, there is no observable rise in its acidity. But if the cations occupy sites II and III, significant rise in its acidity is observed [61]. It is due to the lower electrostat: shielding of the cations in these positions [73-74] and to the asymmetric charge distribution caused by cations carrying higher charge. Kladnig [61] observed a strong enhancement of acidity at exchange level greater than 70 per cent in LaY zeolite. This threshold degree of exchange coincides with the 'definite exchange capacity' for a Y type zeolite [110].

The results of this study indicates that the minimum degree of exchange of sodium with lanthanum that is needed to produce a reasonably strong catalyst for residuum hydrocracki should lie between 79-96 per cent. Cumene cracking data of Otouma et al. [87,88] showed that the activity of LaX catalyst did not increase when the degree of exchange was raised from 86 to 96 per cent. This could be used to further narrow down the limit to 79-86 per cent. This range of minimum level of exchange turns out to be in the vicinity of the 'definite exchange capacity in big cavities' i.e. 82 per cen

for X type zeolite. This implies that not only exchange of Na^+ ions from supercages (or big cavities) but also from 'hidden' sites, either in hexagonal prisms or sodalite cages might be needed for optimum activity of the LaX catalysts.

5.2 Nickel Exchanged Zeolite X(NiX):

5.2.1 Effect of Reaction Temperature:

The dependence of the conversion and the distribution of the products on reaction temperature over NiX-80 catalyst, examined in the range of 370-455 ^{o}C, are exhibited in Figure 5 In the whole range of temperature covered, the conversion increased linearly. While the yields of middle distillates as well as gas oil decreased, that of naphtha increased with an increase in temperature. The degree of saturation of kerosene showed a decreasing trend with increasing temperature

The increase in the total conversion of residuum with increasing reaction temperature is in broad agreement with the results of Ciapetta and Hunter [29]. These authors who studie the isomerization of n-hexane over nickel (4-6 per cent) on silica-alumina catalysts, found that at higher reaction temperature, around 400^{o}C, hydrocracking reaction becomes the major reaction. The decrease in the yield of kerosene and the increase in that of naphtha particularly became significant at higher temperature which may be due to the onset of secondary reactions resulting in further cracking of higher

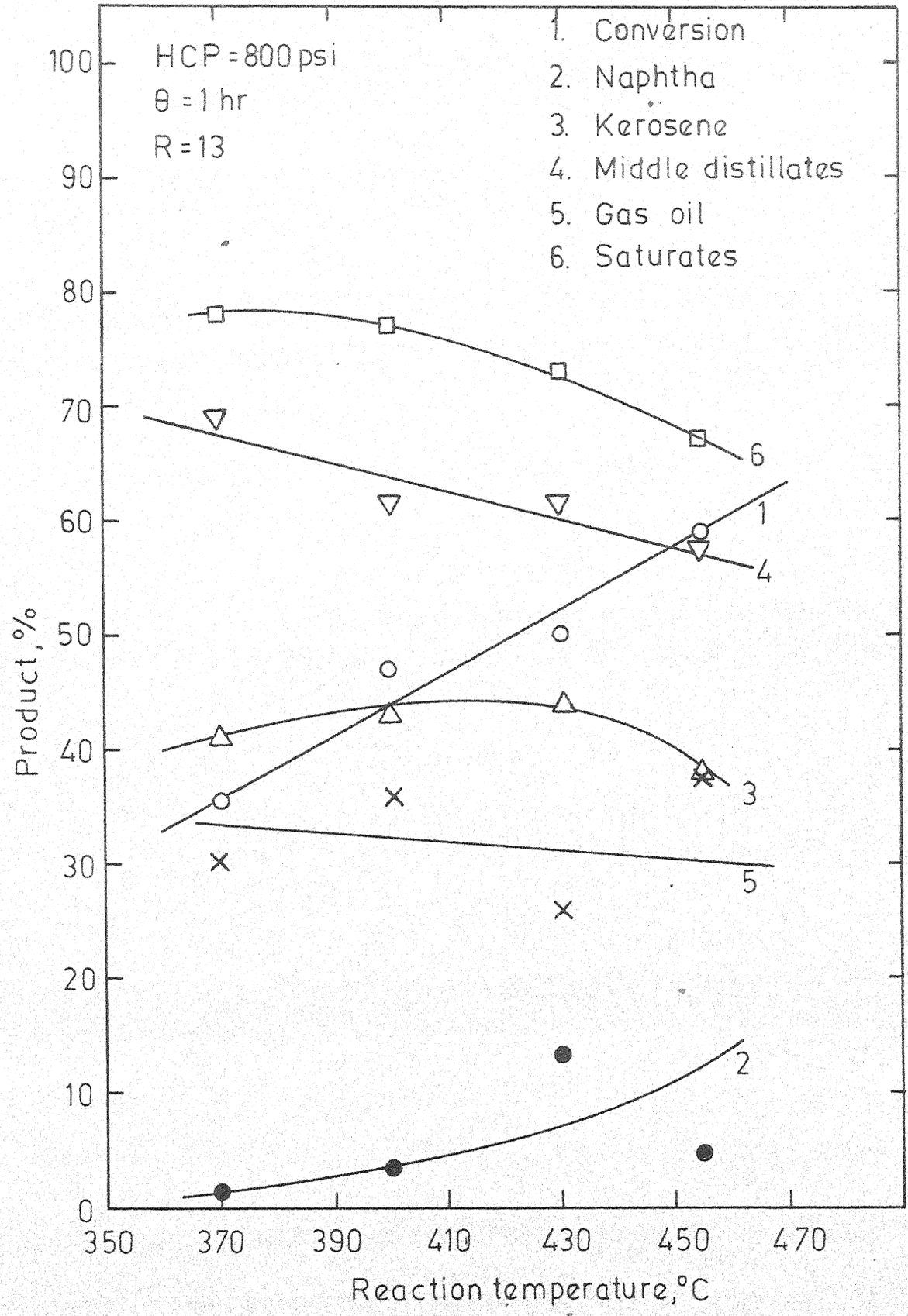

Fig. 5.8 - Effect of temperature on product distribution for NiX-80.

product molecules into more lighter ends, gas and coke [96].

With increasing reaction temperature, the decrease in the degree of saturation of kerosene obtained over NiX-80 catalysts at the first thought may appear inconsistent special because nickel metal is well known for good hydrogenating activity. However, Elkady et al [40] who investigated the upgrading of petroleum residue over NiMo/Al and CoMo/Al catalysts found that at higher temperature, hydrogenation-cracking equilibrium shifted towards cracking. This displacement of the equilibrium reaction would result in a decreased proportion of the saturates.

Figure 5.9, which is a plot of the dependence of the conversion on operating temperature, presents a comparative study of the different catalysts used. The catalysts included in this figure are LaX-96, LaX-79, NiX-80 and amorphous silica alumina. It is clear that the activity of all the zeolite catalysts remains higher than that of silica-alumina. This is to be expected since the zeolite catalysts are known for their supercracking activities. This again corroborates the close correlation between the acidity of the catalyst with its activity in residuum hydrocracking.

The effect of the nature of the cation present in the zeolite catalysts may also be seen in this figure. The characteristic bell shaped dependence of the conversion on

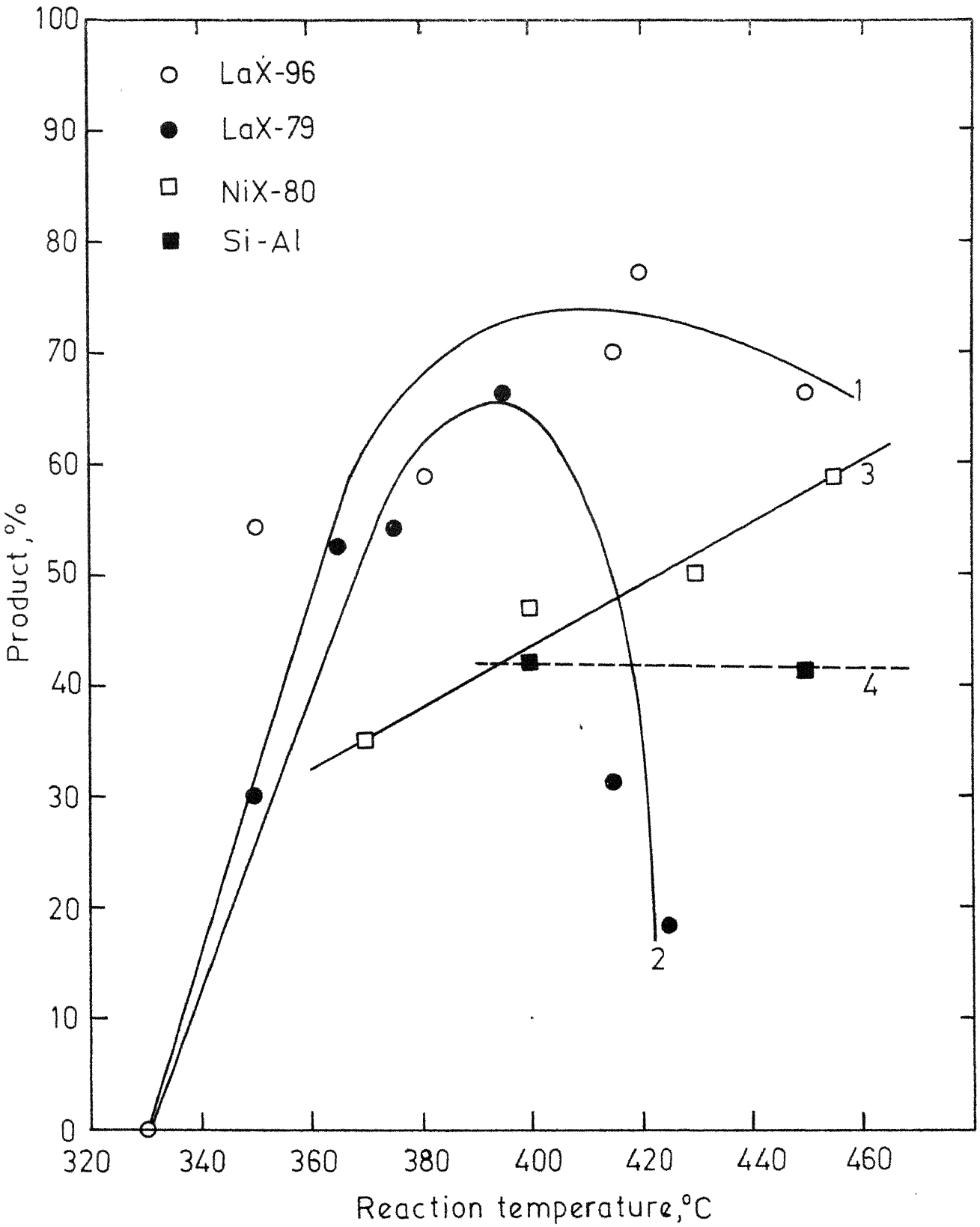

Fig. 5.9 - A comparison between LaX, NiX and Si-Al catalysts

Conversion?

reaction temperature observed inthe case of LaX catalysts (curves 1 and 2) is missing in the case of NiX and on the contrary, a linear dependence is observed in the temperature range studied. Also the level of conversion over LaX-96 remained higher as compared to that over NiX-80. Even LaX-79 having about the same degree of exchange, gave better convers until a temperature of about 400°C. It, therefore, appears that lanthanum cations are more suitable for obtaining better conversion of Assam crude residue.

A notable difference between LaX and NiX catalysts is the location of the cations in the zeolite lattice. In exchanged zeolite X, when completely dehydrated, while La^{3+} ions are distributed in sites SI and SII, Ni^{2+} ions occupy SII and SII' in addition to sites SI and SI' and the populati of nickel cation in SI sites is limited to 12 ions per unit cell (PUC) [48]. Thus more of Ni^{2+} ions occupy accessible sites as compared to La^{3+} ions which should result in higher activity for NiX. However, as revealed by x-ray results, discussed in Section 4.4.2, NiX catalysts are known to suffer partial loss of structure during calcination [36, 55, 93, 108] or during ion exchange [108]. This can explain the lower activity observed in case of NiX-80 compared to LaX catalysts inspite of the more favourable position of Ni^{2+} ions in the zeolite lattice.

A look at Table 4.4 reveals that the surface area of NiX-80 is 217 m^2/g whereas that of LaX-96 is 327 m^2/g , which is about 50 per cent more. Also the pore size distribution for NiX-80 shows that nearly 58 per cent of pore volume is in the size range of 4 to 60 Å which is close to that observed in case of amorphous silica-alumina catalyst. Lanthanum exchanged catalysts have only 25 to 30 per cent pores in this size range. All these results also support the hypothesis of loss of structure in NiX catalysts.

5.2.2 Effect of Hydrogen Charging Pressure:

With NiX-80 catalyst, the range of hydrogen pressure covered was from 500 to 1200 psi. The operating temperature was 425°C at a charge to catalyst weight ratio of 13. The results are illustrated in Figure 5.10. It is apparent from this figure that hydrogen charging pressure (HCP) is not a very significant parameter. The conversion of the residuum to liquid products first decreased slightly and then picked up as hydrogen pressure was raised. The yields of naphtha, kerosene and diesel first increased and then decreased with an increase inHCP, while the yield of gas oil in the product followed a reverse trend indicating that the cracking reaction are suppressed at higher pressure.

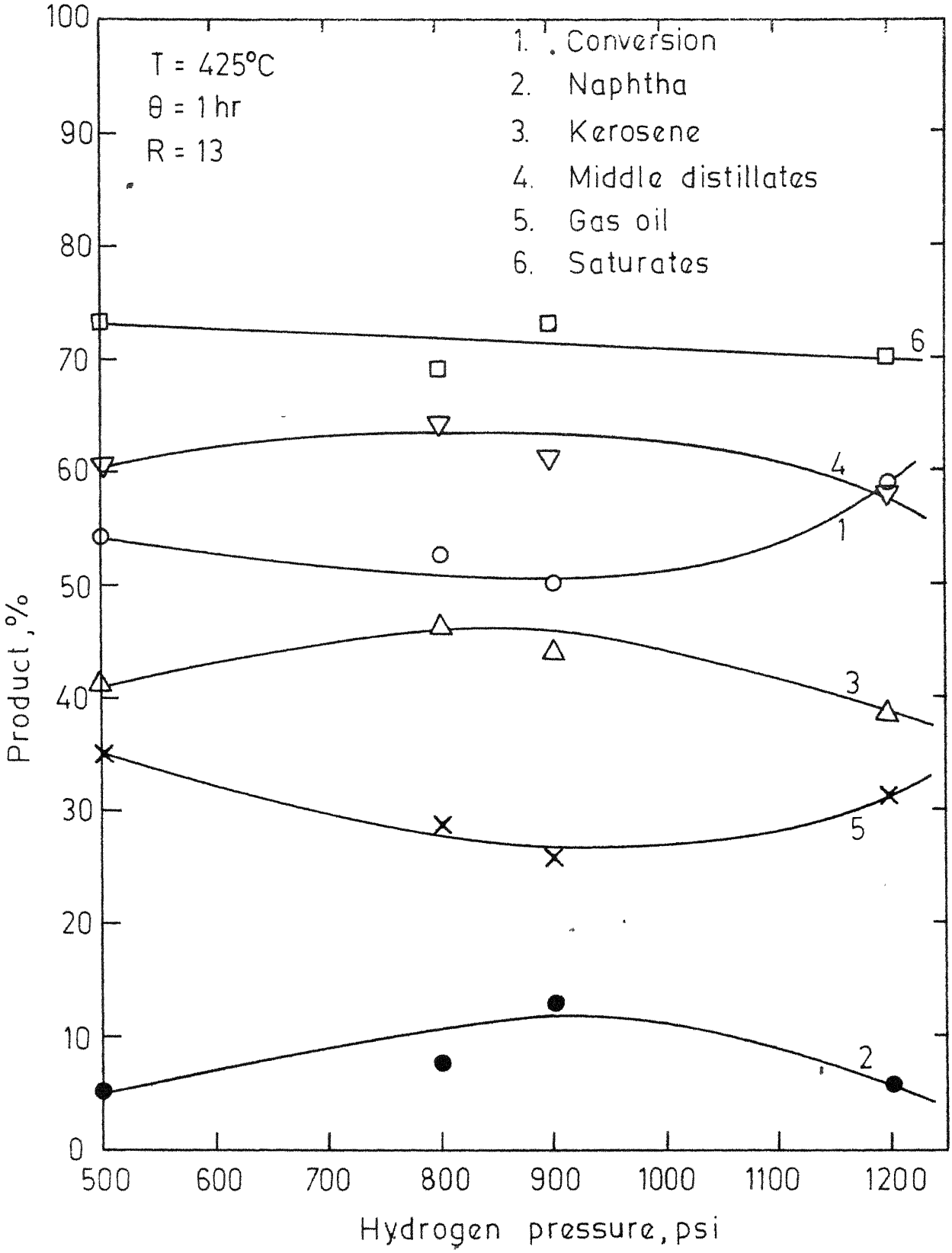

Fig. 5.10 - Effect of hydrogen pressure on product distribution for NiX-80.

5.2.3 Effect of Reaction Time:

The variations in the conversion and distribution of the products obtained over NiX-80 catalyst with reaction time are depicted in Figure 5.11. The conversion first increased, attained a maximum and then decreased with increasing reaction time. The yields of naphtha, kerosene and middle distillates increased with increasing time while that of gas oil decreased. The effect of reaction time on the degree of saturation of kerosene fraction was similar to that on the conversion. These results are similar to those obtained in case of LaX catalysts.

5.3 Amorphous Silica-Alumina:

Conventional silica-alumina was used as diluent to lanthanum exchanged zeolite catalyst in order to minimize the gas formation. Neither significant increase in conversion to liquid product nor decrease in gas formation could be achieved when 50 per cent dilution of LaX-96 catalyst with silica-alumina was tried. The conversion was not only low but also very much comparable to that with silica-alumina alone. Under similar operating conditions, the conversions with different ratios of LaX-96 and silica-alumina such as 1.0, 0.5 and 0.0. were 43, 47 and 84 per cent, respectively. The effect of reaction temperature on the conversion over silica-alumina catalyst is included in Figure 5.9 for comparison.

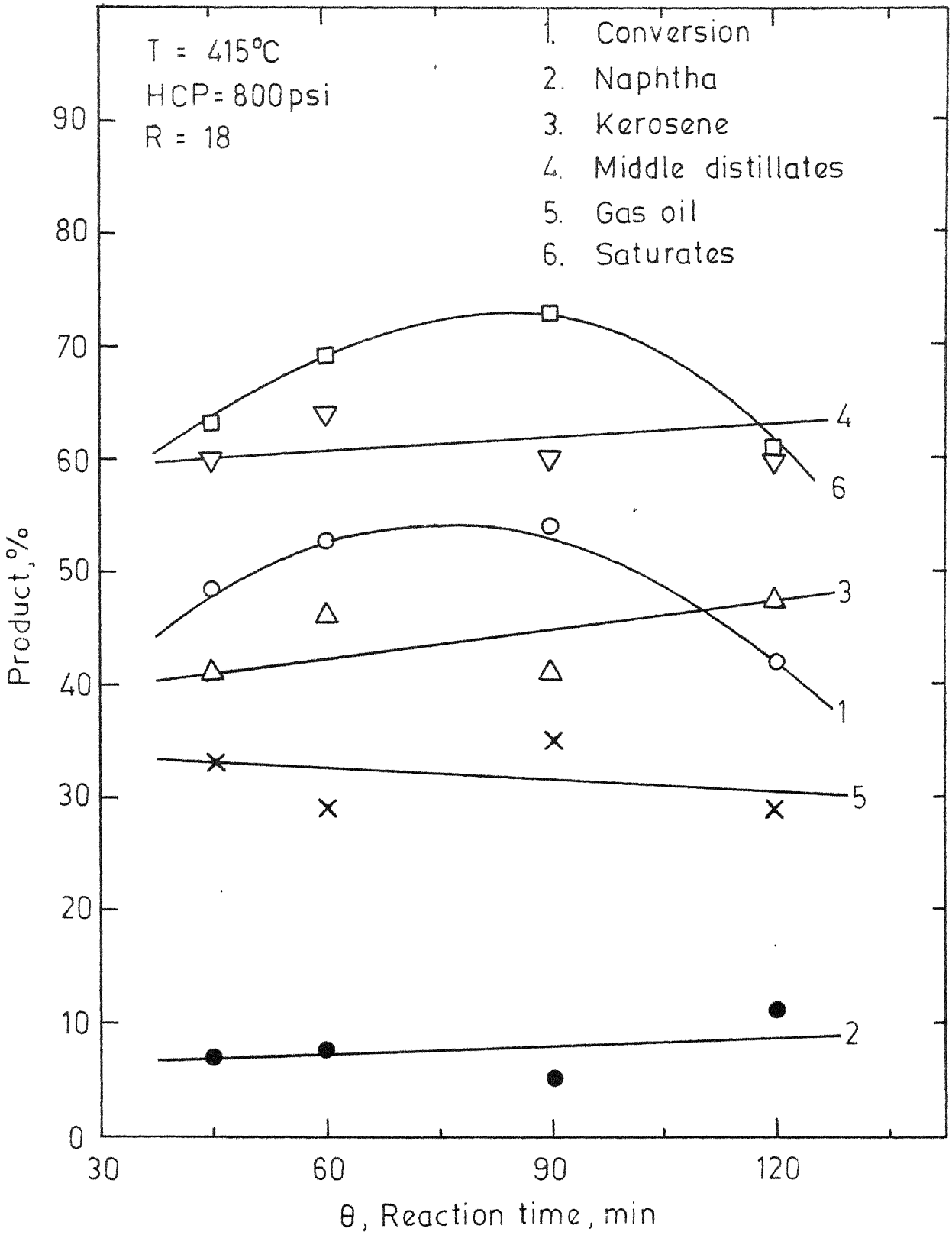

Fig.5.11 - Effect of reaction time on the product distribution for NiX-80.

5.4 Effect of Particle Size of LaX Catalyst:

As discussed in Chapter 2, the performance of the catalyst is influenced by its particle size because of mass transfer limitations. To discern this effect in the present work, LaX-96* catalyst of -20 +35 mesh size was used. NaX in powder form obtained from Union Carbide was mixed with about 10 per cent sodium silicate which served as binder. This was pelletized and baked before crushing to the desired size. Figure 5.12 shows the effect of reaction temperature on the conversion and the distribution of the products obtained over this catalyst. The dependence of the conversio and yields of the different cuts are essentially similar to that obtained over the pellets of LaX-96 (Figure 5.2). However, the level of activity of LaX-96* remained lower than that in case of LaX-96. The lower activity obtained with smaller size catalyst particles is rather intriguing and contrary to the theoretical expectancy. It should be mentioned here that the nature and amount of binder used in the two cases may have been significantly different resulting in different activities. Also looking back, it seems probable that part of powdered catalyst charged might have been lost during evacuation in the activation step leaving a much higher charge to catalyst weight ratio than initially intended. These factors may explain the unexpectedly lower

*is used to distinguish the powder form from pellet form discussed earlier.

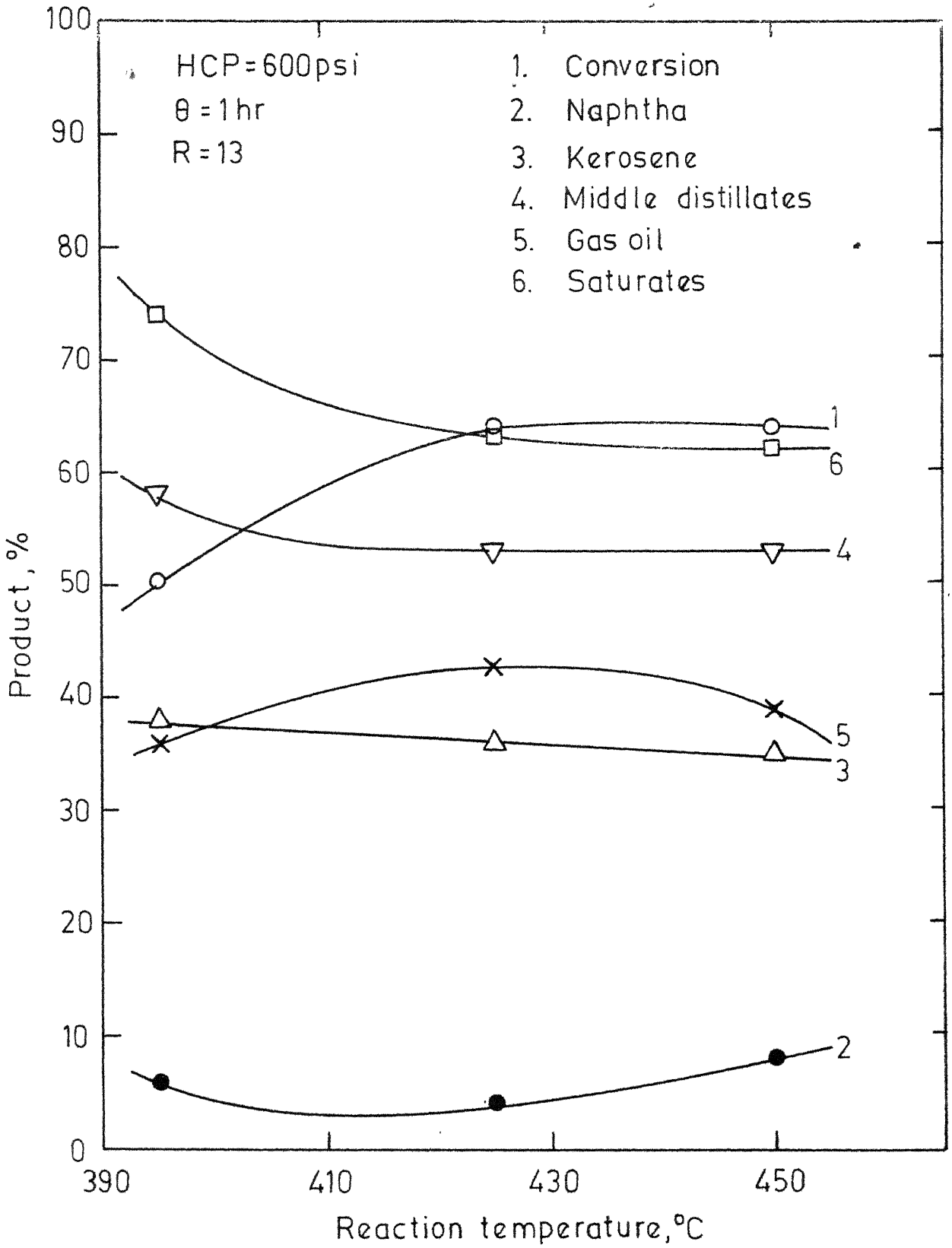

Fig. 5.12- Effect of temperature on product distribution for -20+35 mesh LaX-96.*

activity of LaX-96*. Interestingly, while the level of conversion is in some doubt because of the aforesaid reasons, the pattern of product distribution still remains valid.

Figure 5.13 shows the conversion and product distributi as a function of reaction time. Unlike the case of pellets, the conversion remained independent of time. In case of pellets, lower conversion at a lower reaction time may be due to decrease in apparent reaction rate by mass transfer limitation. When smaller particles are used this effect may be relatively small or absent.

5.5 Lanthanum Exchanged Zeolite Y Catalyst:

The dependence of the conversion and the distribution of the products obtained over LaY-86* on temperature are shown in Figure 5.14. Although the data points are scanty, the trend is evident and the nature of the curves are essentially similar to those obtained over different LaX catalysts (Figure 5.1 -5.2). Figure 5.15 presents the variation of the conversi and the product distribution with hydrogen charging pressure. Essentially similar effect of reaction time on the conversion and the product distribution (Figures 5.6 and 5.16) proves the existence of a similar cracking mechanism of residuum molecules,as discussed earlier in Section 5.1.1,over LaY-86* also. A comparison of Figures 5.12 and 5.14 will show that

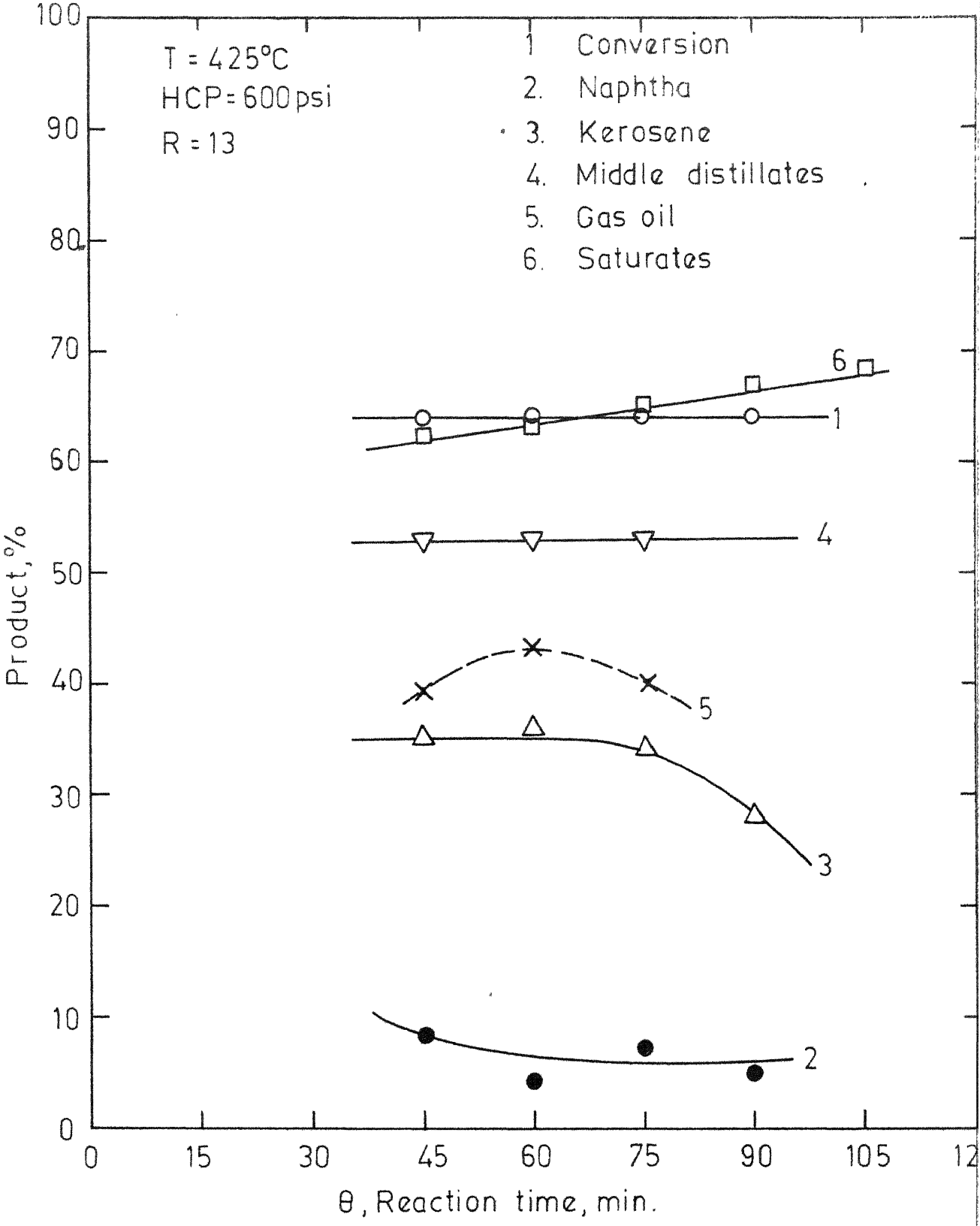

Fig.5.13-Effect of reaction time on product distribution for -20 + 35 mesh LaX-96.*

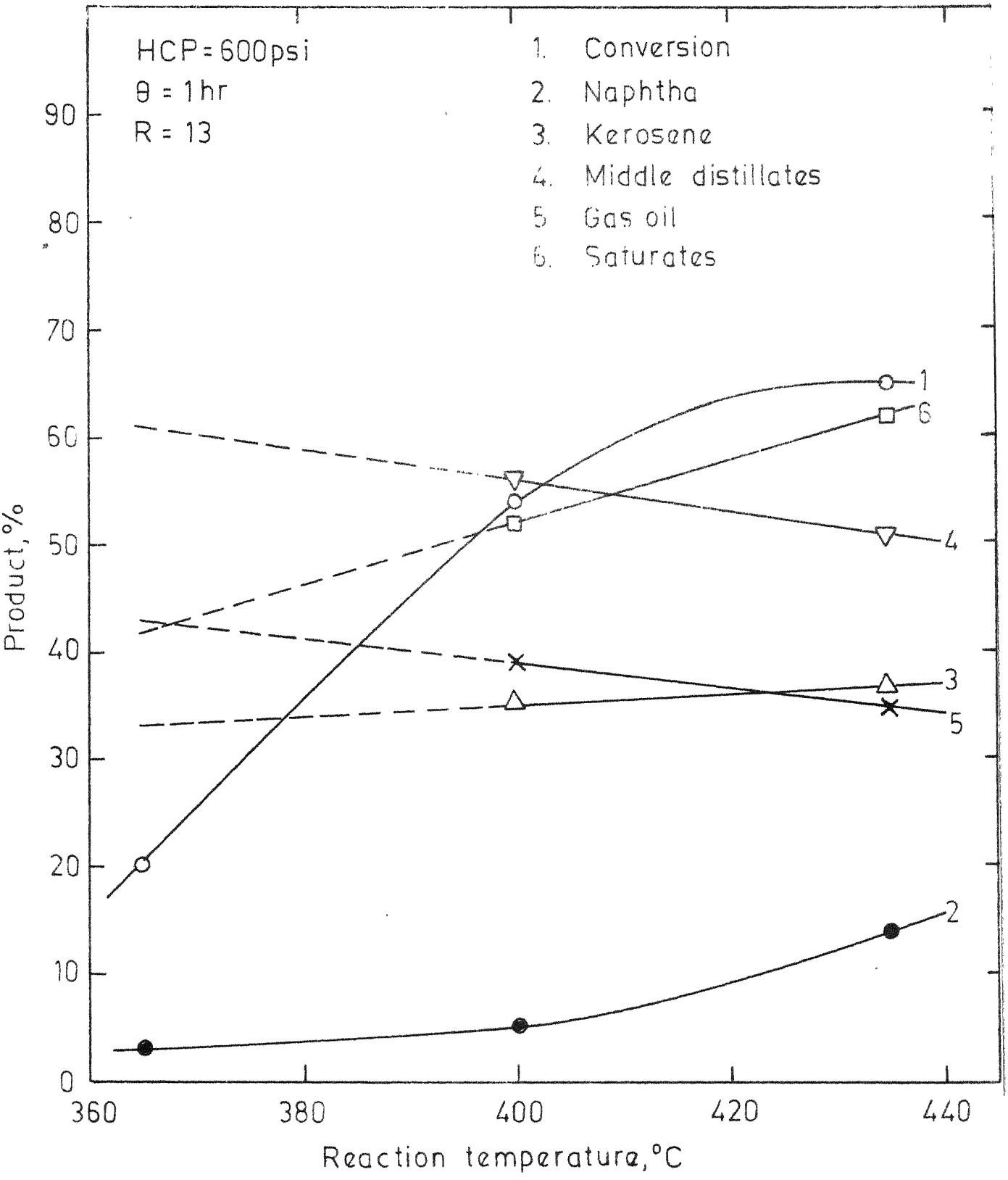

Fig.5.14 - Effect of temperature on product distribution for -20+35 mesh LaY-86.*

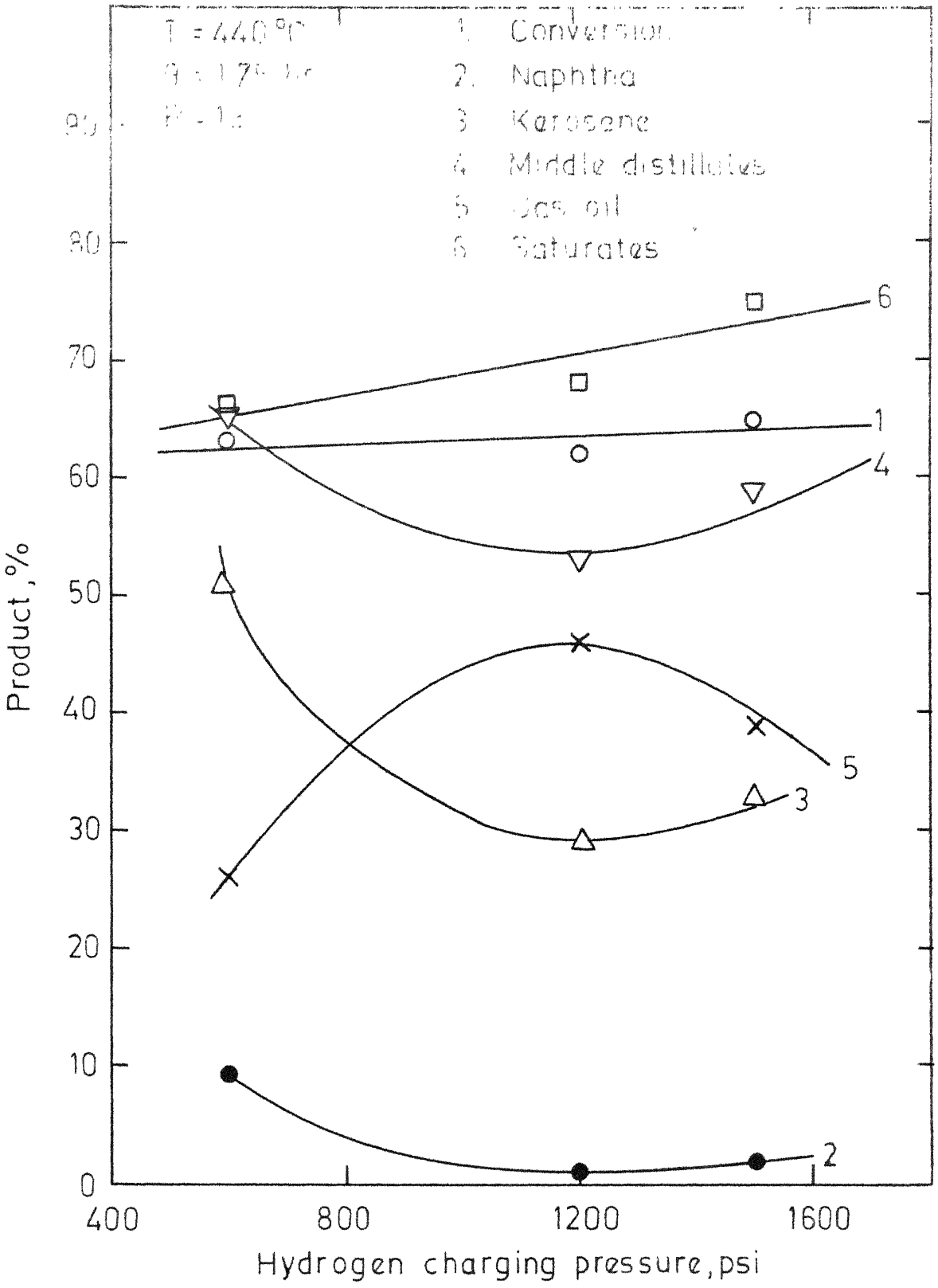

Fig 5.15 - Effect of hydrogen pressure on product distribution for -20+60 mesh LaY-86*

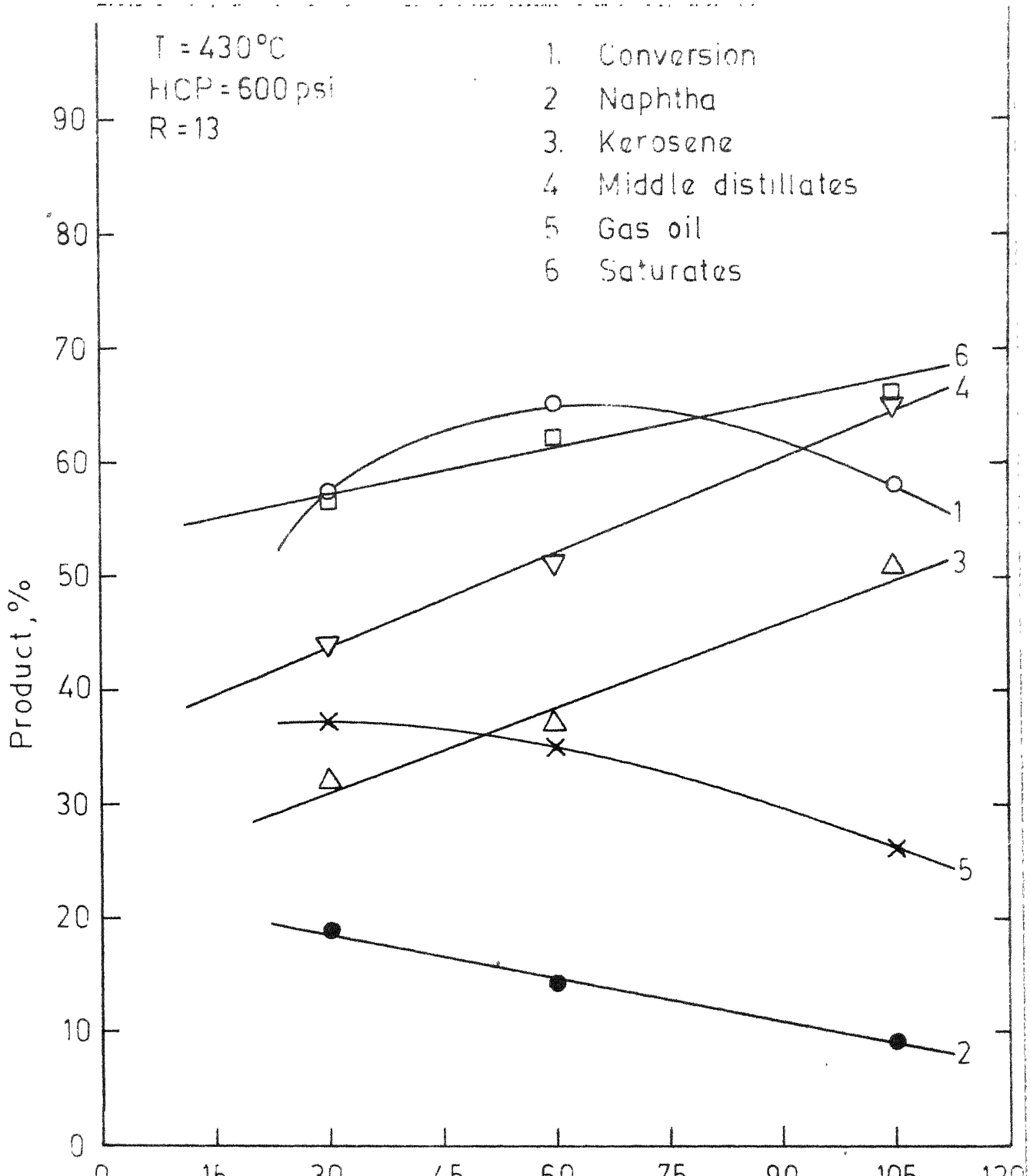

Fig. 5.16 - Effect of reaction time on product distribution for -20+60 LaY-86.*

the conversion in both cases is essentially same with slightly higher value in case of LaY.

5.6 Effect of Temperature Variation During Reaction Time:

Figure 5.17 shows the variation in temperature as a function of time during a run for a few cases over LaX-96*. The corresponding variation in pressure is shown in Figure 5.1 When the temperature was held constant throughout a run, the pressure rise was essentially linear. When the temperature was varied during the progress of the reaction as shown by curve 1 in Figures 5.17 and 5.18, the conversions obtained were significantly higher than the other two cases, curves 2 and 3. At constant temperatures of 395°C and 425°C the conversi was 27 and 64 per cent, respectively, while in the case where temperature varied from 350 to 420°C during the run, the conversion was 90 per cent. In case of LaY-86*, similar effect can be seen in Figure 5.19. A more detailed experimenta study would be required to determine the exact nature of temperature programming which will give best results and also to explain this behaviour. However, at this stage, it seems certain that a temperature programmed reactor will prove superior to isothermal operation.

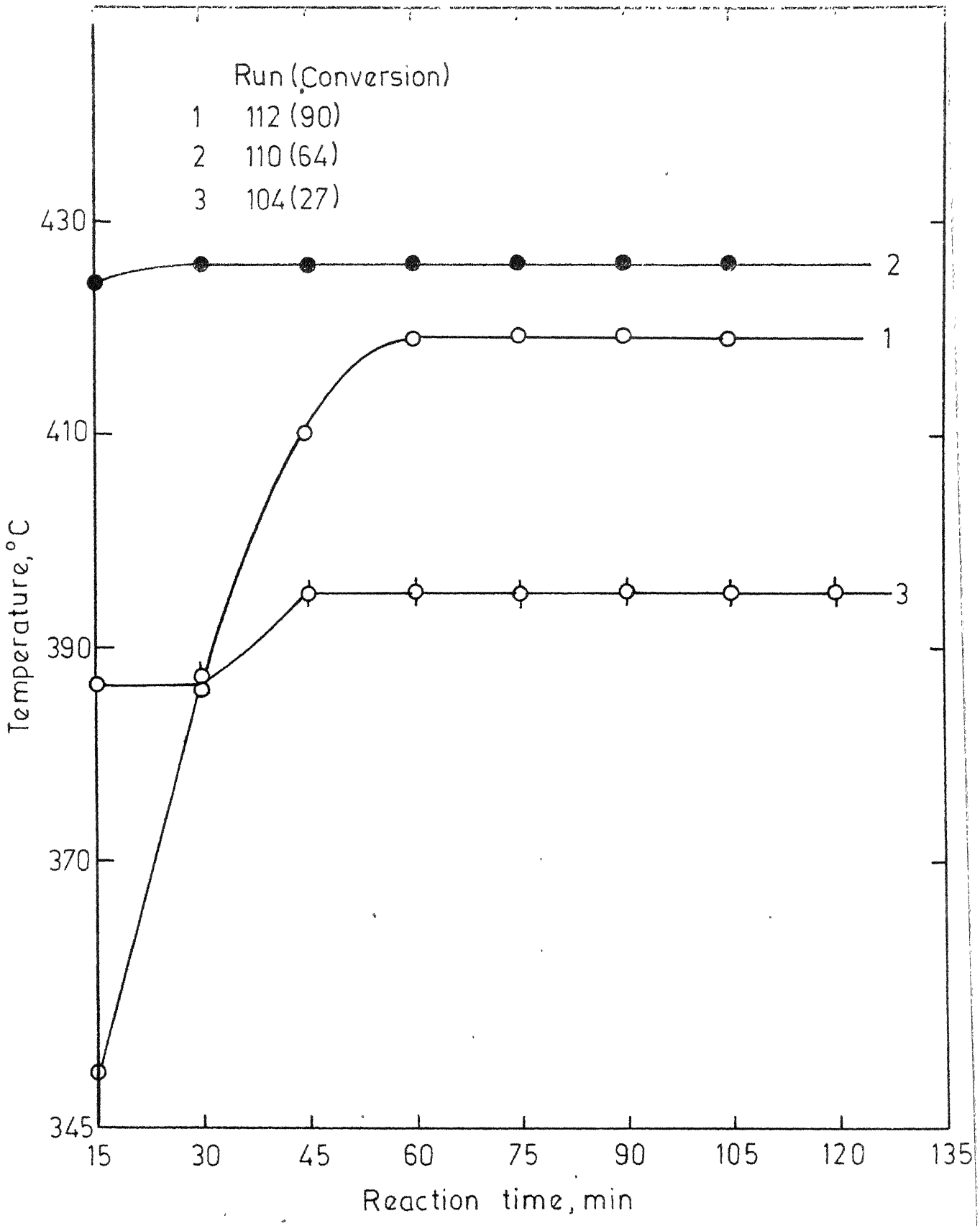

Fig.5.17 - Variation in temperature with reaction time for -20+35 mesh LaX-96* during a run.

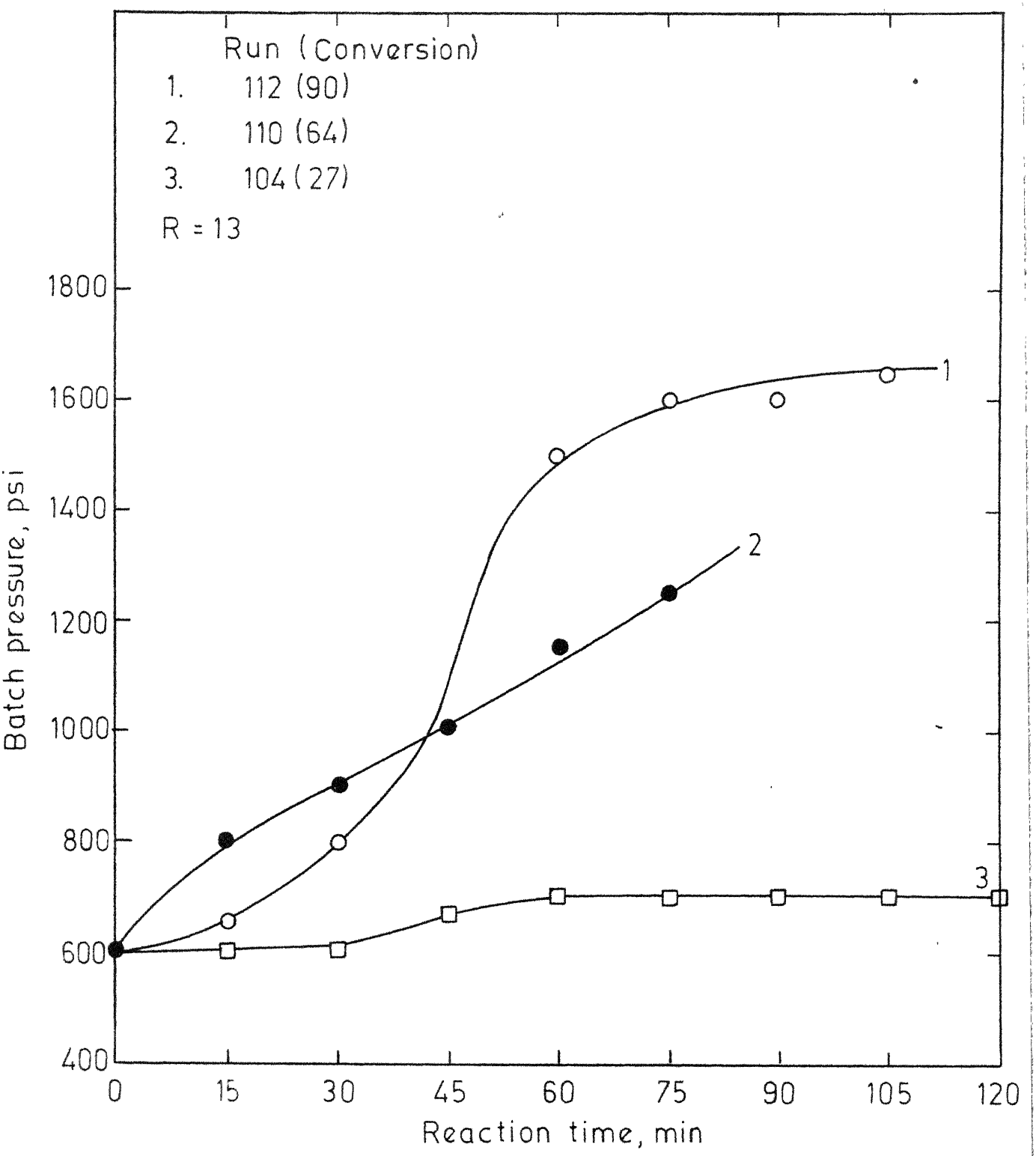

Fig 5.18 - Variation in pressure with reaction time for -20+35 mesh LaX-96* during a run.

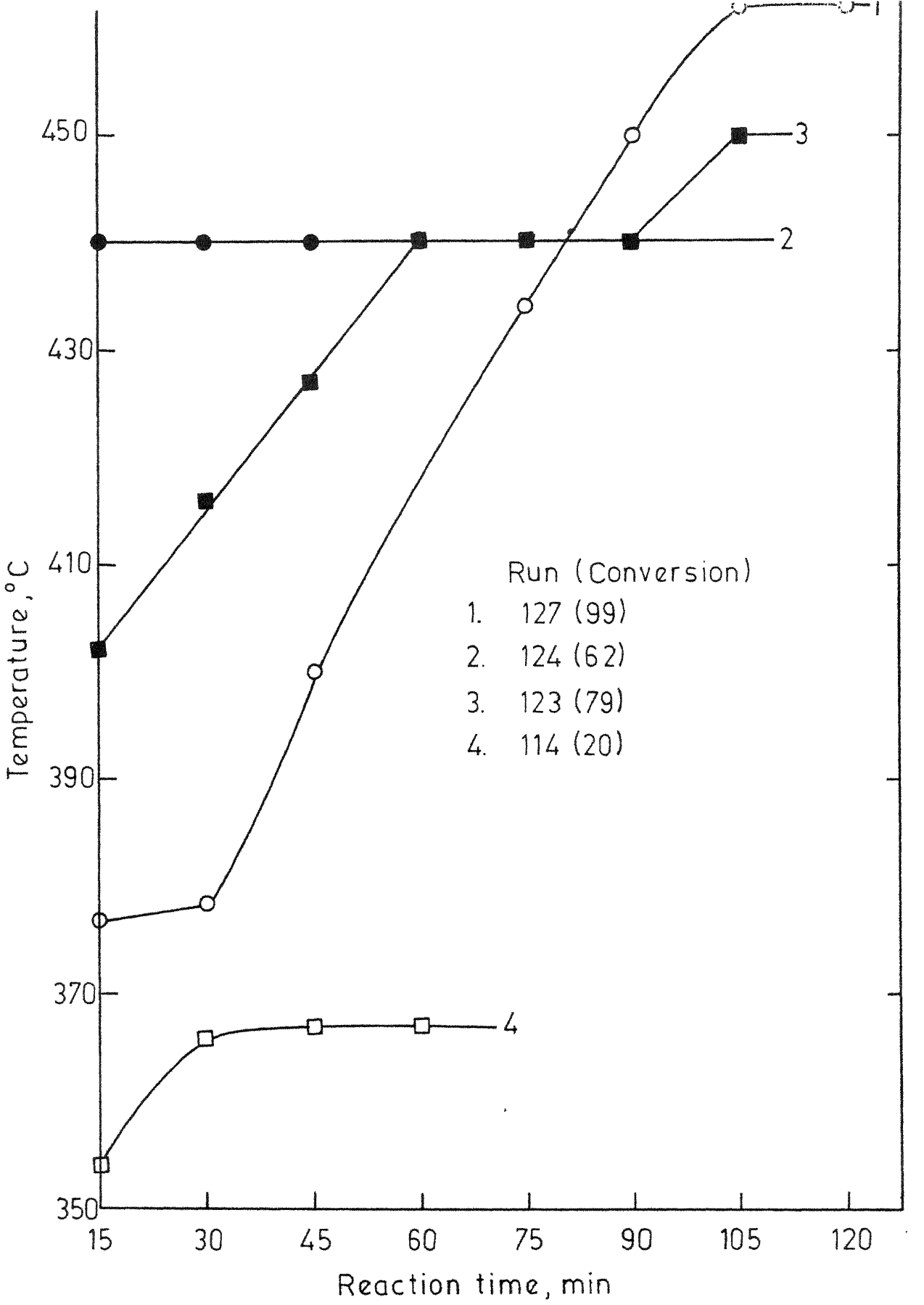

Fig.5.19 - Variation in temperature with reaction time for -20 + 35 mesh LaY-86* during a run.

CHAPTER 6

CONCLUSIONS AND RECOMMENDATIONS

6.1 Conclusions:

Hydrocracking of Assam crude residue obtained from Gauhati Refinery was investigated in a batch reactor. Faujasite type zeolite catalysts were used after ion-exchanging with a rare earth or a transition metal. The catalysts, so developed, were characterized using x-ray diffraction, flame photometry, DTA, TGA, surface area, pore volume and pore size distribution. Following important observations were made:

1. Lanthanum exchanged NaX zeolite was quite suitable for hydrocracking of Assam crude residue and gave higher degree of conversion as well as larger proportion of middle distillates as compared to nickel exchanged catalysts.
2. Degree of exchange of lanthanum had an important bearing on the process; a higher degree of exchange resulting in a higher degree of conversion.
3. The degree of saturation of kerosene obtained with LaX catalyst was usually high and comparable to that obtained with NiX.

4. Temperature was found to be the most significant operating variable. In case of LaX, the conversion first increased, attained a maximum at about 400°C and then started decreasing with further increase in temperature. With NiX, however, a linear increase was persistent in the entire range studied. The proportion of middle distillates, obtained with LaX catalyst first increased with temperature rise and then levelled off whereas in case of NiX, a linear decrease was observed.
5. Hydrogen charging pressure did not affect either the conversion or the product distribution significantly in the range of 600 to 1300 psi.

6.2 Recommendations:

Because of nonavailability of a high pressure flow reactor, the entire study was carried out in a batch reactor in the present investigation. It is, however, recognized that industrially important process has to be carried out only in flow type reactors. It is likely that because of mass transfer effects which may become significant in these trickel reactors, the performance may be somewhat different from that obtained in the present study. It is, therefore,

recommended that similar study be undertaken in a flow type reactor before an industrial process is designed.

Only a limited observations were made on Y type zeolite in this study. It is well-known that Y type zeolites possess higher catalytic activity compared to X type. Further, NaX suffers partial loss of structure on exchange with nickel whereas this is not so with NaY. A more detailed study on these lines may yield a still better catalyst.

It was noticed in the present study that varying the temperature during a run resulted in much better conversion as compared to that obtained in an isothermal operation. This, however, also needs a more detailed study to find an optimal temperature program.

BIBLIOGRAPHY

1. Abidova, M.F., Midzhuraev, R., Sultanov, A.S., Uzeb. Khim. Zh., 12(6), 40(1968); Chem. Abstr. 70: 59, 446 (1969).
2. Aboul-gheit, A.K., Abdou, I.K., J. Inst. Petrol., 58 (564) 305 (1972).
3. Aldridge, L.P., McLaughlin, J.R., Pope, C.G., J. Catal., 30, 409 (1973).
4. Ambs, W.C., Flank, W.H., J.Catal., 14, 118 (1969).
5. Annon, Oil Statistics, 13(4), 7 (1975).
6. Annon, Indian Chem.Eng., 18(1), 1 (1976).
7. Annon, Chem. Ind.Dev., 10(2), 13 (1976).
8. Annon, The Hindue, Monday, September 13, 1976.
9. Barrer,, R.M., Davies, J.A., Rees, L.V.C., J. Inorg. Nucl. Chem., 31, 2599 (1969).
10. Beaumont, R., Barthomeuf, D., J.Catal. 26, 218 (1972).
11. Beaumont, R., Barthomeuf, D., Trambouze, Y., Advan. Chem. Ser., 102, 327 (1971).
12. Beecher, R., Voorhies, A., Jr., Eberley, P., Jr., Ind. Eng. Chem., Prod. Res. Dev., 7, 203 (1968).
13. Benesi, H.A., J.Catal., 8, 368 (1967).
14. Bennett, J.M., Smith, J.V., Angell, J.F., Mat. Res. Bull., 4, 77 (1969).
15. Berenek, L., Kraus, M., Collect. Czech. Chem.Commun., 31, 566 (1966).

16. Beuther, H., Larson, O.A., Ind.Eng.Chem., Proc. Des.Dev., 4, 177 (1965).

17. Beuther, H., Smith, B.K., Proc. 7th Wld. Petrol.Congr., Mexico City, 1967.

18. Bolton, A.P., J.Catal. 22, 9 (1971).

19. Bragg, W.L., 'The Crystalline State', Macmillan, New York, 1933.

20. Breck, D.W., 'Zeolite Molecular Sieve', Wiley-Inter Science, New York, 1974.

21. Breck, D.W., Flanigen,F.M., in 'Molecular Sieves, Society of Chemical Industry, London, 1968.

22. Bridge, A.G.,Scott, J.W., Reed, E.M., Hydrocarbon Process, 54(5), 74 (1975).

23. Cantrell, A., Oil and Gas J., 71(14), 102 (1973).

24. Chen, N.Y., Weisz, P.B.,Chem. Eng. Progr. Symp. Ser., 63(73), 86 (1963).

25. Chen, N.Y., Garwood,W.E., Advan. Chem.Ser., 121, 575(1973).

26. Chernakova,G.N., Orochko,D.I., Rogov, S.P., Agafonov, A.V., Porezhigna, I.Y.,Osipov, L.N., Khim.Technol. Topl. Masel, 18(2), 7 (1973); Chem.Abstr. 79:333, 165 (1973).

27. Chernozhukov, N.I., Kuliev, R.S., Sadykhova, B.A., Rasulova, A.M., Issled. Primen. Gid. Pr. Neftepererab. Neftekhim. Prom., 261 (1968); Chem. Abstr. 72, 134,858 (1970).

28. Choudhary, N., Saraf, D.N., Ind. Eng. Chem., Prod. Res. Dev., 14(2), 74 (1975).

29. Ciapetta,F.G., Hunter, J.B., Ind. Eng.Chem., 45, 147 (1953).

30. Conn, A.L.,Chem.Eng. Progr., 69(12), 11 (1973).

31. Coonradt, H.L., Garwood,W.E., Ind.Eng.Chem., Proc. Des. Dev., 3, 38 (1964).

32. Coughlan, B., Carroll, W.M., JCS Faraday Trans I 72(9), 2016 (1976).

33. Dean, J.A., 'Flame Photometry', McGraw-Hill Book Co., Inc., New York, 1960, p 295.

34. Dempsey, E., Olson, D.H., J. Phys. Chem., 73, 387 (1969).

35. Dorogochinskii, A.Z., Khadzhiev, S.N., Gairbekov, S.M., Mech. Hydrocarbon React. Sympo. 1973 (Publ. 1973), 443-56.

36. Dyer, A., Ogden, A.B., J. Inorg. Nucl. Chem., 37, 2207 (1975).

37. Dyer,A., Molyneux,A., J. Inorg. Nucl. Chem., 32, 2389 (1970).

38. Eberley, P.E., Jr.,Kremlin,E.J., Jr., Advan. Chem.Ser., 102, 374 (1971).

39. Egan,C.J., Langlois,G.E., White, R.J., J.Chem.Soc., 84, 1204 (1962).

40. El Kady, F.Y., Hassan, A.H., Abdou, I.K., J. Inst. Petrol., 55 (545), 338 (1969).

41. Fabuss, B.M., Smith, J.O., Lait, R.I., Fabuss, M.A., Satterfield, C.N., Ind.Eng.Chem., Proc. Des. Dev., 3, 33 (1964).

42. Farrar,G.L., Oil and Gas J., 71 (14), 25 (1973).

43. Federov, V.S., Theor. Found. Chem.Eng. (Trans.), 6(5), 625 (1972).

44. Filimonov,V.A., Popov, A.A., Khavkin,V.A., Perezhigina, I.Y., Osipov, L.N., Rogov, S.P.,Agafonov, A.V., Int. Chem. Eng., 12(1), 21 (1972).

45. Flank, W.H., in 'Analytical Chemistry', R.S. Porter and J.F. Johnson, Ed., Plenum Press, 1974, Vol. 3, p. 649.

46. Flinn, R.A., Larson, O.A., Beuther, H., Ind. Eng. Chem., 52, 153 (1960).

47. Galbreath, R.B., vanDriesen,R.P., Proc. 8th Wld. Congr., 4, 129 (1971).

48. Gallezot, P., Ben Taarit, Y., Imelik, B., J. Phys. Chem., 77, 2556 (1973).

49. Gary, J.H., Handwerk, G.E., Marcel Dekker, Inc., New York, 1975, p.121.

50. Goldstein,M.S., Ind.Eng.Chem., Proc. Des. Dev., 5, 189 (1966).

51. Greensfelder, B.S., Voge, H.H., Good, G.M., Ind.Eng. Chem., 41, 2573 (1949).

52. Haensel,V., Pollitzer, E.L., Watkins, C.H., Proc. 6th Wld. Petrol.Congr., 3, 193 (1963).

53. Hassan, A.H.,El Menoufy, M.F., Indian J.Technol., 13, 411 (1975).

54. Hatch, L.F., Hydrocarbon Process., 48(2), 77 (1969).

55. Herd, A.C., Pope,C.G., J.Chem.Soc. Faraday Trans. I, 69, 833 (1973).

56. Hirschler,A.E., J.Catal., 2, 428 (1963).

57. Horne,W.A., McAfee, J., 'Advances in Petroleum Chemistry and Refining',Vol. 3, p.193, Interscience, New York, 1960.

58. Ivanova, T.M., Romanovski, B.V., Topchieva, K.V., Nefte, Khimiya, 12(4), 549 (1972): Chem.Abstr. 78: 6158 (1973).

59. Jerocki, B., Golebiowski, S., Grochowska, M., Hofman, L., Rutkowski, M., Int. Chem. Eng., 12(1), 201 (1973).

60. Kerr, G.T.,Advan.Chem.Ser., 121, 219 (1973).

61. Kladnig,W., J. Phys. Chem., 80, 262 (1976).

62. Kolesnikov, I.M., Panchenkov, G.M., Tret'yakov,V.A., Russ. J. Phys. Chem., 41, 587 (1967).

63. Lai, P.P., Rees, L.V.C., J.C.S. Faraday Trans I 72(8), 1840 (1976).

64. Langlois, G.E.,Sullivan,R.F., Advan.Chem.Ser., 97, 38(1970).

65. Lapidus, A.L., Isakov, Y.I., Rudakova, L.N., Minachev, K.M., Eidus, Y.T., Bull. Acad. Sci. USSR,Div. Chem. Sci., 21, 1848 (1972).

66. Larson, O.A., Maciver,D.S, Tobin, H.F., Flinn, R.A., Ind. Eng. Chem., Prod. Res. Dev., 1, 300 (1962).

67. Larson, O.A., Am.Chem.Soc., Div. Petrol.Chem., Prepr., 12(4), 13 (1967).

68. Maher,R.K., Hunter, F.D., Scherzer, J., Advan.Chem. Ser., 101, 266 (1971).

69. Manshilin,V.V., Vail, Y.K., Manakov, N.K., Vasilenko,V.F., Kheifets,A.E., Khim.Tekhnol. Topl. Masel, 13(7), 1(1963): Chem. Abstr. 69: 687, 314 (1968).

70. Mehta, B.R., 'Indian and the World Oil Crisis', Sterling Publishers, Pvt. Ltd., New Delhi, 1974, p.113.

71. Minchev, K.M., Gagarin,V.I., Kharlamov, V.I., Bull. Acad. Sci. USSR, Div. Chem.Sci., 19(4), 785 (1970).

72. Molenda, J., Gut, A., Przem. Chem., 51(3), 135 (1972); Chem. Abstr., 76: 156, 331 (1972).

73. Mortier, W.J., Bosmans, H.J., J. Phys. Chem., 75, 3327(1971).

74. Mortier, W.J., Bosmans, H.J., Uytterhoeven, J.B., J. Phys. Chem., 76, 650 (1972).

75. Moscou, L., Lakeman, M., J.Catal., 16, 173 (1970).

76. Moscou, L., Mone, R., J.Catal., 30, 417 (1973).

77. Murphy, J.R., Smith, M.R., Viens, C.H., Proc.Div. Refining, Am.Petrol.Institute, 50, 923 (1970).

78. Musial, E., Rutkowski, M., Int. Chem.Eng., 12(4), 687 (1972).

79. Myers, C.G., Garwood, W.E., Rope, B.W., Wedlinger, R.L., Hawthorne, W.P.,Am.Chem.Soc., Div. Petrol. Chem., Prepr., 7(1), 173 (1962).

80. Nace, D.M., Ind.Eng.Chem., Prod. Res.Dev., 8, 31 (1969).

81. Nelson,W.L., Oil and Gas J., 65 (12), 170 (1967).

82. Nelson,W.L., Oil and Gas J., 71 (47), 54 (1973).

83. Obald,A.G., Oil and Gas J., 70(3), 84 (1972).

84. Olson,D.H., J. Phys. Chem., 72(13), 4366 (1968).

85. Olson, D.H., Kokotailo,G.T., Charnell, J.F., J.Colloid Interface Sci., 28, 305 (1968).

86. Orochro, D.I., Perezhigina, I.Y., Rogov,S.P.,Rysakov, M.V., Chernakova,G.N., Khim. Tekhnol. Topl. Masel, 15(8), 2 (1970); Chem.Abstr. 73: 100,695 (1970).

87. Otouma, H., Arai, Y., Rep. Res. Lab., Asahi Glass Co., Ltd., 19(1), 21 (1969).

88. Otouma, H., Arai, Y., Ukihashi, H., Bull.Chem.Soc. Jap., 42, 2449 (1969).

89. Pansing, W.F., Am.Chem.Soc., Div. Petrol.Chem., Prepr., 9(3), 63 (1964).

90. Penchev,V.,Davidova, N., Kanazirov,V., Minchev, H., Neinska, Y., Advan.Chem.Ser., 121, 461 (1973).

91. Pickert, P.E., Rabo, J.A., Dempsey, E., Schomaker, V., Proc. 3rd Int. Congr. Catalysis, 1, 714 (1965).

92. Pickert, P.E., Bolton,A.P., Lanewala, M.A., Chem.Eng., 75(16), 126 (1968).

93. Pope,C.G., Thomas, M., J.Catal., 40, 67 (1975).

94. Qader, S.A., J. Inst. Petrol (London), 59 (568), 178 (1973).

95. Qader,S.A., Singh,S., Weiser, W.H., Hill,G.R., J. Inst. Petrol. (London), 56 (550), 187 (1970).

96. Qader,S.A., Hill, G.R., Ind. Eng.Chem., Proc. Des. Dev., 8, 98(1968).

97. Rabo, J.A., Schomaker, V., Pickert, P.E., Proc. 3rd Int. Congr. Catalysis, 2, 1265 (1965).

98. Rettalic, W.B.,Doelp, L.C., 'Kirk-Othomer's Encyclopedia of Chemical Technology', 2nd Ed. Vol. 11, p.418, 1966.

99. Richardson, J.T., J. Catal., 9, 182 (1967).

100. Rosseinsky,D.R., Chem.Rev., 65, 467 (1965).

101. Satterfield, C.N.,Coltin, C.K., Pitcher,W.H., Jr., AIChEJ., 19(3), 628 (1973).

102. Schoonheydt, R.A., Vandamme, L.J., Jacobs, P.A., Uytterhoeven, J.B., J.Catal. 43,292-303 (1976).

103. Schuftz, H.F., Weltkamp, J.H., Ind. Eng.Chem., Prod. Res. Dev., 11(1), 46 (1972).

104. Schuftz, H.F.,Weitkamp, J.H., Am.Chem.Soc., Div. Petrol. Chem., Prepr., 16(1),A102 (1971).

105. Scott, J.W., Patterson, N.J., Proc. 7th Wld. Petrol. Congr., 4, 97 (1967).

106. Scott, J.W., Bridge,A.G.,Advan.Chem.Ser., 103, 113 (1971).

107. Selim, M.M.,Rudenko, A.P., Int. Chem.Eng., 15(4), 694(1975).

108. Serpinskii,V.V., Rakhamukov, B.K., Minchev, K.M., Penchev, V., Izv. Akad. Nauk SSSR,Ser. Khim., 23(2), 466 (1973); Mol. Sieve Abstr., 4(1), 23 (1974).

109. Sherry, H.S., Advan. Chem.Ser., 101, 350 (1971).

110. Smith, J.V.,Advan.Chem.Ser., 101, 171 (1971).

111. Sullivan,R.F., Meyer, J.A., 169th ACS Meet., Philadelphia, Pa., April 6, 1975 (Paper PETR-35).

112. Stangeland, B.E., Kittrel, J.R., Ind.Eng.Chem., Proc. Des. Dev., 11(1), 15 (1972).

113. Stormont,D.H., Oil and Gas J., 62 (52), 190 (1965).

114. Thomas,C.L., McNelis,E.J., Proc. 7th Wld Petrol.Congr., 1B, 161 (1967).

115. Turkevitch, J., Catalysis Rev., 1, 1 (1967).

115a. Vogel, A.I., 'A Text Book of Quantitative Analysis', 3rd Ed., Longenans Green, London, 1961

116. Voorhies,A., Jr., Smith,W.M., Advances in Petroleum Chemistry and Refining', Vol. 8, p169, Interscience, New York, 1964.

117. Ward, J.W., Hansford, R.C., Reichle, A.D.,Sosnowski, J., Oil and Gas J., 71 (22), 69 (1973).

118. Ward, J.W., Am.Chem.Soc.,Div. Petrol.Chem., Los Angeles Meet., March 28, 1971.

119. Ward, J.W., J. Phys.Chem., 72, 4211 (1968).

120. Ward, J.W., J.Catal., 13, 321 (1969).

121. Way, J.T., J. Roy. Agri.Soc.,11, 313 (1850).

122. Weiss, A.H.,Friedman, L., Ind. Eng.Chem., Proc. Des. Dev., 2, 163 (1963).

123. Weisz, P.B.,Chem.Tech., 3(8), 498 (1973).

124. Weitkamp, J.H.,Schultz, H.F., J.Catal., 29, 361 (1973).

125. Winsor, J.,Chem.Eng. (London), 61, 194 (1972).

126. Zhorov, U.M., Panchenkov,G.M., Khim.Tekhnol. Topl. Masel. 18(10), 5 (1973).

127. Zhorov, U.M., Panchenkov,G.M., Tatraintseva, C.M., Kuzinin,S.T., Zenkouskii, S.M., Int. Chem.Eng., 11(2), 256 (1971).

APPENDIX A

X-RAY POWDER DIFFRACTION DATA FOR DIFFERENT ZEOLITE CATALYSTS

TABLE A.1: X-RAY DATA FOR NaX-100

d (Å)	I/I_o per cent	hkl	
14.6566	100	111	
8.9162	30	220	
7.5828	21	311	
7.1380	3	222	a = 24.9954 Å,
5.7536	39	331	Si/Al = 1.23
5.5289	1	420	Al/U.C.= 86
4.8217	10	511, 333	
4.4329	19	440	
3.9602	8	620	
3.8176	60	533	
3.7155	4	622	
3.3473	49	642	
3.0562	9	733	
2.9883	2	820, 644	
2.9478	16	822, 660	
2.8892	49	751, 555	
2.7968	19	840	
2.7450	5	753, 911	
2.6672	19	664	
2.6240	10	931	
2.4069	12	(10,2,2), 666	
2.2106	8	880	

TABLE A.2: REPORTED DATA FOR NaX-100[21]

$a = 24.93$ Å Si/Al = 1.25

d (Å)	I/I_o per cent	hkl
14.465	100	111
8.845	18	220
7.538	12	311
5.731	18	331
4.811	5	333,511
4.419	9	440
4.226	1	531
3.946	4	620
3.808	21	533
3.765	3	622
3.603	1	444
3.500	1	711,551
3.338	8	642
3.253	1	731,553
3.051	4	733
2.944	9	822,660
2.885	19	751,555
2.794	8	840
2.743	2	911

TABLE A.3: X-RAY DATA FOR LaX-58

d ($\overset{o}{A}$)	I/I_o, per cent	hkl
14.4413	100	111
8.8628	47	220
7.2310	4	222
6.2567	13	400
5.7425	48	331
4.8243	10	511,333
4.4285	2	440
4.2402	3	531
4.1617	1	600,442
3.8184	85	533
3.5065	3	711,551
3.3461	84	642
3.0583	2	733
2.9535	23	822,660
2.8929	53	751,555
2.8002	39	840
2.7549	2	911,753
2.6703	21	664
2.6255	18	931
2.5559	16	844
2.4555	4	(10,2,0),862

Table A.3 (contd)

d o (A)	I/I_o per cent	hkl
2.4113	9	(10,2,2),666
2.2919	2	(10,4,2)
2.2567	2	(11,1,1),(775)
2.2142	25	880
2.1890	12	(11,3,1),(971),955
2.1227	13	(11,3,3),973
2.0668	2	(11,5,1),777
1.9565	6	(12,4,2),(11,8,0),(886)
1.9099	2	(13,1,1),(11,7,1),(11,5,5),(993)
1.8887	3	(12,4,4)
1.8715	33	(13,3,1),(11,7,3),(9,7,7)
1.7935	3	(13,5,1),(11,7,5)
1.7715	15	(10,10,0),(10,8,6),(14,2,0)
1.7244	7	(11,9,3),(997)
1.6066	6	(15,3,3),(13,7,5),(11,11,1)(9,9,9)
1.5420	1	(16,2,2),(14,8,2),(10,10,8)
1.5314	2	(13,7,7),(11,11,5)
1.5189	6	(16,4,0),(12,8,8)
1.4771	6	(16,4,4),(12,12,0)
1.3831	5	(16,8,0)
1.3145	4	(19,1,1),(17,7,5),(13,13,5),(11,11,1

TABLE A.4: X-RAY DATA FOR LaX-79

d o (A)	I/I_o per cent	hkl
14.5362	100	111
8.8894	11	220
7.2427	14	222
4.8088	8	511
4.1713	34	422
3.8144	52	533
3.5065	7	711
3.3473	12	642
3.2608	7	553
3.1318	3	800
3.0359	8	733
2.9497	14	822
2.8711	7	555
2.8011	9	840
2.7491	12	911
2.6710	4	664
2.6255	9	931
2.5150	6	755
2.4552	10	10,2,0
2.4201	4	773

Table A.4 (contd)

d_o (A)	I/I_o per cent	hkl
2.2132	14	880
2.1860	14	11,3,1
2.1463	3	10,6,0
2.1232	5	11,3,3
1.9549	9	12,4,2
1.7890	8	12,6,4
1.7703	5	10,10,0
1.6053	8	11,11,1

TABLE A.5: X-RAY DATA FOR LaX-96

d o (A)	I/I_o per cent	hkl
14.5124	100	111
8.8628	11	220
7.2310	13	222
5.7722	3	331
4.8165	8	511, 333
4.4285	3	440
4.2223	4	531
4.1704	10	442, 600
3.8160	59	533
3.5038	8	711, 551
3.3436	9	642
3.2561	4	731, 553
3.1393	3	800
3.0349	5	733
2.9469	11	822,660
2.8811	4	751, 555
2.7972	6	840
2.7467	13	911, 753
2.6672	3	664
2.6232	8	931
2.5516	1	844

Table A.5 (contd)

d o (A)	I/I_o per cent	hkl
2.5156	4	933, 771, 755
2.4529	6	(10,2,0),862
2.4163	3	(10,2,2), (6,6,6)
2.2116	8	880
2.1855	6	(11,3,1), 971, 955
2.1463	1	(10,6,0), 866
2.1227	3	(11,3,3), 973
2.0646	3	(11,5,1), 777
2.0102	2	(11,5,3), 975
1.9545	6	(12,4,2), (10,8,0),886
1.7894	4	(12,6,4),(14,0,0)
1.7696	3	(14,2,0),(10,10,0),(10,8,6)
1.7557	3	(13,5,3),(11,9,1)
1.7217	1	(11,9,3),(997)
1.6923	1	(13,7,1), (13,5,5),(11,7,7)
1.6053	4	(15,3,3),(13,7,5),(11,11,1),(9,9,9)
1.5404	1	(16,2,2),(14,8,2),(10,10,8)

TABLE A.6: X-RAY DATA FOR NiX-80

d ($\mathring{A}$)	I/I_o per cent	hkl
14.4178	84	111
8.8187	18	220
7.5635	9	311
6.3032	5	400
5.7057	55	331
4.7959	9	511,333
4.4219	36	440
4.2583	5	531
3.9377	5	620
3.8015	63	533
3.3448	100	642
3.0491	10	733
2.9402	17	822,660
2.8793	39	751,555
2.7908	14	840
2.6610	16	664
2.3995	11	(10,2,2) (6,6,6)
2.3123	5	(10,4,0), (8,6,4)
2.2813	5	(10,4,2)
2.2475	7	(11,1,1) (775)

A
Table A.6 (contd)

d_o (A)	I/I_o per cent	hkl
2.2257	2	(880)
2.2008	5	(11,3,1), (9,7,1), (9,5,5)
2.1270	3	(11,3,3), (9,7,3)
2.8248	6	(13,3,3), (995)
1.7504	4	(13,5,3), (11,9,1)

APPENDIX B

EXPERIMENTAL RESULTS

TABLE B.1: OPERATING CONDITIONS

Run No.	Catalyst	Charge, g Catalyst, g	Operating Conditions				Conversion, percent
			Temp., °C	Pressure, PSI Initial	Pressure, PSI Final	Reaction time, hr	
1	2	3	4	5	6	7	8
1	NaX	11	360	600	1300	3.00	34.0
2	LaX-80	6	395	500	1400	3.50	54.0
3	LaX-80	13	380	600	1300	4.25	50.0
4	LaX-80	13	405	1200	1560	1.50	30.0
5	LaX-80	11	400	600	-	1.25	20.0
6	LaX-80	13	410	700	1250	2.00	27.0
7	LaX-79	8	415	600	1400	2.00	30.0
8	LaX-79	13	420	800	1500	2.00	23.0
9	LaX-79	13	410	1100	1700	2.00	29.0
10	LaX-79	13	425	600	1850	3.00	17.0
11	LaX-79	13	365	600	1200	2.00	52.0
12	LaX-79	13	365	600	1150	2.00	51.0
13	LaX-79	13	375	700	1250	2.25	54.0
15	LaX-79	13	355	600	650	1.00	27.0
16	LaX-79	13	355	600	650	1.00	15.0
17	LaX-79	13	395	800	1240	2.00	66.0
18	LaX-79	13	395	1000	2200	1.75	48.0
19	LaX-79	13	395	900	1250	2.00	60.0
20	LaX-79	13	395	600	600	2.00	-
21	LaX-79	13	385	1000	1375	2.00	54.0

Table B.1 (contd)

1	2	3	4	5	6	7	8
22	LaX-79	13	325	800	900	2.00	-
23	LaX-79	13	350	600	700	2.50	29.0
24	LaX-79	13	345	600	800	2:50	36.0
25	LaX-79	13	345	700	800	3.25	37.0
26	LaX-79	13	345	850	1000	3.25	27.0
27	LaX-79	13	345	900	1100	3.25	27.0
28	LaX-79	13	360	650	875	4.00	40.0
31	LaX-96	32	350	600	900	3.00	54.0
32	LaX-96	13	400	650	1200	2.00	49.0
33	LaX-96	13	400	600	1200	3.00	54.0
34	LaX-96	13	400	700	1000	1.00	54.0
35	LaX-96	13	400	1100	1350	1.00	67.0
36	LaX-96	13	400	1100	1400	1.00	38.0
38	LaX-96	40	380	600	1900	2.00	59.0
39	LaX-96	20	385	600	1450	2.00	76.0
40	LaX-96	13	400	600	1400	2.00	84.0
41	LaX-96	13	435	850	1300	2.00	32.0
42	LaX-96	13	420	600	1400	2.00	77.0
43	LaX-96	26	415	600	1200	2.00	70.0
44	LaX-96	18	445	600	750	1.75	53.0
45	LaX-96	13	330	1300	1375	3.00	0.0
46	LaX-96	13	360	1300	1600	3.00	60.0
47	LaX-96	13	36.0	1300	1700	3.00	61.0
48	LaX-96	13	368	1000	1300	3.00	56.0

Table B.1 (contd)

1	2	3	4	5	6	7	8
49	LaX-96	13	365	700	900	3.0	56.0
50	LaX-96	13	405	1300	1950	1.50	67.0
51	LaX-96	13	440	1200	1950	0.5	63.0
52	LaX-96	13	440	1000	1900	0.5	48.0
53	LaX-96	13	440	800	1800	0.5	36.0
54	LaX-96	13	445	600	1250	0.5	61.0
55	LaX-96	13	440	1200	1450	0.16	34.0
56	LaX-96	13	460	800	1550	0.5	58.0
57	LaX-96	13	455	600	1700	1.5	68.0
58	LaX-58	13	360	800	1150	2.0	44.0
59	LaX-58	13	400	450	1750	2.0	46.0
60	LaX-58	13	410	900	1750	2.0	30.0
61	LaX-58	13	410	1200	2000	2.0	35.0
62	LaX-58	13	450	800	2000	0.16	55.0
63	LaX-58	13	450	400	2000	0.25	63.0
64	LaX-58	13	450	600	2000	0.25	67.0
65	LaX-58	13	460	700	1250	0.25	26.0
66	LaX-58	13	400	800	1600	2.00	25.0
67	LaX-58	13	400	1100	1950	1.00	57.0
68	LaX-58	13	410	400	1350	1.00	35.0
69	LaX-58	13	455	800	1800	0.25	27.0
70	Si-Al	13	415	600	800	2.00	7.0
71	Si-Al+LaX-96	13	405	600	800	2.00	7.0
72	Si-Al+LaX-96	13	395	600	1200	2.00	27.0

Table B.1(cntd)

1	2	3	4	5	6	7	8
73	Si-Al	13	400	600	1500	0.50	42.0
74	Si-Al(50 % +LaX-96 each)	13	405	600	1850	2.00	47.0
75	LaX-58	13	410	600	1350	2.00	11.0
76	LaX-58	13	410	900	1700	2.00	16.0
77	LaX-58	13	410	500	2000	2.25	24.0
78	LaX-58	13	435	900	1900	0.25	47.0
79	LaX-58	13	465	900	1950	0.25	43.0
80	LaX-58	13	430	600	1500	2.00	20.0
81	NiX-80	18	410	800	1700	2.00	42.0
82	NiX-80	18	410	800	1550	1.00	52.0
83	NiX-80	18	420	900	1900	0.75	48.0
84	NiX-80	18	420	500	1450	1.50	54.0
85	NiX-80	18	430	1200	1960	1.00	56.0
86	NiX-80	13	355	1200	1300	2.00	32.0
87	NiX-80	13	370	800	980	2.00	35.0
88	NiX-80	13	400	850	1200	1.00	1.0
89	NiX-80	13	430	1200	1900	1.00	59.0
90	NiX-80	13	430	900	1680	1.00	50.0
91	NiX-80	13	450	1200	1900	0.50	41.0
92	NiX-80	13	455	800	1600	1.00	59.0
93	NiX-80	13	455	500	1100	1.00	50.0
94	NiX-80	13	400	800	1200	0.25	50 .0
95	NiX-80	13	450	800	1400	2.00	13.0
96	Nix+LaX-96 (50% each)	13	440	700	1400	2.00	27.0

Table B.1 (contd)

1	2	3	4	5	6	7	8
97	NiX+LaX-96 (50% each)	13	400	700	950	2.00	37.0
98	Si-Al	13	450	800	1900	1.00	40.0
99	LaX-96*	13	395	600	1100	2.00	47.0
100	LaX-96*	13	400	600	950	1.00	62.0
101	LaX-96*	13	405	700	1000	0.75	34.0
102	LaX-96*	13	430	800	1200	1.00	64.0
103	LaX-96*	13	450	800	1650	1.00	57.0
104	LaX-96*	13	395	600	700	2.00	27.0
105	LaX-96*	13	420	600	1050	2.00	47.0
106	LaX-96*	13	435	600	1600	2.00	59.0
107	LaX-96*	13	450	700	1800	2.00	27.0
108	LaX-96*	13	400	700	1100	1.00	50.0
109	LaX-96*	13	425	800	1250	1.00	64.0
110	LaX-96*	13	425	600	1250	1.25	64.0
111	LaX-96*	13	425	600	1250	1.50	64.0
112	LaX-96*	13	425	600	1650	1.75	90.1
113	LaX-96*	13	435	600	1500	0.75	64.0
114	LaY-86*	13	365	600	800	1.00	20.0
115	LaY-86*	13	400	600	1000	1.00	54.0
116	LaY-86*	13	415	600	650	0.75	10.0
117	LaY-86*	13	415	700	1650	1.25	43.0
118	LaY-86*	13	430	600	1500	0.50	57.0
119	LaY-86*	13	435	600	1800	1.00	65.0

Table B.1 (contd)

1	2	3	4	5	6	7	8
120	LaY-86*	13	410	300	1600	1.00	70.0
121	LaY-86*	13	440	600	1700	1.75	63.0
122	LaY-86*	13	430	700	900	2.00	17.0
123	LaY-86*	13	440	800	1400	1.75	79.0
124	LaY-86*	13	440	1200	1600	1.50	62.0
125	LaY-86*	13	440	1500	1900	1.75	65.0
126	LaY-86*	13	440	1000	1450	2.00	40.0
127	LaY-86*	13	440	1000	1500	2.00	99.0

TABLE B.2: PRODUCT CHARACTERISTICS

Run No.	Distillation Results						F/A Results of Kerosene	
	IBP, °C	Mid B.P. °C	Naphtha, per cent	Kerosene, per cent	Middle distillates, per cent	Gas Oil, per cent	Saturates, per cent	Unsaturates, per cent
1	2	3	4	5	6	7	8	9
1	85	282	4.0	45.2	64.0	32.0	-	-
2	90	262	10.4	48.2	60.5	29.1	65	35
3	70	255	13.3	43.4	58.0	28.7	65	35
4	90	244	10.0	51.3	63.5	26.5	51	49
5	95	305	6.7	36.7	50.0	23.3	52	48
6	60	285	21.8	26.8	41.4	36.8	46	54
7	90	350	9.0	26.8	35.8	42.4	19	81
8	85	232	17.8	45.0	59.5	22.7	53	47
9	60	262	20.5	34.1	47.8	31.7	55	45
11	90	247	10.9	54.1	67.6	21.5	70	30
12	85	291	7.8	38.0	62.5	29.7	79	21
13	60	235	17.0	46.0	60.8	22.2	77	23
16	100	360	6.7	18.4	36.6	56.7	75	25
17	105	291	4.0	40.4	61.4	34.6	80	20
18	90	303	8.3	36.8	51.0	40.7	58	42

Table B.2 (contd)

1	2	3	4	5	6	7	8	9
21	100	315	3.5	28.6	54.0	42.5	64	36
24	130	315	0.0	34.3	60.0	40.0	63	37
25	110	351	0.0	24.5	44.6	55.4	63	37
26	110	336	0.0	25.0	51.8	48.2	62	38
27	140	320	0.0	25.0	57.5	42.5	73	27
28	105	320	3.2	34.0	54.0	42.8	67	33
31	140	350	0.0	22.5	44.5	55.5	77	23
32	90	282	6.0	43.4	62.5	31.5	76	24
33	115	299	1.2	41.2	62.5	36.3	71	29
34	120	335	0.7	29.0	52.0	47.3	79	21
35	110	345	1.0	30.0	48.5	50.5	78	22
36	115	325	1.7	34.4	56.8	41.5	77	23
38	93	286	5.0	43.0	62.0	33.0	77	23
39	95	302	6.0	37.5	55.0	39.0	78	22
40	90	300	6.0	38.0	57.0	37.0	78	22
41	115	314	4.2	36.5	48.0	47.8	66	34
42	95	275	6.7	45.7	65.7	27.6	77	23
43	105	335	1.5	30.5	50.5	48.0	80	20
44	100	332	3.0	32.0	50.0	47.0	78	22

Table B.2 (contd)

1	2	3	4	5	6	7	8	9
46	110	300	2.2	42.8	65.0	32.8	78	22
47	100	284	6.5	42.4	61.0	32.5	80	20
48	100	335	4.8	32.7	46.4	48.2	76	24
49	135	-	0.0	22.3	39.8	60.2	72	28
50	95	314	5.0	35.8	52.0	43.0	76	24
51	95	323	4.9	33.0	49.0	46.1	73	27
52	95	303	6.9	37.5	52.7	40.4	70	30
53	100	295	13.0	35.2	46.4	40.6	59	41
54	102	297	6.4	36.6	58.2	35.4	74	26
55	125	358	1.0	22.[illegible]	42.0	57.0	68	32
56	80	324	5.7	31.6	47.8	46.5	69	31
57	80	332	6.5	31.5	46.5	47.0	73	27
58	105	360	0.0	29.0	42.5	57.5	73	27
59	90	350	8.7	26.5	39.0	52.3	48	52
60	90	300	11.2	33.3	48.0	40.8	30	70
61	90	316	12.2	27.0	43.4	44.4	48	52
62	90	328	7.5	30.6	57.0	35.5	58	42
63	85	>360	8.0	[illegible]	33.5	58.5	56	44

Table B.2 (contd)

1	2	3	4	5	6	7	8	9
64	90	330	9.0	31.0	43.0	48.0	67	33
65	125	360	2.9	29.0	40.0	57.1	44	56
66	80	300	18.0	30.0	43.3	38.7	38	62
67	85	290	7.2	40.5	53.6	39.2	67	33
68	110	320	5.7	36.6	48.0	46.3	59	41
69	90	350	10.0	27.5	37.5	52.5	32	68
72	115	270	10.0	42.5	55.0	35.0	55	45
73	100	250	11.7	46.7	53.7	29.6	62	38
74	90	290	7.0	38.5	54.3	38.7	49	51
75	105	300	5.9	38.2	50.0	43.1	10	90
76	105	285	4.0	44.0	64.0	32.0	10	90
77	125	320	2.8	33.3	53.0	44.0	10	90
78	95	295	10.0	35.8	51.5	39.5	63	37
79	80	300	14.0	28.6	33.8	47.2	50	50
80	95	310	7.4	41.0	59.5	33.1	38	62
81	95	250	11.0	47.0	60.0	29.0	61	39
82	100	270	7.4	46.4	64.0	28.6	69	31
83	95	280	7.0	41.0	60.0	33.0	63	37

Table B.2 (contd.)

1	2	3	4	5	6	7	8	9
84	90	290	5.0	41.0	60.0	35.0	73	27
85	100	295	5.0	40.0	59.0	36.0	74	26
86	120	330	0.0	37.5	58.1	41.9	69	31
87	100	305	1.0	41.0	69.0	30.0	78	22
88	95	295	2.9	42.9	61.5	35.6	72	28
89	120	295	5.7	38.7	58.0	36.3	70	30
90	95	235	13.0	44.0	61.3	25.7	73	27
91	110	285	1.6	46.0	67.3	31.1	69	31
92	100	325	4.4	38.3	57.4	38.2	67	33
93	120	295	2.9	42.8	63.0	34.1	70	30
94	110	300	4.0	40.0	72.0	24.0	–	–
97	110	330	0.0	30.0	55.0	45.0	–	–
99	95	265	7.0	49.0	69.0	24.0	–	–
100	140	330	0.0	30.0	54.0	46.0	–	–
101	130	340	0.0	28.0	50.0	50.0	–	–
102	95	290	5.0	41.0	64.0	36.0	–	–
103	90	290	10.0	40.0	54.0	36.0	65	35
104	100	–	2.0	32.0	56.0	42.0	73	27

Table B.2 (contd)

1	2	3	4	5	6	7	8	9
105	100	280	7.0	43.0	65.0	28.0	65	35
106	90	240	18.0	43.0	57.0	25.0	63	37
107	70	340	12.0	25.0	37.0	51.0	38	62
108	80	300	6.0	38.0	58.0	36.0	74	26
109	90	310	4.0	36.0	53.0	43.0	63	37
110	80	310	7.0	34.0	53.0	40.0	65	35
111	80	—	5.0	28.0	—	—	63	37
112	60	320	5.0	33.0	50.0	45.0	67	33
113	90	305	8.0	35.0	53.0	39.0	62	38
114	90	—	3.0	—	—	—	—	—
115	90	310	5.0	35.0	56.0	39.0	52	48
117	70	305	14.0	31.0	41.0	45.0	63	37
118	70	280	19.0	32.0	44.0	37.0	56	44
119	80	305	14.0	37.0	51.0	35.0	62	38
120	65	270	15.0	39.0	50.0	35.0	73	27
121	65	250	9.0	51.0	65.0	26.0	66	34
122	85	320	3.0	33.0	56.0	41.0	75	25
124	105	332	1.0	29.0	53.0	46.0	68	32

Table B.2 (contd)

1	2	3	4	5	6	7	8	9
125	105	315	2.0	33.0	59.0	39.0	75	25
126	105	305	0.0	36.0	54.0	46.0	75	25
127	120	335	0.0	24.0	51.0	49.0	70	30